6.6 CONSIDERATION OF ALTERNATIVE CONCEPTUAL MODELS

The SZ site-scale flow model propagates information through the SZ flow and transport model abstraction (SNL 2007 [DIRS 177390]) to the performance assessment calculations, which are used to evaluate potential risks to groundwater users downgradient from the repository area. The results of these performance assessment calculations depend upon the specific discharge of groundwater leaving the repository area as well as on the flow paths and the distribution of flow among the various hydrostratigraphic units that carry, deflect, or otherwise affect the flow. For this report only, the specific discharge was evaluated with SPDIS.EXE (STN: 611598-00-00 [DIRS 180546]), which calculates the average travel distance divided by corresponding travel time to reach a specified northing location (e.g., 5 km downgradient) across 100 particles. It is important to note that SPDIS.EXE yields a convenient metric to compare specific discharges, which represents surrogates for flow fields generated from the model. The alternative conceptual models (ACMs) presented here were investigated because they represented a hydrologic concern such as water table rise due to climate change or were related to a model feature (anisotropy) that had a possibility of affecting the specific discharge calculations. This section presents analyses of the ACMs, their representation in the numerical model, and a discussion about possible impacts on the model outputs. ACMs affecting model outputs are discussed here, although this uncertainty is not directly propagated to the radionuclide breakthrough curves in the TSPA calculations. Specifically, it should be noted that the SZ flow and transport abstraction model does not use the SZ site-scale flow model as a source of direct input to the assessment of uncertainty in groundwater specific discharge. The two direct inputs used to establish the groundwater specific discharge multiplier are DTNs: MO0003SZFWTEEP.000 [DIRS 148744] and LA0303PR831231.002 [DIRS 163561] (SNL 2007 [DIRS 177390], Table 4-1 and Section 6.5.2.1).

The calibrated SZ site-scale flow model described in detail in Section 6.5 also provides the basis for the ACMs discussed here. That is, the same numerical grid and HFM were used throughout this section. Various parameterization schemes were used to define the ACMs (e.g., change in potentiometric surface). The following ACMs were evaluated:

- Removal of vertical anisotropy: This ACM relates to removal of vertical anisotropy in permeability
- Removal of horizontal anisotropy: This ACM relates to removal of horizontal anisotropy in the volcanic units downgradient from Yucca Mountain
- Removal of the altered northern region: This ACM relates to removal of the permeability multipliers that reduce the permeability in the northern region, which help the model honor the observed high head
- Increase in permeability in the *z*-direction for the Solitario Canyon Fault
- Water table rise: This ACM relates to future water table rise.

6.6.1 Removal of Vertical Anisotropy

Anisotropy occurs when hydraulic properties have different values in the three principal directions: vertical, horizontal along the direction of maximum permeability, and horizontal along the direction of minimum permeability. The ratio of horizontal to vertical permeability, 10:1, is in the generally accepted range provided by the Expert Elicitation Panel (CRWMS M&O 1998 [DIRS 100353], Table 3-2). The results upon removal of vertical anisotropy (i.e., 1:1) are shown in Figure 6-18. Specific discharge across the 5-km boundary increases by 28% from 0.36 to 0.46 m/yr. Weighted RMSE increase significantly (89%) from 0.82 to 1.55 m and non-weighted RMSE increase 20% from 24.39 to 29.21 m. Differences in fluxes through the boundary zones defined in Table 6-11 changed by no more than 8% (decreases from –101 to –107 kg/s and –57 to –62 kg/s on the west and north boundaries, respectively). Not surprisingly, without vertical anisotropy, particles travel deeper in the system (from 353 m for the anisotropic case to –175 m without vertical anisotropy). Overall, 10:1 vertical anisotropy yields better flow calibration because removal of vertical anisotropy degrades the accuracy and representativeness of the model results.

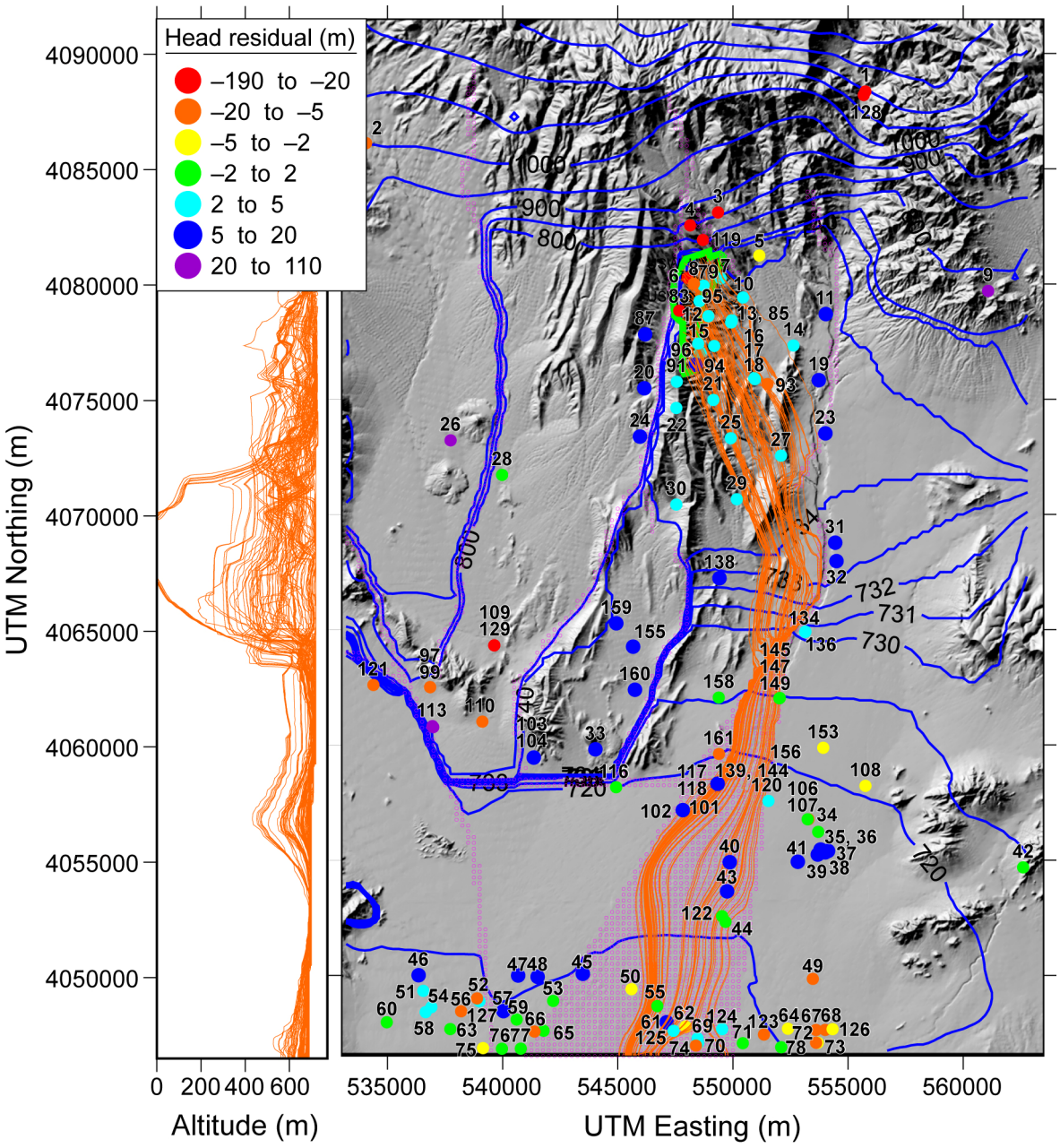

Source: SNL 2007 [DIRS 179466] (for repository outline).

NOTE: For illustration purposes only. Altitude is in meters above mean sea level. Legend represents the water level difference in meters (simulated value minus measured value). The wells are numbered to correspond to the second column of Table 6-8 (multiple-depth wells only show the number corresponding to the highest screened interval altitude).

UTM = Universal Transverse Mercator.

Figure 6-18. Particle Tracks for a Model without Vertical Anisotropy

6.6.2 Removal of Horizontal Anisotropy

Anisotropy in the volcanic units near Yucca Mountain was investigated using an ACM with variable horizontal anisotropy ratios (north–south to east–west permeability changes). The area to which the anisotropy ratio was applied is bounded by the quadrilateral shown in Figure 6-12. This effect was investigated by rerunning the calibrated model with a 1:1 horizontal permeability ratio in this region and checking the sensitivity of the modeled water levels and flow paths. A detailed description of the development of the horizontal anisotropy distribution used in this model is found in *Saturated Zone In-Situ Testing* (SNL 2007 [DIRS 177394], Section 6.2.6 and Appendix C6). This alternate conceptual model is carried through to TSPA where flow fields are generated using the distribution defined in *Saturated Zone In-Situ Testing* (SNL 2007 [DIRS 177394], Section 6.2.6 and Appendix C6). Modeling the Yucca Mountain volcanic zones as isotropic yielded insignificant changes to the weighted RMSE for head residuals (0.82 m). Specific discharge across the 5-km boundary decreases by 31% from 0.36 to 0.25 m/yr and associated pathlines are shown in Figure 6-19. The pathlines, as expected, have a more easterly trend immediately downstream from the repository as compared to the calibrated model (Figure 6-17). Also, pathlines go somewhat deeper to 319 from 353 m for the horizontally isotropic case. Because horizontal anisotropy impacts specific discharge results, this parameter has been included in the TSPA analysis and, is therefore fully accounted for in terms of effect on repository performance.

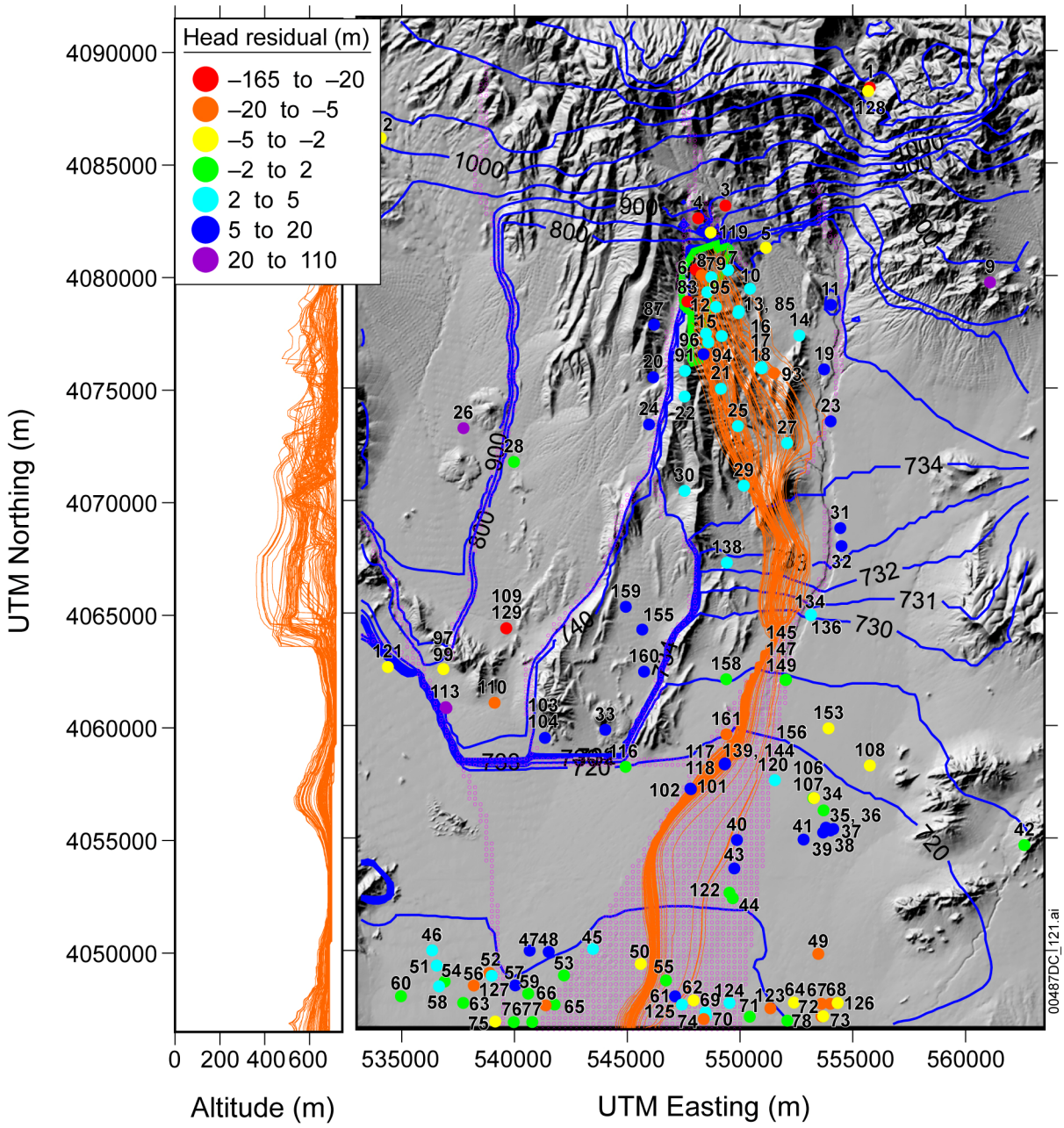

Source: SNL 2007 [DIRS 179466] (for repository outline).

NOTE: For illustration purposes only. Altitude is in meters above mean sea level. Legend represents the water level residual (m) (simulated value minus the observed value). The wells are numbered to correspond to the second column of Table 6-8 (multiple-depth wells only show the number corresponding to the highest screened interval altitude).

UTM = Universal Transverse Mercator.

Figure 6-19. Particle Tracks for Isotropic Yucca Mountain Volcanic Units

6.6.3 Removal of LHG and Change to the Solitario Canyon Fault Anisotropy

A LHG just north of Yucca Mountain has been inferred from hydraulic head measurements. Previous revisions of the AMR assumed an artificial low-permeability east-west feature included in the model simply to obtain an acceptable representation of the LHG. This model implements the LHG with a more defensible conceptual model—the altered northern region (see Sections 6.3.1.11 and 6.4.3.7 where alteration due to the Claim Canyon Caldera north of Yucca Mountain divides hydrogeologic units into distinct northern and southern zones). Although the genesis of the LHG has yet to be fully explained, logic dictates that so long as the LHG in this region is faithfully represented (regardless of its conceptualization), effects on flowpaths are minimal because the region is upgradient from the zone of interest (and away from zones that are weighted heavily during calibration). However, removal of the LHG from the conceptual model yielded an increase in specific discharge across the 5-km boundary to 4.79 m/yr (an increase by nearly a factor of 15) because the zone of reduced permeability was eliminated from the altered northern region (permeability multipliers set to one, but no recalibration performed) and the overall flux of water through the northern model boundary was significantly increased. The weighted RMSE was increased by nearly a factor of 8 to 6.20 m. Clearly, removal of the LHG from the conceptual model yields a model that does not match observations, hence its existence (not its conceptualization) is critical to an accurate model.

Changing the vertical anisotropy in the Solitario Canyon Fault from a factor of 10 to 1,000 its across-the-fault permeability yielded a 3% increase in specific discharge across the 5-km boundary to 0.37 m/yr. Weighted head residuals, however, actually decreased by 2 % to 0.80 m (non-weighted residuals increased by 1% to 24.67 m). This indicates that different conceptualizations for anisotropy of the Solitario Canyon Fault do not impact water levels, but can impact specific discharge to some degree.

6.6.4 Water Table Rise

6.6.4.1 Water Table Rise below Repository

In addition to modeling SZ flow under contemporary conditions, it is also necessary to consider conditions as the climate changes in the future. A higher water table is expected in the Yucca Mountain region for future wetter climatic conditions. A rise in the water table could impact radionuclide transport in the SZ, but it is handled in a simplified manner. A higher water table has clear impacts on radionuclide transport in the UZ by shortening the transport distance between the repository and the water table. SZ modeling analyses considered in this report indicate that a rise in the water table will cause some of the flow paths from below the repository to the accessible environment to be in units with lower values of permeability than the ones saturated by the present-day water-table conditions.

Several independent lines of evidence are available for estimating the magnitude of rise in the water table below the repository at Yucca Mountain under previous glacial-transition climatic conditions (Forester et al. 1999 [DIRS 109425], pp. 56 and 57). Mineralogic alteration (zeolitization and tridymite distribution) in the UZ at Yucca Mountain shows no evidence that the water table has risen more than 60 m (200 ft) above its present position in the geologic past (Levy 1991 [DIRS 100053], p. 477). Analyses of $^{87}Sr/^{86}Sr$ ratios in calcite veins of the

unsaturated and saturated zones at Yucca Mountain indicated previous water-table elevations of 85 m (279 ft) higher than present (Marshall et al. 1993 [DIRS 101142], p. 1,948). Recently completed wells at paleospring discharge locations near the southern end of Crater Flat, which are inactive sites of Pleistocene spring discharge, revealed shallower-than-expected groundwater with depths of only 17 to 30 m (56 to 100 ft) to the water table (Paces and Whelan 2001 [DIRS 154724]; BSC 2004 [DIRS 168473], Table I-1). These findings indicate that the water-table rise during the Pleistocene at these paleospring locations could not have been more than about 30 m (100 feet) due to formation of discharge locations. The results of the mineralogical and geochemical studies showing a maximum water-table rise of up to 85 m reflect evolution of past climates for the last 1 million years, which included the effects of glacial climates. The maximum water-table rise under monsoon and glacial-transition climates is, therefore, expected to be less than 85 m because the monsoon and glacial-transition climates are warmer and dryer than the glacial climate (Sharpe 2003 [DIRS 161591]).

Interpretation of the water levels in wells at the southern end of Crater Flat, in relation to water-table rise, is complicated by several factors. The paleospring discharge locations at the southern end of Crater Flat are not along the flow path from Yucca Mountain. Also, a higher groundwater flow rate (increased hydraulic gradient) is expected under future wetter climatic conditions. However, the principles of hydrogeology specify that a uniform rise in the water table could only occur if the increased saturated thickness (and its effect on transmissivity) accommodates the additional groundwater flow through the aquifer. For the geology within the model domain, an increase in gradient to accommodate the increase in flow will results in a nonuniform water-table rise with higher increases upgradient of flow. A higher groundwater flow rate implies a higher hydraulic gradient, a larger transmissivity, or both along any given flow line. Thus, the water table at upgradient locations would be expected to rise more than the water table at downgradient locations, resulting in a nonuniform rise in the water table across the flow system.

Two-dimensional groundwater flow modeling of the response to doubling mean annual precipitation indicated a maximum water table rise of 130 m (430 ft) in the vicinity of Yucca Mountain (Czarnecki 1985 [DIRS 160149]). This result is potentially overestimated because the analysis by Czarnecki (1985 [DIRS 160149]) was limited to two dimensions. In addition, average precipitation under monsoon and glacial-transition climates is less than twice the present-day value in the Yucca Mountain area, and the percolation flux resulting from the precipitation increase was also conservatively modeled (Czarnecki 1985 [DIRS 160149]). More recent groundwater flow modeling of the regional flow system under paleoclimate conditions (the DVRFS) simulated water levels of 60 to 150 m (200 to 490 ft) higher than present below Yucca Mountain (D'Agnese et al. 1999 [DIRS 120425], p. 2). Coarse resolution of the numerical grid in this model is believed to have resulted in potential overestimation of water table rise (150 m).

The uncertainty in water-table rise has been evaluated by considering these multiple lines of evidence and new geochemical data using a multidisciplinary workshop approach, as documented by *Total System Performance Assessment Model/Analysis for the License Application* (SNL 2007 [DIRS 178871]). Given that these various sources of information on water-table rise result in significant variations in the estimate and that none of the sources is clearly definitive, a subjective approach to quantifying uncertainty was used and a consensus

uncertainty distribution was derived. The median value from the uncertainty distribution for the average water-table rise beneath the repository from that assessment is 50 m (SNL 2007 [DIRS 178871]). This 50-m increase in the water table elevation at the repository is consequently used in the adaptation of the SZ site-scale flow model described below.

6.6.4.2 Incorporation of Water-Table Rise into the SZ Flow and Transport Models

The effects of climate change on radionuclide transport simulations in the SZ are incorporated into the TSPA analyses by scaling the simulated SZ breakthrough curves by a factor representative of the alternative climate state (SNL 2007 [DIRS 178871]). The scaling factor used in this approach is the ratio of average SZ groundwater flux under the future climatic conditions to the flux under present conditions. This approach approximates the impacts of future, wetter climatic conditions in which the SZ groundwater flux will be greater. However, this approach implicitly models the same flow path for radionuclide transport through the SZ under wetter climatic conditions of the future. In reality, significant rise in the water table due to climatic changes would result in different flow paths through the SZ system, including the potential for encountering different hydrogeologic units by radionuclides during transport.

The objective of this modeling task is to adapt the SZ site-scale flow model to include the effects of estimated water-table rise. The SZ site-scale transport model is used in a separate report to compare the results of particle-tracking simulations using this adapted model to the simple flux scaling approach used in TSPA analyses. Flow modeling for this task is presented in this report and the transport simulations are presented in *Site-Scale Saturated Zone Transport* (SNL 2007 [DIRS 177392], Appendix E). The flux-scaling approach to simulation of climate change results in more rapid radionuclide transport in the SZ, relative to the more realistic situation in which water-table rise is included in the modeling (SNL 2007 [DIRS 178871]). The purpose of this section is to provide an adapted version of the SZ site-scale flow model for incorporation in the SZ site-scale transport model.

6.6.4.2.1 Estimating Water Table Rise from Climate Change

Rise in the water table during wetter glacial transition conditions at Yucca Mountain is a complex function of greater recharge to the SZ and changes to the amount and spatial distribution of lateral fluxes from the regional SZ system. Although the analyses discussed in this report are for glacial-transition climatic conditions, they are a reasonable approximation of changes to the SZ for time periods beyond 10,000 years in the future. The conclusions are thus applicable to TSPA analyses that extend to peak simulated dose. Simulations of groundwater flow under wetter climatic conditions with the SZ regional-scale flow model (D'Agnese et al. 1999 [DIRS 120425]) indicate that groundwater flow paths from below Yucca Mountain do not significantly change under glacial climatic conditions. These simulations also show that groundwater surface discharge from the SZ for the wetter glacial climatic conditions would not occur along the flow path from Yucca Mountain at any location closer than the regulatory boundary of the accessible environment, approximately 18 km south of the repository.

The estimated elevation of the water table under wetter, glacial-transition conditions within the domain of the SZ site-scale flow model was calculated in an Excel spreadsheet by assuming linear increases in the elevation of the water table. This estimated increase in water level was

calculated by assuming a 20-m rise at locations with a present-day water table elevation of 700 m, a 50-m rise at locations with a present-day water table elevation of 740 m, and a 100-m rise at locations with a present-day water table elevation of 1,000 m. The estimated higher water table for glacial-transition climatic conditions at other locations was calculated by linear interpolation or extrapolation. In addition, the rise in the water table was limited by the topographic surface.

This approach results in a water-table rise of approximately 50 m in the area beneath the proposed repository, which is the median value from the uncertainty distribution derived for this parameter (SNL 2007 [DIRS 178871]). The approach also approximately preserves the direction of the horizontal hydraulic gradient at the water table, which is consistent with the results of the SZ regional-scale flow model with regard to the simulated flow paths from beneath the repository under wetter climatic conditions (D'Agnese et al. 1999 [DIRS 120425]).

The estimated elevation of the water table under wetter, glacial-transition climatic conditions, as calculated with the approach described above, is shown in Figure 6-20. Note that the pattern of the contours for the water table is generally similar to the present water table (see Figure 6-4), with the exception of the area in Fortymile Canyon in the northern part of the model domain. The deflection of the water table contour in Fortymile Canyon corresponds to an area in which the water table rise has been limited by the topographic surface. There is little information upon which to base estimates of the water table configuration under future climatic conditions in the area to the north of Yucca Mountain in the SZ site-scale flow model domain. Regardless, the approach used to estimate water-table rise to the north of the repository has little impact on the simulated flow system down gradient of Yucca Mountain in the SZ site-scale flow model.

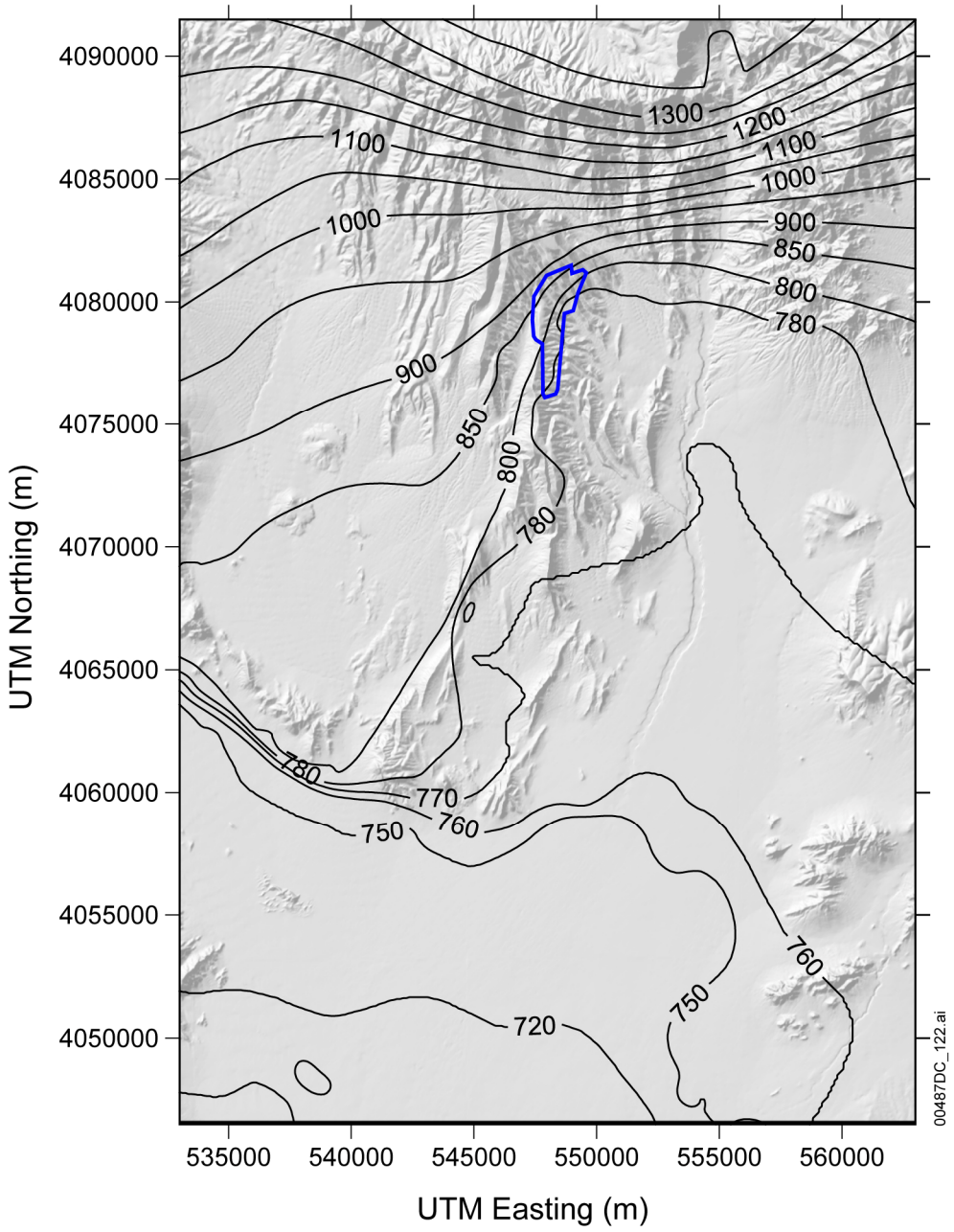

Sources: SNL 2007 [DIRS 179466] (repository outline); Output DTN: SN0702T0510106.006 (water table rise).

NOTE: Repository outline shown with a bold blue curve. For illustration purposes only.

UTM = Universal Transverse Mercator.

Figure 6-20. Estimated Water Table Elevations for Future Glacial-Transition Climatic Conditions

Figure 6-21 shows the estimated depth to the water table under wetter, glacial-transition climate conditions, as calculated by the approach described above. The areas in which the estimated water table is within 5 m of the topographic surface are shaded blue. The larger of these areas in the southwestern part of the domain contains three distinct paleospring deposits located along U.S. Highway 95 and at the southern end of the Crater Flat. This shows consistency between the

estimated higher water table and the geologic features associated with Pleistocene spring discharge. The specific paleospring locations are probably controlled by structural features too small to be resolved with this model. Another site of shallow estimated groundwater shown in Figure 6-21 is Fortymile Canyon. Paleospring deposits are not observed in Fortymile Canyon, but it is reasonable to postulate that such deposits would not be preserved in this geomorphic location. It is also reasonable that the water table would rise to the extent that upper Fortymile Wash would become a perennial gaining stream in Fortymile Canyon under wetter climatic conditions. The areas of predicted shallow groundwater near and on the southern boundary of the model domain do not correspond to specifically identified paleodischarge locations, but paleospring deposits could have been buried by aggradation of alluvium in these locations.

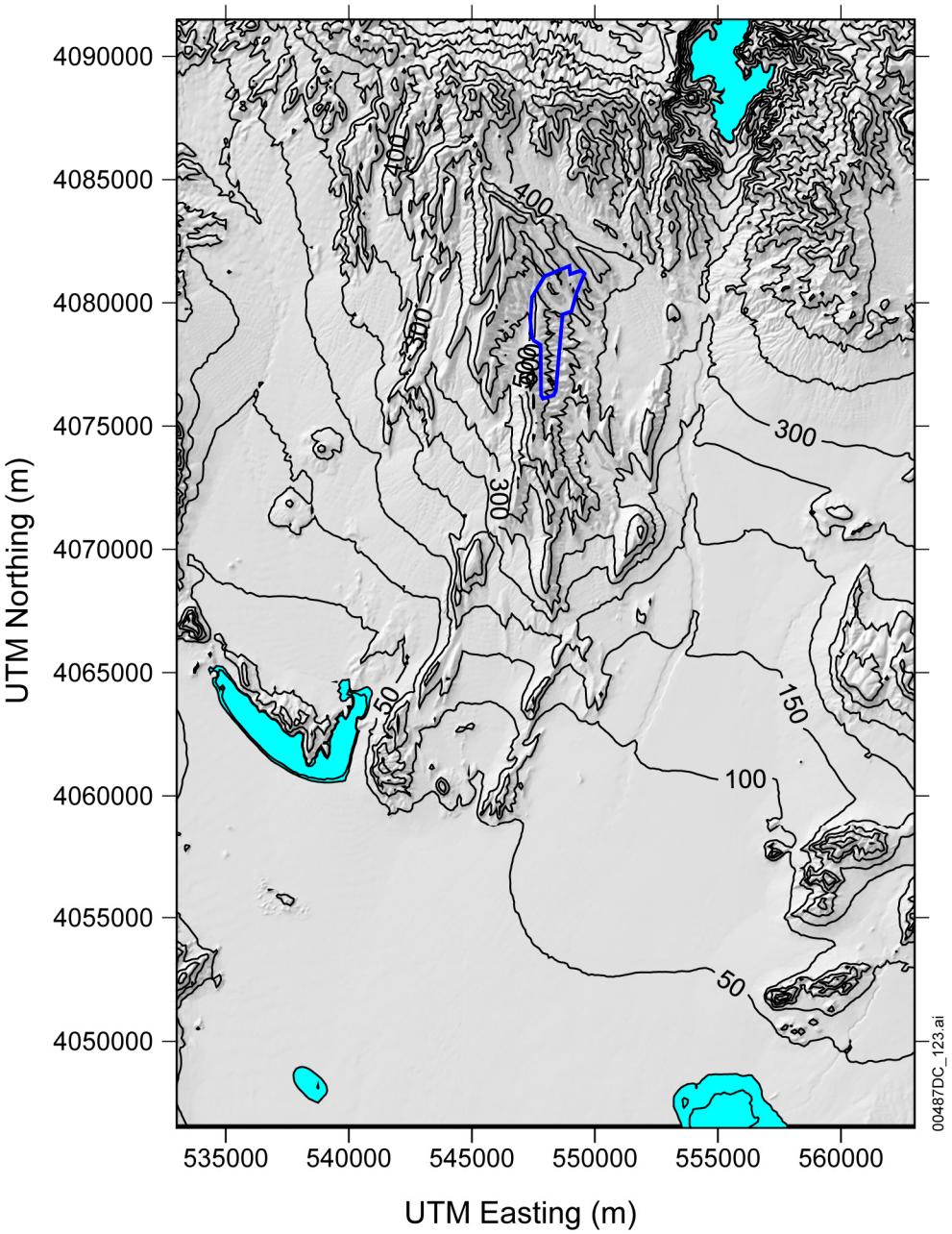

Sources: SNL 2007 [DIRS 179466] (repository outline); Output DTN: SN0702T0510106.006 (depth to water).

NOTE: Repository outline shown with a bold blue line. Areas with estimated depth to the water table of less than 5 m are shaded blue. For illustration purposes only.

UTM = Universal Transverse Mercator.

Figure 6-21. Estimated Depth to the Water Table for Future Glacial-Transition Climatic Conditions

Analyses of the impacts of climate change and water table rise on groundwater flow in the area near Yucca Mountain have been conducted using an independently developed site-scale flow model by Winterle (2003 [DIRS 178404], 2005 [DIRS 178405]). These modeling studies included increased values of specified head at the flow model boundaries, increased recharge,

and potential discharge of groundwater from springs activated by the higher water table. Winterle (2003 [DIRS 178404], 2005 [DIRS 178405]) concluded that neither the increase in the water-table elevation nor the discharge of groundwater from springs significantly affected the flow paths from beneath Yucca Mountain. Comparison of the predicted locations of shallow groundwater under glacial-transition climatic conditions (Figure 6-21) with the simulated locations of potential discharge locations (Winterle 2005 [DIRS 178405], Figure 3) indicates similar results. Both approaches indicate similar patterns of potential discharge at the southern end of Crater Flat and in two areas near the southern boundary of the SZ site-scale flow model domain. However, this report's analysis results predict potential discharge in Fortymile Canyon, wheras the Winterle (2005 [DIRS 178405], Figure 3) results apparently do not.

In summary, a reasonable estimate of the water table elevation under wetter, glacial-transition conditions is developed for the SZ site-scale flow model domain. The estimated rise in the water table is consistent with the conclusion that the general direction of flow paths from beneath the proposed repository would not change for wetter climatic conditions, although differences in hydrogeologic units occurring at the water table below the repository would have an impact on local flowpaths. In addition, the pattern of the estimated rise in the water table is generally consistent with the locations of paleospring deposits within the domain.

6.6.4.2.2 Water Table Rise in the SZ Site-Scale Flow Model

The SZ site-scale flow model is adapted to the higher estimated water table for glacial-transition climatic conditions by creating a new grid with an upper surface corresponding to the higher water table. The lateral and bottom boundary locations remain the same in this adaptation of the model. The spatial distributions of hydrogeologic units at the water table in the flow model under present-day conditions and in the adapted model with the higher estimated water table are shown in Figures 6-22 and 6-23, respectively.

Comparison of Figures 6-22 and 6-23 indicates potentially significant differences in the hydrogeologic units present in the SZ below the repository and along the inferred flow path to the south and east of the repository at depths corresponding to the position of the water table at the different climatic conditions. The upper volcanic confining unit is more widely distributed at the water table below the repository under estimated future glacial-transition climatic conditions than it is under present-day conditions, particularly under the northern and eastern parts of the repository. Under estimated future conditions, to the south of the repository, the alluvium unit is present at the water table over a somewhat broader area compared to present-day conditions.

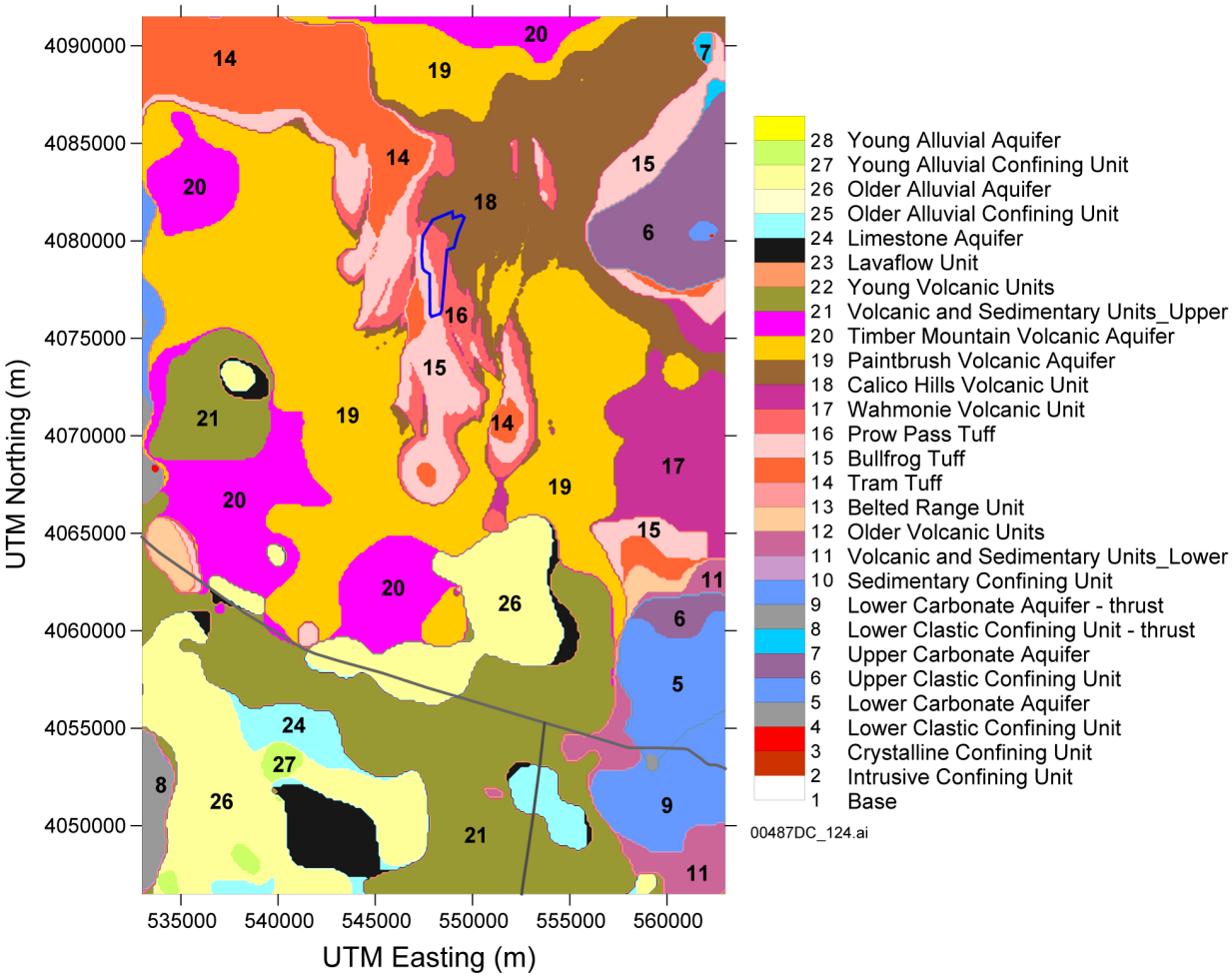

Source: SNL 2007 [DIRS 179466] (repository outline).

NOTE: Repository outline shown with a bold blue curve. For illustration purposes only.

UTM = Universal Transverse Mercator.

Figure 6-22. Hydrogeologic Framework Model Units at the Water Table for Present-Day Conditions

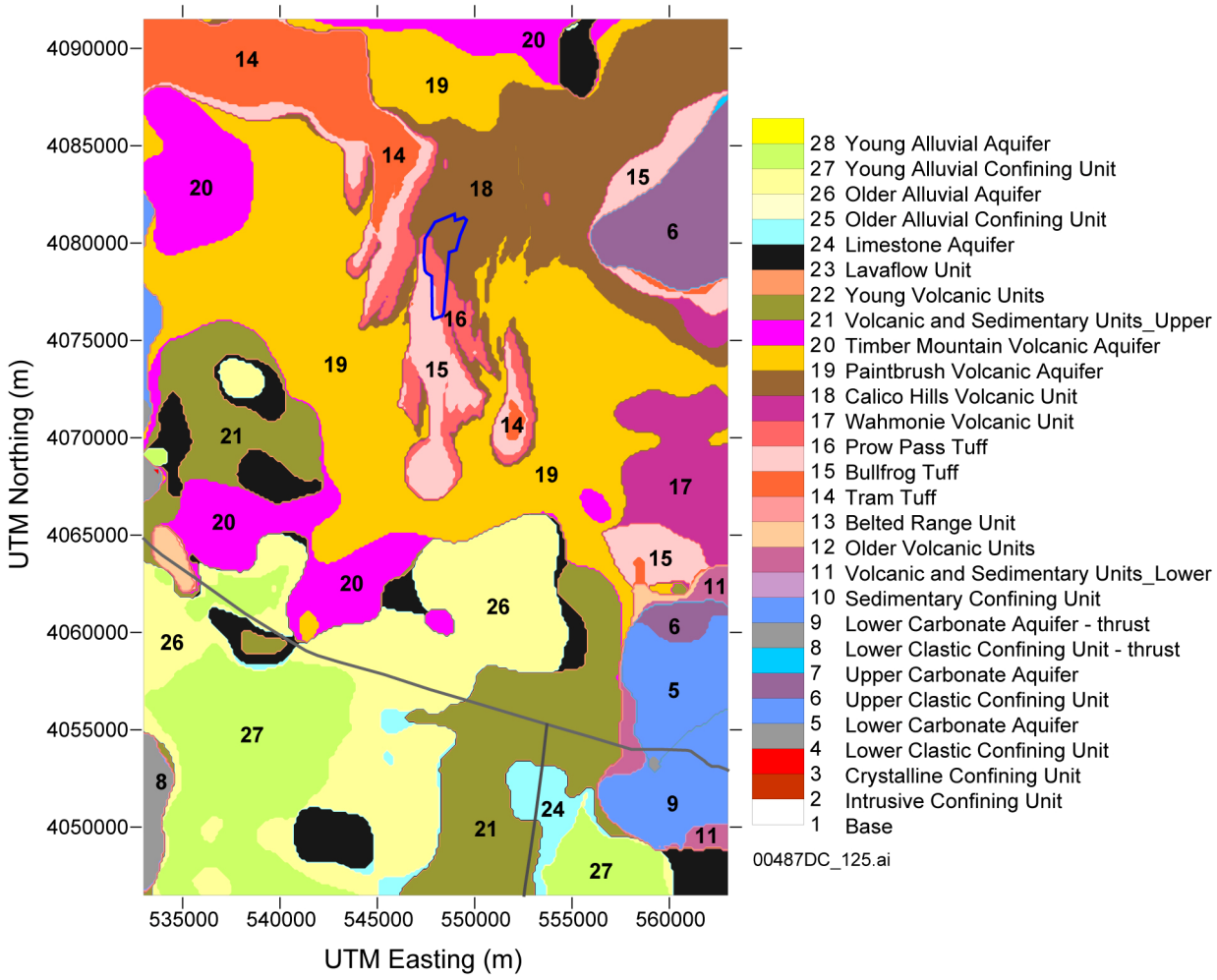

Source: SNL 2007 [DIRS 179466] (repository outline).

NOTE: Repository outline shown with a bold blue curve. For illustration purposes only.

UTM = Universal Transverse Mercator.

Figure 6-23. Hydrogeologic Framework Model Units at the Water Table for Estimated Future Glacial-Transition Climatic Conditions

Figure 6-24 illustrates the modeled potentiometric surface for the flow model using calibrated effective permeabilities subject to water-table rise. The specific discharge across the 5-km boundary was 1.26 m/yr after the water-table rise. The SZ site-scale transport simulations with the higher water table are considered in *Site-Scale Saturated Zone Transport* (SNL 2007 [DIRS 177392], Appendix E).

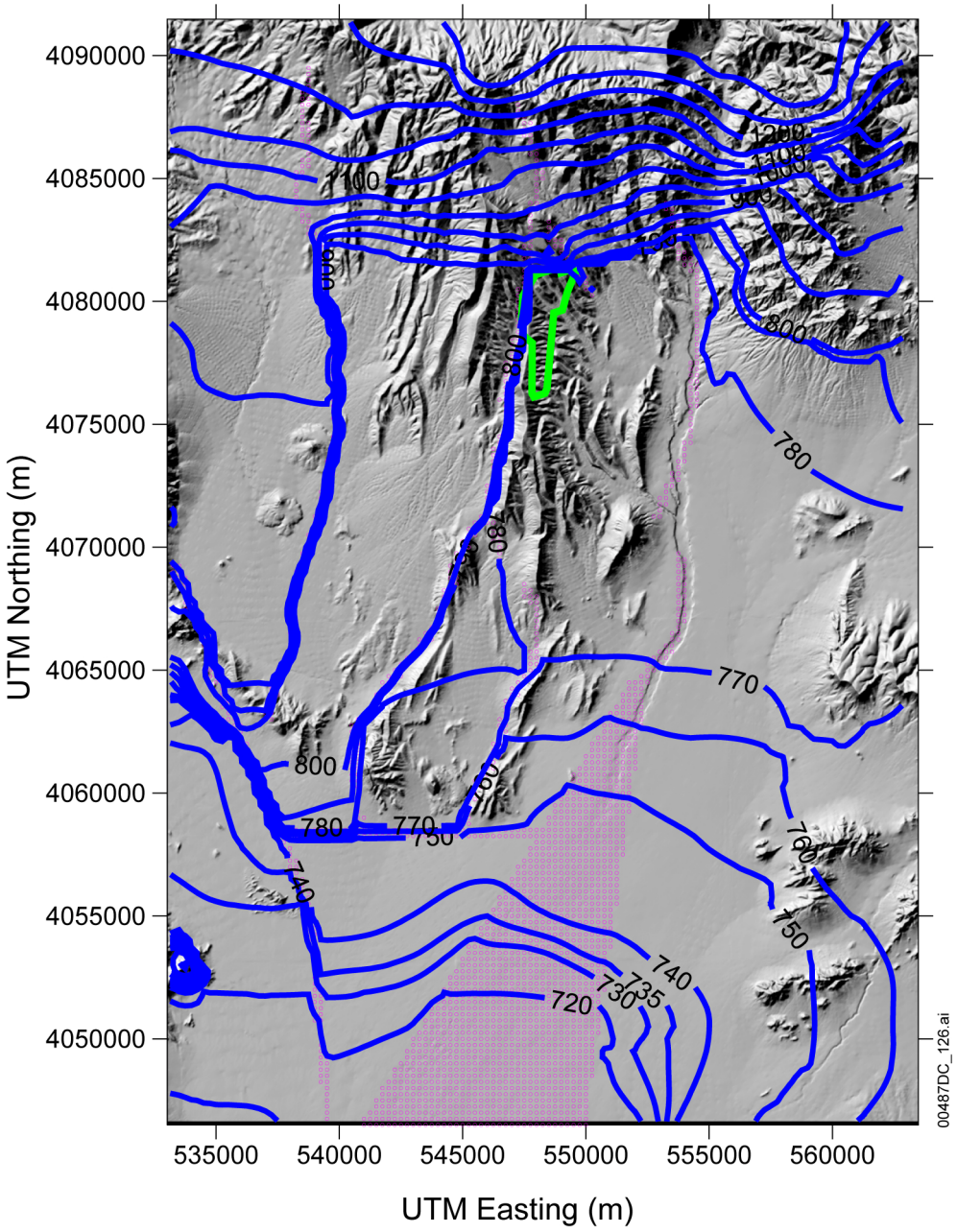

Source: SNL 2007 [DIRS 179466] (repository outline).

Output DTN: SN0702T0510106.006 (FEHM model of water-table rise).

NOTE: For illustration purposes only. The contours represent the modeled potentiometric surface. Altitude is in meters above mean sea level. Pink represents special geologic features (see Table 6-7 and Figure 6-12).

UTM = Universal Transverse Mercator.

Figure 6-24. Simulated Potentiometric Surface After a Rise in the Water-Table

6.7 UNCERTAINTY

Characterizing and understanding the flow through the saturated zone is important for assessing the overall containment strategy for safely sequestering radioactive materials at the Yucca Mountain repository. Uncertainty in flow modeling arises from a number of sources including, but not limited to, the conceptual model of the processes affecting groundwater flow, water–level measurements and simplifications of the model geometry, boundary conditions, hydrogeologic unit extent and depth, and the values of permeability assigned to hydrogeologic units. This section discusses and attempts to quantify uncertainties in the SZ site-scale flow model because all uncertainty contributes to inaccuracy in system representation and response (uncertainty in model predictions). Such uncertainty is an inescapable aspect of geologic modeling. In addition to the discussion in this section, parameter uncertainty is addressed in the model abstraction document (SNL 2007 [DIRS 177390], Section 6.5) and a thorough discussion of uncertainty analysis is given in Appendices H and I. *Saturated Zone Flow and Transport Model Abstraction* (SNL 2007 [DIRS 177390], Sections 6.5.2.1 and 6.5.2.10) includes additional quantitative analysis on horizontal anisotropy in permeability and groundwater specific discharge. *Saturated Zone In-Situ Testing* (SNL 2007 [DIRS 177394]) addresses the uncertainty related to the spatial distribution of the observation wells. Overall, it is understood that model predictions are always uncertain, thus it is important to minimize and quantify this uncertainty. It should be noted that the uses of PEST V11.1 (STN: 611582-11.1-00; [DIRS 179480]) and SPDIS (STN: 611598-00-00; [DIRS 180546]) are non-quality affecting analyses of the qualified results produced by PEST V5.5 (STN: 10289-5.5-00; [DIRS 161564]) and that they in no way change the conclusions of this report. Instead, this analysis sheds light on some of the details going on behind the scenes during the calibration process (e.g., differentiating null from solution space errors and evaluating data worth and parameter importance).

Estimating uncertainty in a modeled process is a wide ranging field of active research spanning many disciplines including hydrologic modeling, surface water flow and transport, medical imaging, geophysics, etc. A fundamental aspect of geologic modeling is the calibration phase where model parameters (in this case permeabilities) are adjusted until the model's replication of historical field measurements is judged to be "reasonably good." It is then assumed that this constitutes sufficient justification to use the model to make predictions to be used in site management. For the SZ site-scale flow model developed here, PEST ([DIRS 161564], 2006 [DIRS 178612]) was used to minimize the objective function comprising a weighted sum of squares of water-level measurements and fluxes across the lateral model boundaries (minimize the differences between measured and modeled data). Additional information was also used to hand calibrate the model, namely gradients that indicate that flowpaths emanating from below the repository should travel in a southeasterly direction. Future efforts could explicitly include soft data (e.g., local specific discharge estimates from well tests or elicitation) in the PEST calibration process.

When performing an uncertainty assessment on model results, which are solely dependent upon the parameter values supplied to the model, it is important to recognize two fundamental types of uncertainty in a model: null space and solution space uncertainties (see Appendix H). Null space uncertainty is that which arises in a calibrated model prediction due to the necessary simplifications made during model development (e.g., using a predefined HFM, applying constant BCs, representing heterogeneity with a homogenized geologic unit, single porosity

model of a dual porosity medium, etc.). It represents the differences between real world predictions and their simulated equivalents arising from the inability of model parameters to represent the innate complexity of the real world. Solution space uncertainty is contained in a model parameter that arises from the fact that its estimation through calibration is based on noisy data (including that induced by the simplification process required when constructing a hydrologic model).

Regularization theory shows how parameters employed by a calibrated model must, of necessity, be "smoothed" or "blurred" versions of real-world hydraulic properties (Appendix H). Figure 6-25 is a conceptualization of how estimated modeled parameters are "contaminated" during the modeling process. The figure reflects how model (effective) parameters are the transformation of real world parameters through the current conceptual model of the system. This transformation yields estimates for the simplified parameter field, which is required for solution of the inverse problem (model calibration). This indicates that it should not be presumed that estimated parameters always match real world parameters except in an average sense over large areas (and possibly with an averaging kernel that crosses parameter boundaries). The "resolution matrix" presented conceptually in Figure 6-25 encapsulates the details of the conceptual model development (averaging process during parameterization). The more diagonally dominant the resolution matrix, the closer the model parameters approximate the real world hydraulic properties throughout the model domain. Off-diagonal elements indicate spatial averaging or "contamination" of model parameters induced by necessary simplification and homogenization required for calibration of the model.

$$\begin{bmatrix} \hat{k}_1 \\ \vdots \\ M \\ O \\ D \\ E \\ L \\ \\ P \\ A \\ R \\ A \\ M \\ E \\ T \\ E \\ R \\ S \\ \vdots \\ \hat{k}_n \end{bmatrix} = \begin{bmatrix} 0.74 & \cdots & p & a & r & a & m & e & t & e & r & \cdots & \cdots & \cdots & \cdots & \cdots & \cdots & \cdots & \cdots & h \\ \vdots & 0.91 & \cdots & \cdots & d & i & l & u & t & i & o & n & \cdots & \cdots & \cdots & \cdots & \cdots & \cdots & \cdots & o \\ a & \vdots & 0.84 & \cdots & \cdots & \cdots & \cdots & d & u & e & \cdots & \cdots & \cdots & \cdots & \cdots & \cdots & \cdots & \cdots & \cdots & m \\ s & \vdots & \mathrm{r} & \mathrm{e} & \mathrm{a} & \mathrm{l} & \cdots & \cdots & \cdots & t & o & \cdots & \cdots & \cdots & \cdots & \cdots & \cdots & \cdots & \cdots & o \\ s & p & \vdots & \vdots & 0.69 & s & i & m & p & l & i & f & i & c & a & t & i & o & n & g \\ y & a & \vdots & \mathrm{w} & \mathrm{o} & \mathrm{r} & \mathrm{l} & \mathrm{d} & \cdots & \cdots & a & n & d & \cdots & \cdots & \cdots & \cdots & \cdots & \cdots & e \\ m & r & c & \vdots & \vdots & \vdots & 0.91 & \cdots & \cdots & \cdots & \cdots & \cdots & \cdots & \cdots & m & o & d & e & l & n \\ e & a & o & \vdots & \vdots & \vdots & \mathrm{a} & \mathrm{s} & \cdots & \cdots & \cdots & \cdots & \cdots & \cdots & \cdots & \cdots & \cdots & \cdots & \cdots & i \\ t & m & n & t & \vdots & \vdots & \vdots & \vdots & 0.88 & \cdots & \cdots & \cdots & \cdots & \cdots & \cdots & \cdots & \cdots & \cdots & \cdots & z \\ r & e & t & h & \vdots & \mathrm{e} & \mathrm{s} & \mathrm{t} & \mathrm{i} & \mathrm{m} & \mathrm{a} & \mathrm{t} & \mathrm{e} & \mathrm{d} & \cdots & \cdots & \cdots & \cdots & \cdots & a \\ i & t & a & r & c & \vdots & \vdots & \vdots & \vdots & \vdots & 0.79 & \cdots & \cdots & \cdots & \cdots & \cdots & \cdots & \cdots & \cdots & t \\ c & e & m & o & o & \vdots & \vdots & \vdots & \vdots & \vdots & \mathrm{b} & \mathrm{y} & \cdots & \cdots & \cdots & \cdots & \cdots & \cdots & \cdots & i \\ \vdots & r & i & u & n & m & \vdots & \vdots & \vdots & \vdots & \vdots & \vdots & 0.66 & \cdots & \cdots & \cdots & \cdots & \cdots & \cdots & o \\ \vdots & \vdots & n & g & c & o & \vdots & \vdots & \vdots & \vdots & \vdots & \vdots & \mathrm{t} & \mathrm{h} & \mathrm{e} & \cdots & \cdots & \cdots & \cdots & n \\ \vdots & \vdots & a & h & e & d & \vdots & \vdots & \vdots & \vdots & \vdots & \vdots & \vdots & \vdots & 0.98 & \cdots & \cdots & \cdots & \cdots & \cdots \\ \vdots & \vdots & t & \vdots & p & e & \vdots & \vdots & \vdots & \vdots & \vdots & \vdots & \vdots & \mathrm{m} & \mathrm{o} & \mathrm{d} & \mathrm{e} & \mathrm{l} & \cdots & \cdots \\ \vdots & \vdots & i & \vdots & t & l & \vdots & \vdots & \vdots & \vdots & \vdots & \vdots & \vdots & \vdots & \vdots & \vdots & 0.32 & \cdots & \cdots & \cdots \\ \vdots & \vdots & o & \vdots & u & \vdots & \vdots & \vdots & \vdots & \vdots & \vdots & \vdots & \vdots & \vdots & \vdots & \vdots & \vdots & 0.75 & \cdots & \cdots \\ \vdots & \vdots & n & \vdots & a & \vdots & \vdots & \vdots & \vdots & \vdots & \vdots & \vdots & \vdots & \vdots & \vdots & \vdots & \vdots & \vdots & 0.87 & \cdots \\ \vdots & \vdots & \vdots & \vdots & l & \vdots & d & e & v & e & l & o & p & m & e & n & t & \vdots & \vdots & 0.93 \end{bmatrix} \begin{bmatrix} k_1 \\ k_2 \\ \vdots \\ R \\ E \\ A \\ L \\ \\ P \\ A \\ R \\ A \\ M \\ E \\ T \\ E \\ R \\ S \\ \vdots \\ k_n \end{bmatrix}$$

NOTES: Specifically, real-world parameters are averaged during the parameter estimation process required for model calibration. A better resolution matrix will have smaller off-diagonal elements (increased diagonal dominance) yielding model parameters that are closer approximations to the real parameters. Unfortunately, this can only occur where real-world heterogeneity is small and calibration data are ubiquitous and noise-free.

Figure 6-25. Conceptual Representation of the Resolution Matrix Illustrating How Estimated Model Parameters Are "Contaminated" During the Modeling Process

The following description distinguishes null space uncertainty from solution space uncertainty with regard to its impact on model predictions of specific discharge 5 km from the proposed repository. Despite the fact that specific discharge 5 km from the repository is only a surrogate for the flow fields passed on to TSPA, it was selected as the predictive metric for this analysis because it reflects changes in the flow field . Solution space uncertainty is a product of a noisy data set (uncertainty in calibration data) plus model imperfections (structural noise introduced through the use of effective parameters). Solution space uncertainty may be reduced through the calibration process, but null space error is irreducible given an established conceptual model and calibrating data set. Null space uncertainty can only be reduced by collecting additional data that contain information relevant to the currently inestimable combination of parameters (null space). Null space exists because we acknowledge that the model complexity (due to, for example, the constraints of HFM2006 that assign uniform permeability to an individual hydrogeologic unit) falls short of what can be uniquely estimated given the current calibration data set. That is, it is a direct consequence of the limited descriptive capacity for a data set to reproduce modeled hydraulic properties (i.e., parameters, including spatial variability) upon which a prediction depends. This is especially apparent in our inability to represent hydraulic property detail. If the model prediction depends upon this detail, this prediction is prone to increased uncertainty. Null space is the space spanning parameter set combinations that can be added to the calibrated parameter set without affecting calibration (a null space matrix is orthogonal to parameter space and thus there exist certain combinations of parameters that yield an equally calibrated model but

significantly different predicted model metrics, like specific discharge). Thus, null space uncertainty is the uncertainty in the prediction from a calibrated model due to the inability of the calibrating data set to inform those parameters that contribute to the model output metric (in this case, prediction of specific discharge). Recent advances in uncertainty assessment facilitate quantification of the null space error despite the inability to reduce it (given a specified, calibrated model and data set).

6.7.1 Uncertainty in Specific Discharge

In previous flow and transport and abstraction models of the SZ, the specific discharge was varied from one-tenth of its nominal value to ten times its nominal value in performance assessment calculations (BSC 2001 [DIRS 157132], Section 6.2.5). Based on recent calibration experience and the evaluation of permeability data from Yucca Mountain and other sites, the range was reduced to 1/8.93 times its nominal value to 8.93 times the nominal value (SNL 2007 [DIRS 177390], Section 6.5). The nominal value is obtained from a predictive run of the calibrated SZ site-scale flow model (Section 6.5). It should be noted that because the numerical model is linear, the calibration of the model can be preserved by scaling the fluxes, recharge, and permeabilities by exactly the same ratio. A new uncertainty analysis procedure is available in recent releases of the PEST software. Although PEST V11.1 is not qualified, it is still extremely useful in analyzing and describing the results from qualified codes. A general introduction and discussion of the latest techniques in uncertainty and sensitivity analyses is presented in Appendices H and I.

The PEST V11.1 (STN: 611582-11.1-00; [DIRS 179480]) PREDVAR suite of codes (Watermark Computing 2006 [DIRS 178613]) was used to analyze FEHM's predictive uncertainty for specific discharge. First, null space and solution space uncertainties are quantified. This analysis, if done a priori, can help to determine if calibrating the conceptual model to the existing dataset will significantly reduce uncertainty in the selected predictive model metric. The effect of calibrating each model parameter (or each set of parameters when considering the permeability multipliers for the altered northern region, which were lumped) in reducing uncertainty in specific discharge 5 km from the repository is presented in Figure 6-26. Red bars are normalized contributions to uncertainty (they have unit sum) in specific discharge from uncalibrated parameters and blue bars are the same contribution from calibrated parameters. This figure can be interpreted as the answer to the following question: Assuming perfect knowledge of a parameter, how do the rest contribute to reduction in uncertainty of a prediction? Specifically, the contribution of calibrating each parameter with respect to reducing uncertainty in specific discharge is illustrated. There is seemingly little value gained in reducing uncertainty in specific discharge across the 5-km boundary through the calibration process. The uncertainty for specific discharge decreased 56% after calibration. It is not surprising to see such a small reduction in predictive uncertainty for specific discharge because calibration data did not include an estimate for specific discharge. If a specific discharge measurement was explicitly included in the automatic calibration process, a greater reduction in uncertainty would be expected. In these figures, a parameter's "contribution" to uncertainty is assessed through repeating the predictive uncertainty analysis under an assumption of perfect knowledge of that parameter type and measuring the decrease in predictive error thereby incurred. That is, each parameter is sequentially assigned it calibrated value with zero error bars and the resulting impact on decreased uncertainty in a prediction is assessed. In some circumstances,

post-calibration contribution to predictive uncertainty for a parameter type can exceed its pre-calibration contribution (significant examples include CFTA, CHVU, H95Z, and WASH). This is a reflection of the fact that perfect knowledge of one parameter (zero error bars applied to an estimated parameter) may allow better estimates to be made of another parameter to which it is highly correlated. Thus, to the extent that the prediction depends on the second parameter type, the advantages of assumed perfect knowledge of the first parameter are thereby amplified. Without a detailed analysis beyond the scope of this report, it is difficult to ascertain how hand calibrations contribute to a reduction in predictive uncertainty in specific discharge. Not surprisingly, fault permeabilities dominate specific discharge uncertainty because they have first-order impacts on flow magnitudes and directions.

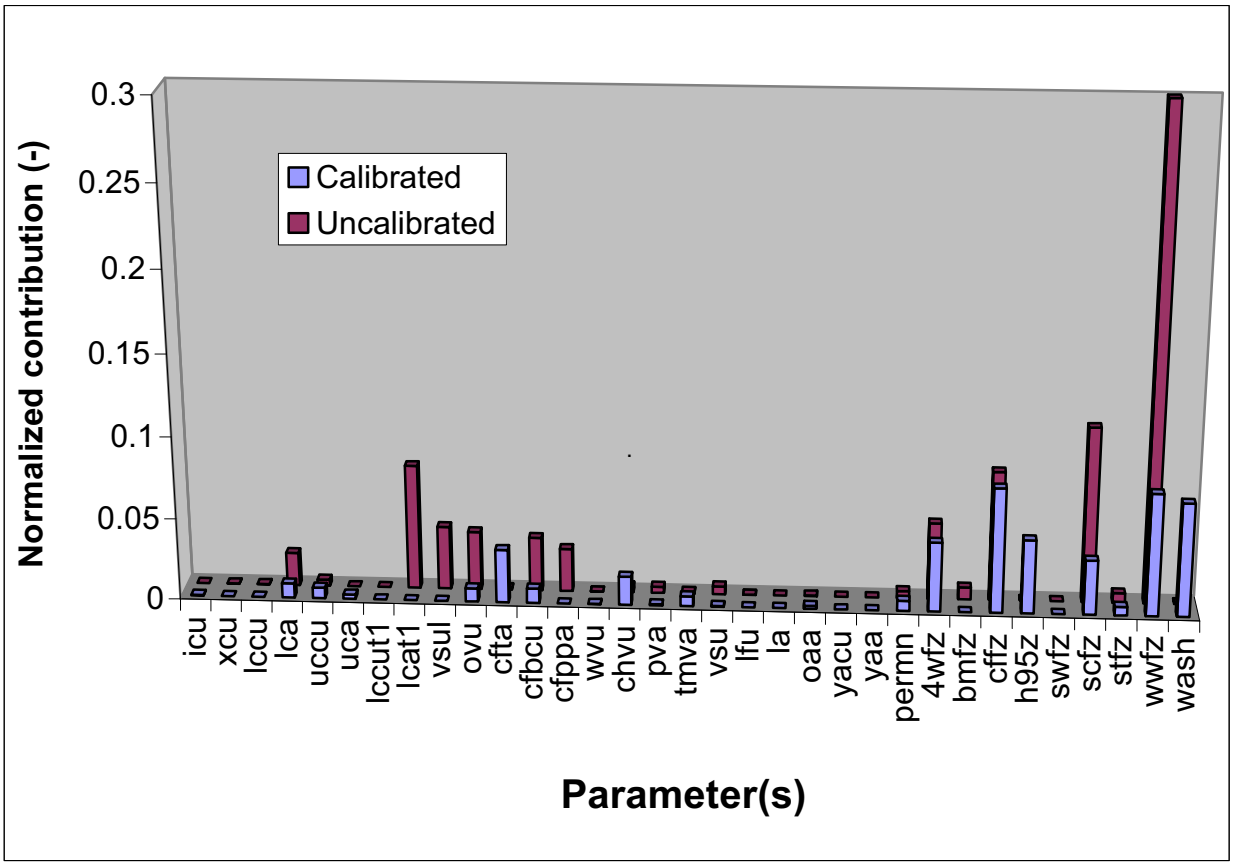

Source: Output DTN: SN0705T0510106.009.

NOTE: Parameter names are listed and defined in Table 6-9, "permn" comprises all permeability multipliers for the altered northern region and the Crater Flat zone.

Figure 6-26. Uncalibrated and Calibrated Model Parameter Impact on Normalized Uncertainty in Specific Discharge

The second sort of analysis that can be performed with PREDVAR is an analysis of the worth of existing observations or groups of observations as related to reducing model predictive uncertainty for specific discharge. This information can also be used to assess the worth of acquiring additional data, something truly valuable to site characterization decision making. In this analysis, the inclusion of a hypothetical observation of specific discharge (SPD) allowed an

analysis of its potential worth to the calibration process. Figure 6-27 shows the relative worth of groups of observations for reducing specific discharge uncertainty. Not surprisingly, observation groups NYE COUNTY, CRATER FLAT, and FLUX are important observations for reducing predictive uncertainty in specific discharge. FLUX is important because it directly impacts overall flows through the model and should therefore be important to specific discharges throughout the model domain. Head observations in the altered northern region (HIGH HEAD), along the inferred flow path (PATH), and those considered perched (PERCHED) are of lesser importance in reducing uncertainty is specific discharge.

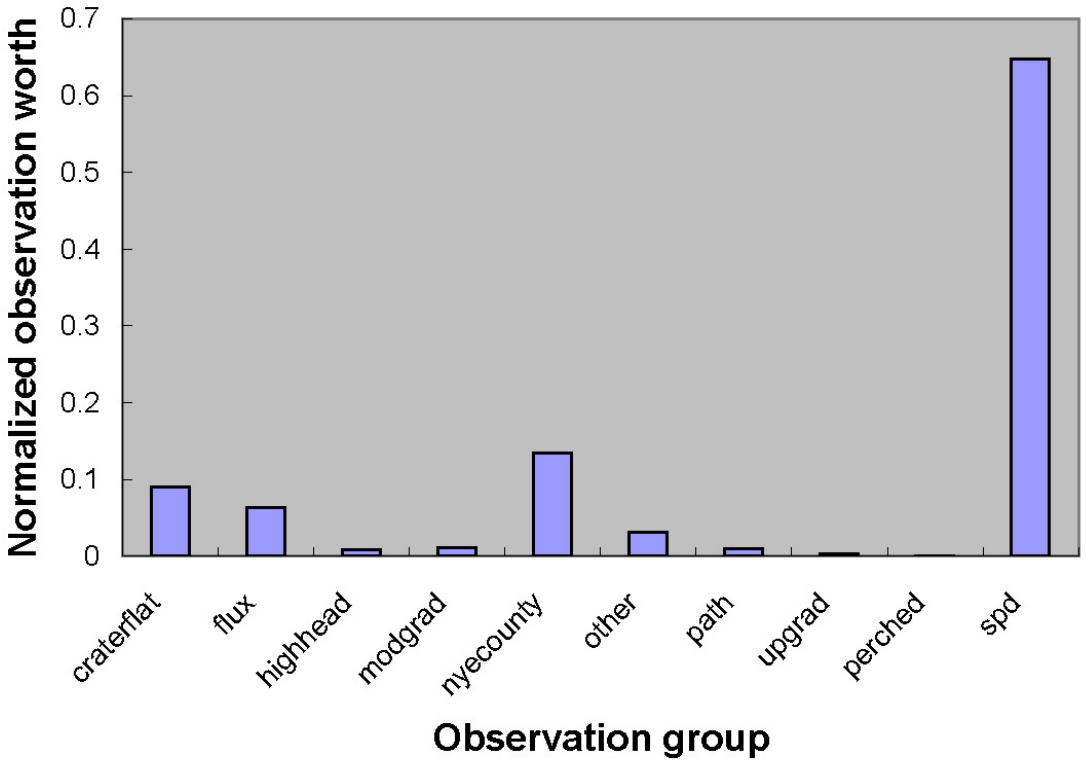

Source: Output DTN: SN0705T0510106.009.

NOTE: Observation groups are listed and defined in Table 6-9, "flux" are the boundary flux target observations and "spd" Is a hypothetical specific discharge observation that could be used in calibration.

Figure 6-27. Value of Observation Group to Reducing Uncertainty in Specific Discharge

6.7.2 Nonlinear Analysis

A methodology for nonlinear analysis of predictive error was applied to the Yucca Mountain model. Its theoretical basis is described in Appendix I. Applying the nonlinear analysis to the specific discharge prediction made by the SZ flow model yielded a maximum of 1.60 m/yr across the 5-km boundary (less than a factor of three times the maximum value of 0.66 m/yr). The nonlinear analysis is undertaken such that model calibration is maintained and only the null space is modified. By changing combinations of parameters that make no impact on the calibration objective function (weighted RMSE between modeled and measured head data and

boundary fluxes), the specific discharge was maximized to a value of 1.60 m/yr (Output DTN: SN0705T0510106.009). This indicates that even a model maintaining calibration can have significant "wiggle room" in its predictions. Note also that this maximization process was undertaken with the specific intent of seeing just how high the specific discharge could go for a nominally calibrated model. The chances for the exact combination of (null space) parameters required to make this happen in real life is low and this maximized specific discharge therefore represents a reasonable upper bound for this calibrated model. Furthermore, visualization of the flow field arising from this combination of permeabilities yielded an unrealistic scenario where flow exited the eastern boundary of the model.

6.7.3 Discussion of the Effect of Hydrogeologic Contact Uncertainty on Specific Discharge

The HFM conceptual model for the SZ site-scale flow model was created from a variety of field data and exists in electronic form as Earthvision surfaces (SNL 2007 [DIRS 174109]). There is uncertainty in the spatial positions of these surfaces primarily due to lack of data. These surfaces were used to generate the finite-element mesh such that each element is assigned those hydrogeologic properties found at the center of the element as discussed in Section 6.4.3.1. There is interest in how uncertainties in the representation of hydrogeologic-unit horizontal locations affect flux or specific discharge calculations. Due to the coarseness of the finite-element mesh, some horizontal uncertainty in the HFM can be entertained. As long as the horizontal spatial ambiguity in the location of hydrogeologic contacts is less than 125 m (one-half the grid block dimension), there is essentially zero impact on model specific discharge or flux calculations.

Because flow leaving the repository area is confined to a few of the most permeable units, the vertical dimension deserves special consideration. From the SZ site-scale flow model, it is known that the fluid leaves the repository area through the Crater Flat Tuffs and migrates to alluvial units. The flow paths in areal and vertical views are reproduced in Figure 6-17. Note that the vertical thickness of the flowing zone varies between 25 and 400 m, and the elevation changes from 400 to 700 m above sea level. From Table 6-4, the spacing in this part of the finite element mesh varies from 10 to 50 m. Consider, for example, that the uncertainty in the vertical location of a geologic contact 50 m in the portion of the model where the flow path is 400 m thick. Changing a single element's hydrogeologic designation, either to or from one unit to another could not result in a change to the average local specific discharge by more than a factor of 50/400 (13%). This is well within the overall specific discharge uncertainty range (Section 6.7.1). The vertically thin flow path south of UTM Northing coordinates 4,065,000 m (Figure 6-17) results in a greater impact from geologic uncertainty. Here the fluid flow is vertically constrained to about 25 m. If the bottom contact of the local hydrogeologic unit were to change by 10 m (the thickness of a single layer), this could result in a change to the average specific discharge in that area of up to 40%. Integrated specific discharge calculations will be affected to a lesser degree. A study of the impacts of hydrogeologic contact location uncertainty reveals:

- Sensitivity to uncertainty in the hydrogeologic contact surfaces in the horizontal directions is much less than in the vertical direction due to the averaging effect of 250-m grid block spacing

- The change in specific discharge due to the 50-m uncertainty in the vertical hydrogeologic surface can produce up to a 13% change in the local specific discharge near the repository and in the alluvial flow regions

- 10-m uncertainty in the vertical hydrogeologic surface can produce up to a 40% change in the local specific discharge in the transitional zone (south of UTM Northing 4,065,000 m).

Because of the averaging effect across elements in the integrated specific-discharge calculations (0 to 18 km), a 50% regional change in a relatively small portion of the 0- to 18-km compliance boundary affects model results only moderately. The range of uncertainty considered for specific discharge in the SZ flow and transport abstractions model is significantly greater than the uncertainty in the HFM (SNL 2007 [DIRS 174109], Section 6.4.3).

6.7.4 Site Data

In the 18-km compliance region (green line on Figure 6-17), performance assessment calculations are also strongly influenced by travel of fluid in the alluvial aquifer. Estimates of groundwater specific discharge in the SZ have been obtained from field-testing at the ATC (SNL 2007 [DIRS 177394], Section 6.4.5). The ATC is approximately located at the boundary of the accessible environment, as specified in regulations for the Yucca Mountain Project, 10 CFR 63.302 [DIRS 176544]. The location of the ATC is approximately 18 km from Yucca Mountain, and testing was performed in the alluvium aquifer. Estimates of groundwater specific discharge at the ATC range from 0.47 to 5.4 m/yr (DTN: LA0303PR831231.002 [DIRS 163561]; SNL 2007 [DIRS 177394], Table 6.5-6). From the calibrated SZ site-scale flow model, the specific discharge to the 18-km compliance boundary is 0.55 m/yr. This calculation integrates transport through all volcanic and alluvial units from introduction below the repository to the 18-km compliance boundary and its relatively low value can partially be attributed to slow flows through the volcanic units.

In addition to the information from the Expert Elicitation Panel (CRWMS M&O 1998 [DIRS 100353]) (related to specific discharge in the volcanics), other data are available for specific discharge in the alluvium (SNL 2007 [DIRS 177394], Tables 6.5-5 and 6.5-6). The measured specific discharge at the ATC spans a factor of 7.8 (i.e., 1.2 to 9.4 m/yr) while at NC-EWDP-22S the range was 11.5 (0.47 to 5.4 m/yr). There are no site data available for specific discharge in volcanic units, but the Expert Elicitation Panel (CRWMS M&O 1998 [DIRS 100353], p. 3-43) typically suggested larger ranges (approximately two orders of magnitude or more). A factor of 1/8.93 to 8.93 times the nominal value that combines volcanic and alluvial uncertainties with Bayesian updating is used as a multiplier for the specific discharge throughout the model domain in the latest performance assessment calculations (SNL 2007 [DIRS 177390], Section 6.5.2). It is worth noting that the specific discharge is variable along any given flowpath and that it can either increase or decrease locally due to flow focusing, hence significant variability and uncertainty is expected locally, but these fluctuations are smoothed when averaged over kilometer-scale portions of the model domain. For example, across the 100 flow paths in the calibrated model, the range of specific discharges spans approximately an order of magnitude across both the 5- and 18-km boundaries. Nevertheless, the overarching criterion that the range in uncertainty of specific discharge encapsulate

uncertainty within the domain (with minimal overestimation) is met by TSPA. Historical details, including figures, of the specific discharge distribution and associated sampling techniques are contained in *Saturated Zone Flow and Transport Model Abstraction* (SNL 2007 [DIRS 177390], Section 6.5.2.1) and no differentiation is made between specific discharge in the volcanics or alluvium.

6.7.5 Remaining Uncertainties in Specific Discharge Estimates

The analyses and corresponding assignment of an uncertainty range for the groundwater specific discharge assume that the porous continuum approach is appropriate for the fractured volcanic tuffs. A remaining uncertainty is whether or not the continuum approach can be employed at the scale of the model. An alternative conceptual model not yet explicitly examined is one in which most of the flow from Yucca Mountain moves through faults rather than through the unfaulted rock. To test this alternative model, the known faults need to be included explicitly in the numerical grid of the SZ site-scale flow and transport models. Although the grid-generation and flow-calculation capabilities exist to do this, the need to calibrate the model efficiently and perform particle-tracking transport simulations has taken priority and led to the adoption of structured grids that make explicit inclusion of faults difficult. Important faults are included in the model to capture their impact on flow and transport. Furthermore, the adoption of a range that includes larger specific discharge values and smaller effective porosities introduces realizations that replicate the behavior of a fault-dominated flow and transport system. Therefore, the suite of performance assessment transport simulations currently used likely encompasses the range of behavior that would be obtained with a fault-based flow and transport model.

Finally, it is noted that model linearity assures that a global, constant-multiplier increase in permeability and corresponding increase in infiltration will yield an equal increase in specific discharge throughout the model domain without impacting the head RMSE. Although the net infiltration was defined by specified data sets (Belcher 2004 [DIRS 173179]; BSC 2004 [DIRS 169861]; Savard 1998 [DIRS 102213]), model permeabilities could be globally adjusted such that flux through the southern boundary increased to match that of the regional model (discussed in Section 6.5.2.2). The resulting 23% increase in specific discharge throughout the model domain is still within the uncertainty range of the entire SZ site-scale flow model and well within the specific discharge multiplier used in TSPA (SNL 2007 [DIRS 177390]); also see Sections 6.7.1, 6.7.4, 7.2.3, and 8.3.1 of this document).

6.7.6 Effect of Perched Water on Flow Paths and Specific Discharge

Perched water was not explicitly modeled in the SZ site-scale flow model because the weights applied to these observations were insignificant (0.1). It is noted that the conceptualization of the LHG through introduction of the altered northern region yielded water levels in wells UE-25 WT#6 and USW G-2 (suspected to be perched) that were much lower than the reported water levels. From Table 6-8, it can be seen that some modeled water levels are about 150 m lower than the data in this area to the north of Yucca Mountain; but this is consistent with the perched water-level interpretation in that area (BSC 2004 [DIRS 170009], Section 5). The area of suspected perched water is near the steepest hydraulic gradient in the model and these hydraulic gradients occur over only a few model elements. Thus, if there is some specific reason

to closely model this portion of the model domain, additional discretization may be needed to quantify possible effects on local flow direction and specific discharge. Fortunately, the LHG is upgradient of the repository and as long as it is honored by the model, it only minimally affects particle flow paths and transport times. Therefore, uncertainty due to perched water on flow paths and specific discharge is not propagated forward into the saturated zone flow and transport abstraction model.

6.7.7 Representing Faults with Reduced Permeability Grid Blocks

Computational limitations (i.e., insufficient memory and/or processor speed) preclude the implementation of a finite-element model of the SZ model domain that explicitly models individual fractures and faults on a one-to-one scale. For example, if the exact location, orientation, and dimensions were known for each fracture/fault in the system, the number of elements (and computation time) required to model the system would increase by several orders of magnitude. Therefore, major faults are conceptualized in the SZ site-scale flow model as zones of enhanced/reduced permeability that simulate inhibited/preferential flow in faults with grid blocks that are nominally 250×250 m^2 in the horizontal directions. Fault properties are necessarily volume-averaged throughout an element. On the one hand, representing faults with 250×250 m^2 elements certainly accounts for the uncertainties in their geographic location. Discussion of the observed relationship between the aquifer test and faults is provided in *Saturated Zone In-Situ Testing* (SNL 2007 [DIRS 177394], Section 6.2.4 and Appendix C7). On the other hand, the hydrogeologic properties are "smeared" across a relatively large area, precluding the use of some fault-specific site data in the calibration targets.

Volume-averaged representations of faults are commonly used in numerical modeling. Furthermore, because element permeability values are calibrated to field observations that are several grid blocks away from faults, it is believed that the large-grid-block representation is adequate for the purpose of flow modeling "away" from the fault. While the precise flow regime within the fault may not be representative, overall flow through the system, particularly at the model boundaries, is not significantly affected by the volume-averaged approach because fault volumes are such small fractions of the model volume (average of ~0.4% each).

6.7.8 Scaling Issues

Scaling issues are some of the most complex hydrology modeling problems to overcome, and it is an active field of contemporary research in geohydrology (Neuman 1990 [DIRS 101464]; Harter and Hopmans 2004 [DIRS 178488]). Although there are many approaches that address the effects of scaling on model results, none has been widely accepted as the best method. Transport models are particularly sensitive to scaling issues in both space and time. For example, distribution coefficients measured on the order of hours to months in the laboratory for a performance assessment model are dubiously applied to contaminant transport over millennia. However, flow modeling is much less sensitive to scaling issues in both space and time. First, time scales are relatively unimportant because hydrogeologic properties change little over the course of millennia. While water-level data and infiltration rates may change over such long time periods, any flow model can easily account for these changes given appropriate boundary conditions. Second, while hydrogeologic properties measured through borehole pumping tests may not be appropriate to apply at distances far from the sample site (distance scaling), the SZ

site-scale flow model described here does not use these measured properties directly. Instead, they are used to aid and validate calibration. Therefore, although it may be inappropriate to assign geologic properties based on distant measurements, the calibration techniques used in this SZ site-scale flow model moderate the negative impact of such scaling issues.

6.7.9 Flowpath Uncertainty

There are several metrics that could be used to evaluate uncertainty in specific discharge, but to be consistent with specific discharge calculations, the flowpath lengths from release below the repository to the 5- and 18-km boundaries are examined. It should be noted that the random distribution of intial particle positions below the repository can significantly impact particle length, if for no other reason than particles are distributed over a 5-km distance in the north-south direction. Flowpaths are notably affected by the N−S:E−W horizontal anisotropy applied to the volcanic units in the anisotropic zone (Figure 6-12). Average flowpath length across the 5-km boundary for 5:1 N−S:E−W horizontal anisotropy is 6.0 km (range of 3.1 to 8.6 km). The flowpath length across the 18-km boundary ranges from 19.4 to 25.4 km, with an average of 22.9 km. Average pathlengths across the 5-km boundary for 20:1 and 0.05:1 N−S:E−W anisotropies are 9.6 and 6.2 km, respectively. Correspondingly, they are 29.7 and 22.8 km across the 18-km boundary. For the isotropic case, average flowpath lengths are 6.0 and 23.2 km across the 5- and 18-km boundaries, respectively.

6.8 DESCRIPTION OF BARRIER CAPABILITY

This model report is a compilation of information and processes affecting flow in the SZ around Yucca Mountain. As such, it provides a description of the SZ barrier flow component. The two main features of the barrier described here are: (1) the specific discharge, which affects the transport time of the radionuclides that may be released at the water table below the repository horizon and travel to the accessible environment; and (2) the flow paths that will affect the travel length and, therefore, transport times.

The result for specific discharge ranges from 0.1 to 0.66 m/yr across the 5-km boundary. The average particle flow path starting at the repository footprint at the water table is likely to remain near the water table, traveling southeast as it leaves the repository area and follow Fortymile Wash, where it traverses primarily alluvial material. Transport times are expected in the range of a few thousands of years (SNL 2007 [DIRS 177392], Section 6.5).

Uncertainty affects permeability ranges and flow paths. These parameters, in conjunction with the head gradient, comprise the components of the specific discharge calculations. The flowpaths proved to be fairly insensitive to changes to the conceptual model provided the moderate and small gradient observations were adequately represented. No single change in permeability caused a corresponding (linear) change in specific discharge because of the constraints imposed by neighboring units.

The SZ flow model is used in the site-scale SZ transport model report (SNL 2007 [DIRS 177392]) to generate both concentrations-versus-time and concentrations-versus-distance curves that are needed to demonstrate the capabilities of the saturated zone as a transport barrier.

INTENTIONALLY LEFT BLANK

7. VALIDATION

Model validation is the process of testing the appropriateness of the conceptual, mathematical, and numeric representation of the system being modeled. The SZ site-scale flow model is designed to provide an analysis tool that facilitates understanding of flow in the aquifer beneath and downgradient from the repository. The flow model is also a computational tool to provide the flow fields for performing radionuclide migration predictions in the saturated zone. For these predictions to be credible, the SZ site-scale flow model must be validated for its intended use. This statement means that there is established confidence that a mathematical model and its underlying conceptual model adequately represents with sufficient accuracy the phenomenon, process, or system in question. Based on the material presented in these sections, this requirement is considered satisfied.

The validation criteria and confidence building activities during development are discussed in Section 7.1; the validation results are discussed in Section 7.2; and the summary of the validation effort is presented in Section 7.3.

The data used in validation activities are discussed in the following sections and are summarized below:

- Observed hydraulic heads and gradients not used for model development and calibration. This includes NC-EWDP Phase V potentiometric data not available when model calibration was conducted (DTN: MO0612NYE07122.370 [DIRS 179337]).
- Hydraulic parameters derived from hydraulic testing at the C-wells, Alluvial Testing Complex, and single-well testing at other wells (SNL 2007 [DIRS 177394]).
- Flowpaths derived from hydrochemistry and isotope analyses (Appendices A and B).

7.1 VALIDATION CRITERIA

The model validation approach for the SZ site-scale flow model is presented in *Technical Work Plan for Saturated Zone Flow and Transport Modeling* (BSC 2006 [DIRS 177375], Section 2.2.2), which states that the SZ site-scale flow model requires Level II validation. The validation plan was developed under the BSC procedures in effect at the time. The BSC Level II validation is equivalent to Level I validation as described in SCI-PRO-002. Nevertheless, the site-scale SZ flow model was validated to Level II requirements. The Level II validation includes the six steps of confidence building during model development as described in SCI-PRO-002 and at least two post-development activities as described in SCI-PRO-006, Section 6.3.2. To satisfy the model validation requirements, the following four post-development validation activities (BSC 2006 [DIRS 177375], Section 2.2.2.1) were performed (comparisons of site data to):

- Predicted hydraulic heads and the observed potentiometric map. New water-level data are compared to modeled water-level data. Validation will be considered acceptable if the absolute value of the difference between simulated and observed hydraulic heads are within 10 m (the minimum model layer thickness).

- Predicted flow paths and those derived from the hydrochemistry and isotope analysis. This method involves the model simulation of flow paths. Validation is considered acceptable if the flow paths simulated by the model are bounded by those inferred from hydrochemical and isotope analyses.

- Calibrated hydraulic parameters and those derived from hydraulic testing at the C-wells, the ATC, the NC-EWDP-22 site, and single-well testing at other wells. If this comparison is used, validation will be considered acceptable if the absolute value of the difference between calibrated permeabilities and those derived from hydraulic testing and laboratory measurement is less than or equal to 50% of the field and laboratory derived hydraulic conductivity (permeability) from material along the flow path from the water table directly beneath the repository to the compliance boundary. For the implementation of this work activity, it should be clarified that the acceptance criterion used herein is model-calibrated permeabilities must be within a factor of 2 (i.e., between 1/2 and 2) of the 95% confidence interval on the field-test-derived mean permeabilities. This method is also relevant to model simulation of specific discharge because specific discharge is directly proportional to hydraulic conductivity (permeability).

- Predicted specific discharge and the conclusions of the Expert Elicitation Panel (CRWMS M&O 1998 [DIRS 100353]). Model validation is acceptable if the modeled output of specific discharge is within the range provided by expert elicitation.

These validation activities and acceptance criteria reflect the essential functions of the SZ system with regard to the transport time and radionuclide mass delivery to the accessible environment. The results of these post-development validations are discussed in Section 7.2.

7.1.1 Confidence Building During Model Development to Establish Scientific Basis and Accuracy for Intended Use

For Level II validation, the development of the model should be documented in accordance with the requirements of Section 6.3.1 (C and D) of SCI-PRO-006. The development of the SZ site-scale flow model was conducted according to the following criteria (italicized). The paragraphs following each criterion describe how it was satisfied.

1. *Evaluate and select input parameters and/or data that are adequate for the model's intended use to be consistent with* SCI-PRO-002 [Attachment 3 Level I (1)].

   The inputs to the SZ site-scale flow model have all been obtained from controlled sources (see Table 4-1). The input parameter and data used to develop and calibrate the SZ site-scale flow model are adequate for the intended use of providing TSPA with flow fields necessary to predict radionuclide transport in the saturated zone below the repository to the accessible environment.

2. *Formulate defensible assumptions and simplifications that are adequate for the model's intended use to be consistent with* SCI-PRO-002 [Attachment 3 Level I (2)].

Discussion of assumptions and simplifications are provided in Sections 5 and 6.3. The conceptual model of flow in the saturated zone and the components of the model are discussed in Section 6.3. As discussed in detail in Section 7, further confidence building in sub-model components of the SZ site-scale flow model was conducted through comparison of the conceptual model of SZ flow with the results of field tests conducted at the C-wells complex and at the ATC. The following observations were made from testing at both the C-wells and the ATC regarding the two assumptions:

- Testing at the ATC indicated that a homogeneous, confined-aquifer analytical solution provided a good match to drawdown data; and,

- Testing at the C-wells indicated that the volcanic tuffs are a fracture-dominated system (SNL 2007 [DIRS 177394], Section 6.5).

Long-term testing at the C-wells yielded responses that could be fitted with effective-continuum physical equations and homogeneous hydrologic properties. These tests support the concept that the saturated zone can be modeled as an effective continuum with homogeneous properties. Thus, this criterion is considered satisfied.

3. *Ensure consistency with physical principles, such as conservation of mass, energy, and momentum, to an appropriate degree commensurate with the model's intended use to be consistent with* SCI-PRO-002 [Attachment 3, Level I (3)].

   Consistency with physical principles is demonstrated by the conceptual and mathematical formulations in Sections 6.3 and 6.5 through selection and use of the flow and transport simulator, FEHM (STN: 10086-2.24-02 [DIRS 179539]) in Section 3. The governing equations for non-isothermal flow implemented in FEHM are based on conservation of mass and energy and Darcy's law. As discussed in detail in Section 7.2, further confidence building in the SZ site-scale flow model was conducted through comparisons to field tests conducted at the C-wells complex and the ATC (SNL 2007 [DIRS 177394], Section 6.5).

4. *Represent important future state (aleatoric), parameter (epistemic), and alternative model uncertainties to an appropriate degree commensurate with the model's intended use to be consistent with* SCI-PRO-002 [Attachment 3, Level I (4)].

   The SZ site-scale flow model is a steady-state model that does not require temporal conditions (initial and future conditions). The model incorporates parameter and alternative models uncertainties. The range of uncertainties is used in the modeling abstraction feeding the TSPA predictions.

5. *Ensure simulation conditions have been designed to span the range of intended use and avoid inconsistent outputs or that those inconsistencies can be adequately explained and demonstrated to have little impact on results to be consistent with* SCI-PRO-002 [Attachment 3, Level I (5)].

The SZ site-scale flow model uses the water-level potentiometric surface (Appendix E) to derive constant-head boundary conditions. The model was calibrated to 161 hydraulic head measurements. Recharge and lateral boundary flux targets were developed from the DVRFS flow model (Belcher 2004 [DIRS 173179]), the UZ flow model (BSC 2004 [DIRS 169861]), and infiltration data through Fortymile Wash (Savard 1998 [DIRS 102213], Section 6.3) Initial conditions were not required for the steady state model. Sections 6.6 and 6.7 provide detailed discussion of various model results.

6. *Ensure that model predictions (performance parameters) adequately represent the range of possible outcomes, consistent with important uncertainties and modeling assumptions, conceptualizations, and implementation. to be consistent with* SCI-PRO-002 [Attachment 3 Level I (6)].

   A discussion of model uncertainties is provided in Section 8.3. Sensitivity of the output to some of the uncertain input parameters is discussed in Sections 8.3.1 through 8.3.2.

7.1.2 Hydraulic Gradient Comparison to Build Model Confidence During Development

To build confidence in the SZ site-scale flow model, a comparison between field data and the model simulations of the hydraulic gradients along the flowpaths from the repository has been performed using water-level data employed as calibration targets. The water-level data from a series of seven wells (Figure 7-1a) extending from the immediate area of the repository (USW H-6) to NC-EWDP-32P are presented in Figure 7-1b. The wells used in gradient calculations were selected because they were on or close to the simulated flowpath and they traverse the Solitario Canyon Fault. The simulated and observed hydraulic gradients for non-validation wells are presented in Table 7-1. The differences in observed and simulated water levels between wells USW H-6 and USW-25 WT-2 are due to the manner in which the model accounts for the effect of the splay of the Solitario Canyon Fault, which lies in the general area of these wells. However, while the model does not accurately simulate the precise location for the drop in head across the fault, largely because of the 250-m grid blocks, the overall hydraulic gradient simulated between USW H-6 and USW-25 WT-2 agrees reasonably well with the measured value (within 14%). For the segments between USW-25 WT-2 and NC-EWDP-22PC/24PB, where the simulated hydraulic gradients differs from the observed gradients by 50 to 152% , however, in absolute terms the differences between the observed and simulated hydraulic gradients is quite close to zero. Consider that the water table is extremely flat in that area and the accuracy of land surface altitude is 0.1 m (BSC 2004 [DIRS 170009]). The relatively large error (58%) for the segment between the new wells NC-EWDP-22PC/24PB to NC-EWDP-19P/2D is again due to the rapid water-level change near U.S. Highway 95 fault, which is not precisely reproduced in the model. Nevertheless, measured and modeled gradients are sufficiently close to lend credibility to and build confidence in the model results.

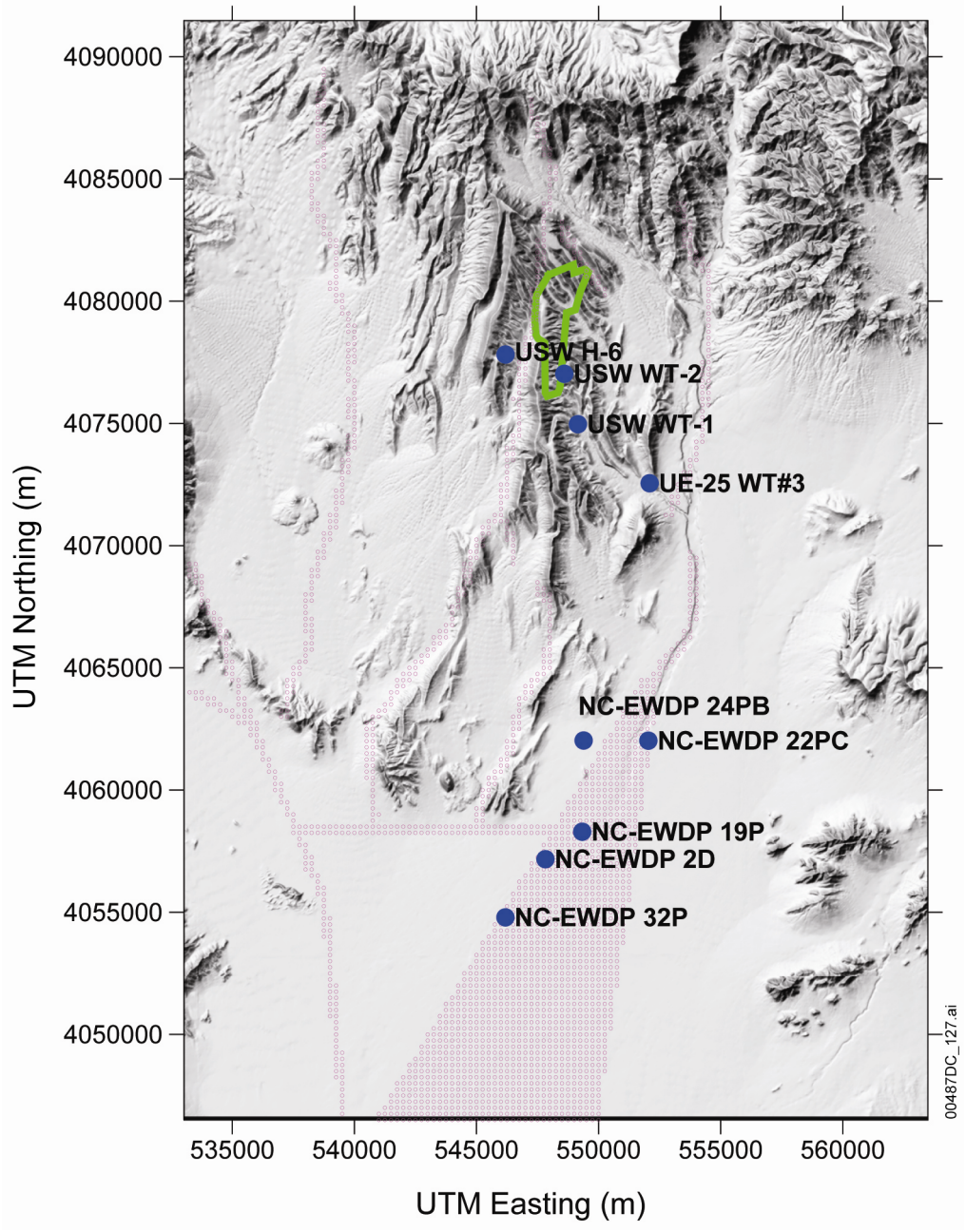

NOTE: Pink represents special geologic features (see Table 6-7 and Figure 6-12).

Figure 7-1a. Location of wells for Measured and Simulated Head Along Flowpath

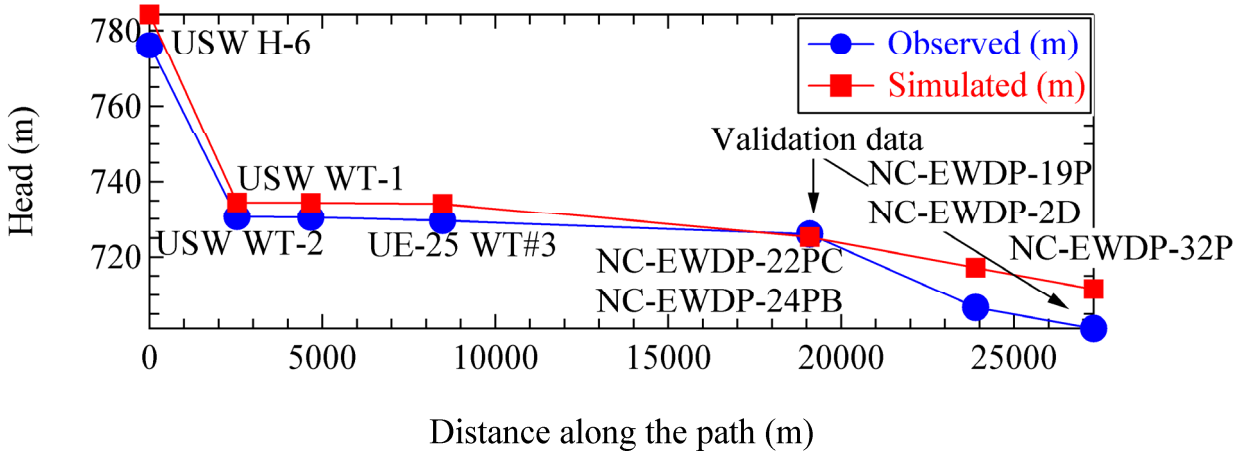

Sources: DTN: GS010908312332.002 [DIRS 163555] (non-NC-EWDP wells); SNL 2007 [DIRS 179466] (repository outline).

Output DTNs: SN0612T0510106.004 (modeled heads); SN0702T0510106.007 (NC-EWDP aggregated Phase III, IV, and V well data).

NOTE: Calculations are from data in Table 7-2. For illustration purposes only.

UTM = Universal Transverse Mercator.

Figure 7-1b. Measured and Simulated Head Along Flowpath

Table 7-1. Predicted and Observed Hydraulic Gradient for Identified Wells Used for Confidence Building During Development

Flow Segment	$\Delta H/\Delta L$ (Measured)	$\Delta H/\Delta L$ (Simulated)	Relative Error
USW H-6 to USW-25 WT-2	1.79×10^{-2}	2.04×10^{-2}	0.14
USW-25 WT-2 to USW-25 WT-1	9.37×10^{-5}	4.68×10^{-5}	−0.50
USW-25 WT-1 to UE-25 WT#3	2.10×10^{-4}	7.89×10^{-5}	−0.63
UE-25 WT#3 to NC-EWDP-22PC/24PB	3.37×10^{-4}	8.48×10^{-4}	1.52
NC-EWDP-22PC/24PB to NC-EWDP-19P/2D	4.03×10^{-3}	1.69×10^{-3}	−0.58
NC-EWDP-19P/2D to NC-EWDP-32P	1.59×10^{-3}	1.62×10^{-3}	0.02

Source: DTN: GS010908312332.002 [DIRS 163555] (non-NC-EWDP wells).

Output DTNs: SN0612T0510106.004 (modeled heads); SN0702T0510106.007 (NC-EWDP aggregated Phase III, IV, and V well data).

NOTES: Calculations are from data in Table 7-2.
NC-EWDP-22PC/24PB uses the average location and head values for wells NC-EWDP-22PC and NC-EWDP-24PB.
NC-EWDP-19P/2D uses the average location and head values for wells NC-EWDP-19P and NC-EWDP-2D.

7.1.3 Confidence Building After Model Development to Support the Scientific Basis of the Model

Model validation requires that mathematical models be validated by one or more of several methods given in Section 6.3.2 (1st and 9th bullets) of SCI-PRO-006. Validation of the SZ site-scale flow model as related to the procedural requirements mandates the following:

1. SCI-PRO-006, Section 6.3.2 (1st bullet): Corroboration of model results with the laboratory, field experiments, analog studies, or other relevant observations, not previously used to develop or calibrate the model.

   The SZ site-scale flow model was validated by comparing results from this model with the laboratory and field experiment and other observations. The validation criteria, testing, and results are described in detail in Section 7.2 of this report. Based on material presented in these sections, this criterion is considered satisfied.

2. SCI-PRO-006, Section 6.3.2 (9th bullet): Technical review through publication in a refereed professional journal. Although this is not required by the TWP, this post-development model validation activity adds to the confidence in the SZ site-scale flow model.

   A previous version of the SZ site-scale flow model and its results are described in the referenced professional publications by Eddebbarh et al. (2003 [DIRS 163577]) and Zyvoloski et al. (2003 [DIRS 163341]). These publications demonstrate additional confidence in the model, when taken in conjunction with the model validation activity described in Item 1 above because the same modeling techniques were used in this report. Moreover, this revision is based on an improved and updated HFM with more accurate fault locations, has more that four times as many grid nodes, and calibration yielded a lower residual (weighted RMSE).

7.2 VALIDATION RESULTS

The validation activities for the SZ site-scale flow model are carried out according to *Technical Work Plan for Saturated Zone Flow and Transport Modeling* (SNL 2007 [DIRS 177375], Section 2.2), which requires Level II model validation of the SZ site-scale flow model based on its relative importance to the performance assessment for the repository. The TWP states that the validation will include confidence building activities implemented during model development. In addition, it states that post-development model validation will consist of a comparison of simulated flowpaths to those derived from hydrochemistry and isotope analyses, plus two or more other comparisons as indicated in the technical work plan.

Water levels and gradients. For purposes of postdevelopment model validation, a comparison of simulated and observed water levels for all new water-level data is presented in Section 7.2.1. This comparison focuses on the NC-EWDP Phase V water-level data (DTN: MO0612NYE07122.370 [DIRS 179337]). A comparison of simulated and observed gradients along the flowpath from the repository is also presented to evaluate the impact of the difference between observed and simulated water levels on the estimates of specific discharge. Specific discharge is directly proportional to the hydraulic gradient. As previously established in

the TWP (BSC 2006 [DIRS 177375], Section 2.2.2), validation is considered acceptable if the differences between simulated and observed hydraulic gradients are not greater than 50% along the flowpath from the water table directly beneath the repository to the compliance boundary (differences may be greater than 50% away from this flowpath).

Specific discharges and permeabilities. The comparison of specific discharges based on calibrated hydraulic parameters (permeabilities) and those derived from hydraulic testing is presented in Section 7.2.2. This section summarizes data from Yucca Mountain and nearby areas available for determining the permeabilities of the hydrogeologic units represented in the SZ site-scale flow model and provides 95% confidences on the means. As discussed in Section 6.7.2 and Appendices H and I, calibrated values of the effective parameters should not be expected to be equivalent to real-world parameters because of the model's inability to represent the innate complexity of the system (heterogeneity). Therefore, the 50% difference between observed and calibrated permeabilities is applied to the range spanned by 95% confidence interval on the mean observed permeability. A factor of 3 (and ⅓) times the specific discharge is allowed between the highest and lowest limits of the range provided by site data and the Expert Elicitation Panel.

New permeability measurements are available from the ATC (SNL 2007 [DIRS 177394], Section 6.4) and are suitable for postdevelopment model validation. The measurements were taken along the flowpath from the repository. Section 7.2.2 compares these measurements with calibrated permeabilities. In addition, because new water-level data and permeability measurements are available at the ATC, simulated and observed values of hydraulic gradient and permeability at this location are used to calculate specific discharge. These calculated values are compared to the model-simulated specific discharge for the test location for purposes of post-development model validation. Furthermore, the ATC tracer tests also independently provide estimates of specific discharge from groundwater flow velocity for a range of flowing porosities (DTN: LA0303PR831231.002 [DIRS 163561]; SNL 2007 [DIRS 177394], Section 6.4); a comparison also was made between these estimates and model results. As established in the TWP (BSC 2006 [DIRS 177375], Section 2.2), validation is considered acceptable if the differences between measured specific discharge values are within the factor of 3 of those from the model.

Flowpaths. The comparison of the simulated flow pathways with those derived from the hydrochemistry and isotope analyses is presented in Section 7.2.4. The hydrochemistry and isotope analyses were not used during model development and calibration and, consequently, are suitable for post-development model validation. The flow-path comparison is considered acceptable if the flowpaths simulated by the model are bounded by those flowpaths inferred from hydrochemical and isotope analyses (Appendices A and B).

7.2.1 Comparison of Observed and Predicted Nye County Water Levels

Because well USW SD-6 received special consideration in *Water-Level Data Analysis for the Saturated Zone Site-Scale Flow and Transport Model* (BSC 2004 [DIRS 170009], Section 6.3.3) and was not used as a calibration target or in the construction of the potentiometric surface (Appendix E), it was selected for use in validation. Moreover, a qualified source of the well's

open interval was not available. *Water-Level Data Analysis for the Saturated Zone Site-Scale Flow and Transport Model* (BSC 2004 [DIRS 170009]) describes the use of this well as follows:

> The water-level information for Borehole USW SD-6 is provided in two DTNs: GS000808312312.007 [DIRS 155270] and GS001208312312.009 [DIRS 171433]. The three water-level elevations in those two DTNs range from 731.10 to 731.70 m. A water level of 731.2 m was used as part of model validation in the calibration of the SZ site-scale flow model (BSC 2001 [DIRS 155974], pp. 48 to 51). This is a more direct use of Borehole USW SD-6 water-level data than is the incorporation of this information into the potentiometric-surface map (Figure 6-1). An argument presented by Williams (2003 [DIRS 170977]) is that the SD-6 data would not have changed the potentiometric-surface map. This can be seen by observing the location of USW SD-6 on Figure 1-2 and noting that the contours on Figure 6-1 would not have changed with the addition of the new wells. The exclusion of Borehole USW SD-6 is justified on the basis of no impact.

Output from the SZ site-scale flow model, 734.8 m, over-predicts (by less than 4 m) the measured value of 731.2 m. USW SD-6 was located at UTM coordinates (547,577 m; 4,077,546 m) from DTN: GS010208312322.001 [DIRS 162908].

Since the calibration of the SZ site-scale model, water-level data for five additional wells have been posted as part of the NC-EWDP. These additions include wells installed at new locations and wells completed near existing locations. Comparison of the water levels observed in the new NC-EWDP wells with water levels simulated by the SZ site-scale flow model at these new locations provides an opportunity to validate the model. In addition, these new NC-EWDP wells can be used when comparing the measured and simulated hydraulic gradients along the flowpath from the repository. This comparison can be used to validate the SZ site-scale model quantitatively.

The SZ site-scale model was calibrated using 161 water-level and head measurements from 132 wells within the model domain, as described in Sections 6.5.1.2 and 6.5.1.3. Fifty-six of these measurements were from wells drilled and completed as part of the NC-EWDP. Measured and simulated heads for the five new Phase V wells to be used in the validation, along with their coordinates, are shown in Table 7-2.

Examination of the residuals reported in Table 7-2 indicates that the errors in simulated water levels depend on their location within the model domain. Figure 7-2 shows that NC-EWDP-32P, with the largest residual of 9.9 m, is located in an area of rapid water-level changes, along the U.S. Highway 95 fault, and the model is not able to fully replicate the steep head gradients observed in this area. Wells NC-EWDP-22PC and -24PB located north of U.S. Highway 95 near Fortymile Wash show small residuals of −0.4 and −1.3 m, respectively. Similar residual errors were observed using the water-level data available during model calibration. NC-EWDP-33P located just south of U.S. Highway 95 and west of Fortymile Wash shows good agreement with a residual of −4.8 m. Finally, NC-EWDP-13P located on the eastern edge of Crater Flats near Windy Wash fault in a region of high water levels also shows a low residual of −4.4 m. Overall, the observed residuals tend to improve for wells located further to the north and east in the

vicinity of Fortymile Wash where wells are in the simulated flowpath from the repository. Thus, these additional water-level data confirm the SZ site-scale model's capability to simulate water levels accurately in this portion of the flowpath from the repository.

Table 7-2. Wells Used in Validation of the Saturated Zone Site-Scale Flow Model with Observed and Predicted Water Levels

Well ID	Easting (UTM) (m)	Northing (UTM) (m)	*z* (elevation) (m)	Observed Head (m)	Modeled Head (m)	Residual Error (m)
NC-EWDP Phase V wells used for validation						
NC-EWDP-13P	543471	4066433	758.9	764.4	760.0	–4.4
NC-EWDP-22PC upper	552036	4062019	702.3	724.9	724.5	–0.4
NC-EWDP-24PB	549387	4062025	621.6	727.2	725.9	−1.3
NC-EWDP-32P upper	546183	4054789	696.4	701.7	711.6	9.9
NC-EWDP-33P upper	545117	4057146	713.1	720.8	716.1	–4.8
Non-NC-EWDP wells used in gradient calculations						
USW H-6 upper	546188	4077816	662.9	776.0	786.2	10.6
USW WT-2	548595	4077028	702.0	730.6	734.6	4.0
USW WT-1	549152	4074967	708.4	730.4	734.5	4.1
UE-25 WT#3	552090	4072550	705.8	729.6	734.2	4.6
NC-EWDP calibration wells used in gradient calculations						
NC-EWDP-19P	549329	4058292	694.7	707.3	717.7	10.4
NC-EWDP-2D	547823	4057170	507.1	706.1	716.6	10.5

Source: DTN: GS010908312332.002 [DIRS 163555] (non-NC-EWDP wells).

Output DTNs: SN0612T0510106.004 (modeled heads); SN0702T0510106.007 (NC-EWDP aggregated Phase III, IV, and V well data).

NOTE: Datum is mean sea level. *z* (elevation) is at the center of the screened interval.

UTM = Universal Transverse Mercator.

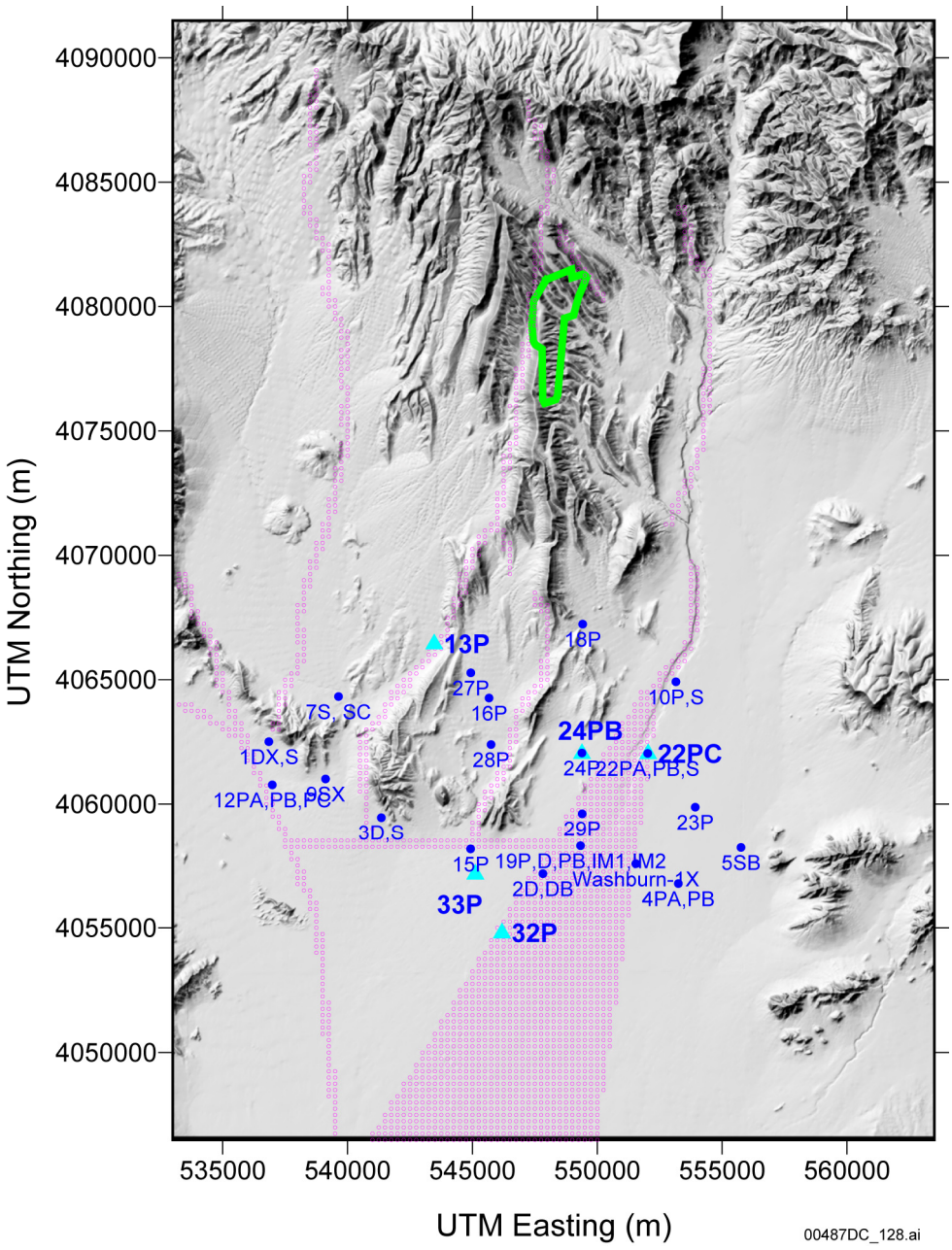

Sources: DTN: GS010908312332.002 [DIRS 163555] (non-NC-EWDP wells); SNL 2007 [DIRS 179466] (repository outline).

Output DTNs: SN0612T0510106.004 (modeled heads); SN0702T0510106.007 (NC-EWDP aggregated Phase III, IV, and V well data).

NOTE: For illustration purposes only. Well coordinates are listed in Table 7-2. Blue dots are NC-EWDP wells used in calibration. Light blue triangles with larger text are Phase V wells used in validation.

UTM = Universal Transverse Mercator.

Figure 7-2. Locations of NC-EWDP Wells

To further validate the SZ site-scale flow model, a comparison was made of the hydraulic gradients along the flowpath using water-level data from two wells that were not used during calibration (NC-EWDP-22PC and -32P). Table 7-3 presents gradients calculated for postdevelopment model validation. Predicted gradients are about a factor of two lower than observed because to the model does not capture the rapid water level change near U.S. Highway 95 fault. However, this region is south of the region of primary interest and, as discussed in Section 7.1.3, the model reproduces observed gradients over the relevant portion of the flowpath from the repository through Fortymile Wash to U.S. Highway 95 quite well. The validation is considered successful because the simulated hydraulic gradient agrees to within 50% with gradient calculations from data.

Table 7-3. Predicted and Observed Hydraulic Gradients for Post-Development Validation

Flow Segment	$\Delta H/\Delta L$ (Measured)	$\Delta H/\Delta L$ (Simulated)	Relative Error
NC-EWDP-24PB to NC-EWDP-32P	3.22×10^{-3}	1.81×10^{-3}	−0.44
NC-EWDP-22PC to NC-EWDP-32P	2.49×10^{-3}	1.39×10^{-3}	−0.44

Sources: DTNs: GS010908312332.002 [DIRS 163555] (non-NC-EWDP wells); SN0612T0510106.004 (modeled heads).

Output DTN: SN0702T0510106.007 (NC-EWDP aggregated Phase III, IV, and V well data).

NOTE: Calculations are from data in Table 7-2.

7.2.2 Comparison of Calibrated Effective Permeabilities to Field Test Results

The numerical model was calibrated by adjusting permeability values for individual hydrogeologic units in the model until the sum of the weighted residuals squared (the objective function) was minimized. The residuals include the differences between the measured and simulated hydraulic heads and the differences between the groundwater fluxes simulated with the SZ regional- and the site-scale models. Permeabilities estimated from hydraulic tests were neither formally included in the calibration nor considered in the calculation of the objective function. The field-derived permeabilities were instead used to check on the reasonableness of the final permeability estimates produced by the calibration.

Discussions of the permeability data from the Yucca Mountain area and nearby NTS as well as the Apache Leap site in Arizona are presented in the following subsections. A discussion of the general inferences about permeability that can be drawn from regional observations is also presented. Following these discussions, a comparison of calibrated effective permeabilities with the 95% confidence interval on the mean of measured permeability values is presented, including the analysis of the potential impact of calibrated permeability values on groundwater specific discharge.

7.2.2.1 General Permeability Data

Many factors affect the permeability of volcanic rocks at Yucca Mountain including: (1) the tendency of the rock either to fracture or to deform plastically in response to stress; (2) the ability of the rock to maintain open fractures, which is a function of the strength of the rock and overburden stress; (3) proximity to major zones of deformation, such as fault zones; and, (4) the degree of mineralization or alteration that would tend to seal fractures and faults. Other factors

being equal, rocks that tend to fracture are at shallow depth, have high compressive strength, are located in a fault zone, or are unmineralized and would be expected to have high permeabilities compared to rocks that do not possess these attributes. In addition to actual variations in permeability, the scale of measurement may also influence the permeability estimated by a test. This effect is most often observed when results of permeability tests conducted on cores that do not contain fractures are compared to the results of tests conducted in boreholes that contain fractured intervals. At Yucca Mountain, the relatively high permeabilities estimated from cross-hole tests compared to single-hole tests in the same rock unit have been attributed to the effects of scale (Geldon et al. 1998 [DIRS 129721]). In this case, the cause of the permeability increase in the cross-hole tests is attributed to the greater likelihood of including relatively rare but highly transmissive and continuous features in the larger rock volume sampled by the cross-hole tests. This assumption is reevaluated below based on recent analyses of air-injection tests conducted at the Apache Leap test site near Globe, Arizona. Permeability data from single- and multiple-borehole hydraulic tests at Yucca Mountain and single-borehole tests elsewhere at the NTS have been compiled and compared to permeabilities estimated during calibration of the SZ site-scale flow model.

7.2.2.1.1 Calico Hills

First, the geometric-mean permeability estimated for the Calico Hills Formation from single-hole tests ($k = 0.078 \times 10^{-12}$ m^2) is less than that estimated from cross-hole tests ($k = 0.17 \times 10^{-12}$ m^2). This observation indicates that factors other than the test method and the scale of the test are influencing results. One such factor may be proximity to faults. Several of the single-hole tests conducted in the Calico Hills Formation were performed in the highly faulted area near borehole UE-25 b#1, whereas faults were present only at deeper stratigraphic horizons at the C-wells where the cross-hole tests were done (Geldon et al. 1998 [DIRS 129721], Figure 3). Nonetheless, geologic contacts with open partings may also have enhanced permeability in the Calico Hills Formation at the C-wells (Geldon et al. 1998 [DIRS 129721], Figure 5). Second, both estimates of the mean Calico Hills Formation permeability are either larger than the mean permeability estimated for the carbonate aquifer from Yucca Mountain data ($k = 0.072 \times 10^{-12}$ m^2) or comparable to mean permeabilities estimated for the carbonate aquifer from data elsewhere at the NTS ($k = 0.6 \times 10^{-12}$ m^2). Although the permeability of the Calico Hills Formation may be locally higher than the mean permeability of the carbonate aquifer, it is unlikely that this relative difference between the two formation permeabilities can exist in general. The carbonate aquifer, along with the alluvial aquifers, is widely viewed as a major water-supply source in Southern Nevada (Dettinger 1989 [DIRS 154690]). In contrast, the Calico Hills Formation has properties similar to those of rocks deemed suitable for nuclear weapons tests below the water table at Pahute Mesa. The rocks at Pahute Mesa had properties (low intrinsic permeability due to zeolitization and sparse, poorly connected fractures) that were predicted, and later observed, to result in only small amounts of seepage into open test chambers during their construction (Blankennagel and Weir 1973 [DIRS 101233], pp. B30 to B31). Similar rocks in the unsaturated zone at Rainier Mesa produced perched water from isolated fault zones during construction of tunnels into the mesa; however, because the fault zones drained quickly and fault zones intersected later during tunneling also initially produced water, the fault zones were inferred to be relatively isolated both horizontally and vertically (Thordarson 1965 [DIRS 106585], pp. 42 to 43). At Yucca Mountain, the apparently widespread presence of perched water on top of the zeolitic Calico Hills Formation in northern Yucca Mountain

(Patterson 1999 [DIRS 158824]) indicates that the formation generally has low permeability compared to the rate of water percolation through the unsaturated zone, which has been estimated to average between 1 and 10 mm/yr in the vicinity of the repository under the present climate (Flint 1998 [DIRS 100033]). Water flowing under a unit gradient at a rate of 10 mm/yr (3.17×10^{-10} m/s) would seep through a rock having a permeability of $0.0000323 \times 10^{-12}$ m^2 (assuming a viscosity of 0.001 N-s/m^2 and a water density of 1,000 kg/m^3); so the field-scale vertical permeability of the Calico Hills Formation, which includes the effects of fracturing, presumably has permeabilities less than this value. Based on core measurements, the geometric-mean hydraulic conductivity for the zeolitic Calico Hills Formation is 4.5×10^{-11} m/s (Flint 1998 [DIRS 100033], Table 7), which is significantly higher than the low permeability ($0.0000323 \times 10^{-12}$ m^2) thought necessary for perched water. The calibrated effective permeability for the Calico Hills Volcanic unit was 0.46×10^{-12} m^2, which is on par with results from cross-hole testing.

7.2.2.1.2 Alluvial Testing Complex

From July through November 2000, pumping tests were conducted in well NC-EWDP-19D. The first test involved production from the entire saturated thickness of 136 m. The results indicated a transmissivity of about 21 m^2/day and an average hydraulic conductivity of 0.15 m/day, approximately equivalent to a permeability of 0.2×10^{-12} m^2 (SNL 2007 [DIRS 177394], Section 6.4.5 and Appendix F7). Subsequently, four screened intervals having a combined thickness of 84 m were tested individually. The combined transmissivities of these intervals totaled about 145 m^2/day, greatly exceeding the transmissivity determined for the initial open-hole test. There are at least two likely causes for the discrepancy. First, pumping apparently resulted in further well development, as fine materials were drawn into the well and discharged with the water. Second, the screened intervals are probably interconnected hydraulically, consistent with the complexity of fluvial-alluvial depositional environments, so that actual thicknesses of the producing zones were significantly greater than the screened intervals. The average permeability of the section is probably greater than the initial permeability determined from the open-hole test (0.2×10^{-12} m^2) but less than those calculated for the two deeper screened intervals, 1.5×10^{-12} and 3.3×10^{-12} m^2. Although thin, discontinuous zones may locally have higher permeabilities, these results indicate that significantly thick (greater than 10 m) and areally extensive zones at NC-EWDP-19D probably have average permeabilities between 0.1×10^{-12} and 1×10^{-12} m^2 (SNL 2007 [DIRS 177394], Sections 6.4.5 and Appendix F7).

7.2.2.1.3 Apache Leap

Fractured welded tuffs and relatively unfractured nonwelded tuffs occur both above and below the water table. Permeabilities measured in the unsaturated zone at Yucca Mountain using air may, therefore, have some relevance to the permeability values of similar rocks located below the water table. In the unsaturated zone, air-injection tests have been conducted from surface-based boreholes in both welded and nonwelded tuffs (LeCain 1997 [DIRS 100153]) and from test alcoves in and adjacent to the Ghost Dance Fault zone in the densely welded Topopah Spring tuff (LeCain et al. 2000 [DIRS 144612]). At Yucca Mountain, no water-injection tests were done in these same intervals to directly compare to the results of the air-injection tests. However, some understanding of the probable relation between permeabilities estimated from

air- and water-injection tests at Yucca Mountain can be made on the basis of tests in nonwelded to partially welded tuff at the Apache Leap experimental site in Arizona, where borehole air- and water-injection tests were made at ambient moisture conditions in the same depth intervals (Rasmussen et al. 1993 [DIRS 154688]). The Apache Leap data (Rasmussen et al. 1993 [DIRS 154688], Figure 5b) reveal a complex relation between permeabilities calculated from the two types of tests. Air-injection tests yielded lower permeabilities than water-injection tests in borehole intervals for which permeabilities calculated using both fluids indicated that fractures were sparse or absent. In these intervals, matrix pore water probably obstructed air movement. However, in test intervals for which air and water permeabilities were both relatively high, the air-injection tests resulted in permeabilities comparable to or higher than permeabilities from the water-injection tests. In these intervals, both fluids probably moved into drained fractures. Additionally, because gravitational influences on air are not as pronounced as for water in the unsaturated zone, air had more possible pathways for movement than water, so air permeabilities were often higher than water permeabilities. Overall, the correlation between air and water permeabilities from the borehole injection tests at Apache Leap was $r = 0.876$ (Rasmussen et al. 1993 [DIRS 154688], Figure 5b).

The test data from Apache Leap indicate that permeabilities calculated from air-injection test data in the unsaturated zone at Yucca Mountain probably provide good approximations to the water permeabilities, particularly in the densely welded intervals where drained fractures dominate the overall air permeability. The surface-based tests in four boreholes at Yucca Mountain showed that the highest air permeabilities (up to 54.0×10^{-12} m^2) were present at depths less than 50 m in the Tiva Canyon tuff, presumably because low lithostatic stresses at these depths allowed fractures to open (LeCain 1997 [DIRS 100153], Figures 7 to 10). However, permeabilities in the Tiva Canyon tuff typically decreased rapidly with depth, so that the permeabilities at depths greater than 50 m were less than 10^{-11} m^2. The geometric-mean permeabilities of the Tiva Canyon tuff in the four boreholes varied between 3.4×10^{-12} and 8.4×10^{-12} m^2 (LeCain 1997 [DIRS 100153], Table 1), with an overall geometric-mean permeability of 4.7×10^{-12} m^2 based on a total of 23 tests. Geometric-mean permeabilities of the Topopah Spring tuff at the four boreholes varied between 0.3×10^{-12} and 1.7×10^{-12} m^2 (LeCain 1997 [DIRS 100153], Table 5) with an overall geometric-mean permeability of 0.75×10^{-12} m^2 based on the results of 153 tests.

Work by Vesselinov et al. (2001 [DIRS 154706]) at the Apache Leap site has demonstrated that permeabilities determined from multiple single-well air-injection tests and simultaneous numerical inversion of multiple cross-hole air-injection tests provided comparable estimates of the mean permeability of the test volume. However, when the cross-hole tests were analyzed individually with an approach equivalent to type-curve analysis, which requires the assumption of a uniform permeability field and a particular flow geometry (spherical), the resulting mean permeability estimated for the test volume was several orders of magnitude higher than the mean permeability estimated from the single-hole analyses or the more detailed simultaneous numerical inversion of the cross-hole tests. The simultaneous numerical inversion of the cross-hole tests resulted in larger calculated variance in permeabilities than was estimated from the multiple single-hole tests, a result that may have been caused by round-off error associated with the numerical inversion. The conclusions of this work relevant to the present analysis are that the mean permeabilities would not have been a function of test methodology (single-hole or cross-hole analyses) except for the inability of standard cross-hole type-curve methods to

account for heterogeneity and departures of the actual flow field from the assumed flow geometry.

7.2.2.1.4 Tuffaceous Formations

The Prow Pass, Bullfrog, and Tram tuffs of the Crater Flat group contain both nonwelded to partially welded margins and partially to densely welded interiors (Bish and Chipera 1989 [DIRS 101195]; Loeven 1993 [DIRS 101258]). The initially vitric nonwelded to partially welded margins of these units have been largely altered to zeolites during hydrothermal events as a result of their thermodynamically unstable glass composition and their initially high permeabilities (Broxton et al. 1987 [DIRS 102004]). The partially to densely welded parts of these units have devitrified to mostly quartz and feldspar and have higher matrix permeabilities than the nonwelded to partially welded zeolitized margins (Loeven 1993 [DIRS 101258]; Flint 1998 [DIRS 100033]). Additionally, because the welded parts of the tuffs have a greater tendency to fracture, the densely welded parts of these units generally have higher secondary permeability. Thus, unless faults are locally present, the densely welded parts of the Prow Pass, Bullfrog, and Tram tuffs are expected to have substantially higher permeability than the nonwelded margins.

The densely welded parts of the Prow Pass, Bullfrog, and Tram tuffs are likely to have mean permeabilities that are less than the mean air permeabilities of the Tiva Canyon ($k = 4.7 \times 10^{-12}$ m^2) or Topopah Spring ($k = 0.75 \times 10^{-12}$ m^2) tuffs estimated from air-permeability tests (see Section 7.2.2.1.3). This likelihood is because greater lithostatic stresses at depth tend to close fractures and successive hydrothermal events have caused increasing degrees of alteration with depth (Broxton et al. 1987 [DIRS 102004]). Figure 7-3 shows the geometric-mean permeabilities from the single-hole air-permeability tests for the Tiva Canyon and Topopah Spring tuffs and the geometric-mean single-hole water permeabilities calculated for the Calico Hills Formation and the Prow Pass, Bullfrog, Tram, and Lithic Ridge tuffs. The single-hole permeabilities show the expected trends of decreasing permeability with depth. Conversely, the trends in the cross-hole permeability data from the C-wells (see Section 7.2.2.3.2 and Section 7.2.2.6, Figure 7-4) are exactly opposite those expected based on geologic reasoning; these trends could, however, reflect the proximity of each hydrogeologic unit to the Midway Valley fault, which intersects the C-wells in the upper part of the Tram tuff (Geldon et al. 1998 [DIRS 129721], Figure 3). Thus, it appears that permeability trends with depth at the C-wells are controlled by local conditions and do not reflect general trends in permeability established by the single-hole tests and expected from geologic reasoning.

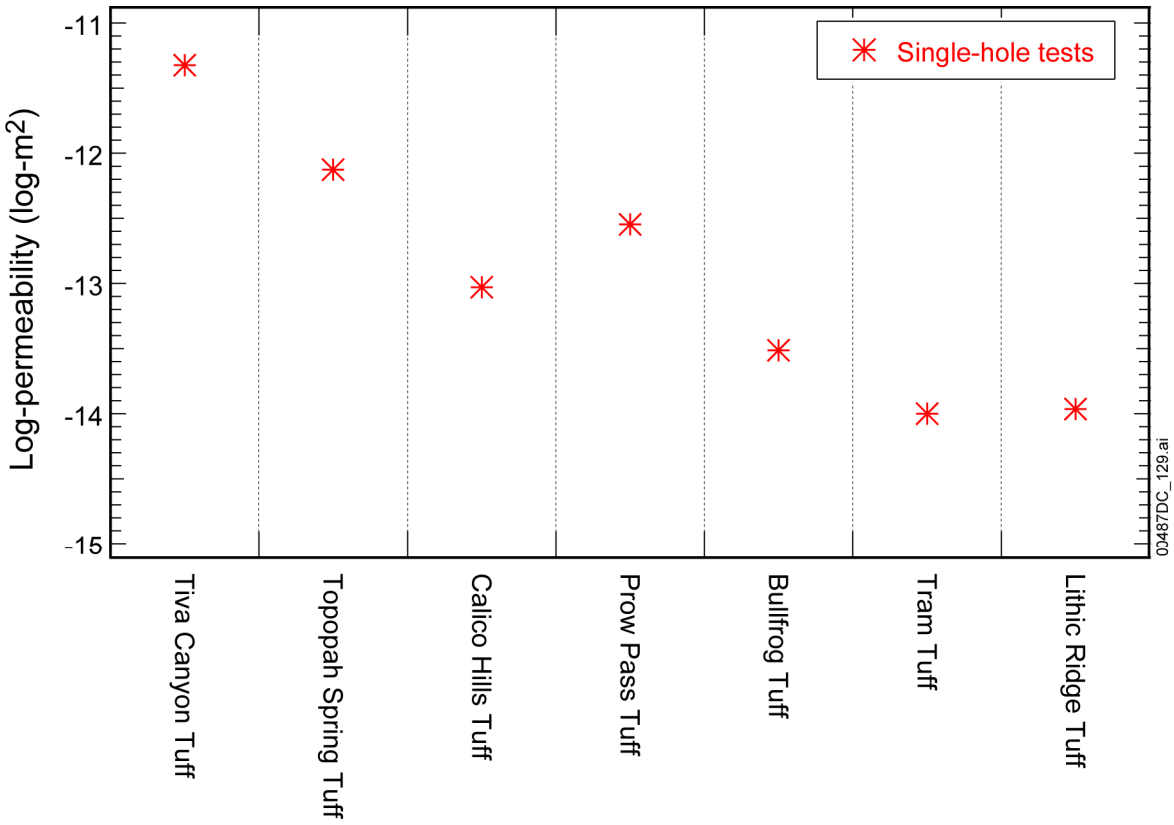

Source: DTNs: GS960908312232.012 [DIRS 114124] (Tiva and Topopah units); SNT05082597001.003 [DIRS 129714] (all other units). Used for corroboration only.

NOTE: All data are the geometric mean. Air permeability tests were conducted in the Tiva Canyon and Topopah Spring Tuffs. Water permeability tests were conducted in the other units.

Figure 7-3. Comparison of Single-Hole Air and Water Permeabilities

7.2.2.2 Implications of Permeability Data

The depth-dependent trends in mean hydrogeologic-unit permeabilities indicated by the combined air-permeability data from the unsaturated zone and the water-permeability data from the SZ (Section 7.2.2.3.2 and Section 7.2.2.6, Figure 7-4) are generally consistent with the trends expected as higher lithostatic stresses and more intense hydrothermal alterations close fractures at increasing depths. Conversely, permeabilities measured from cross-hole tests at the C-wells (Section 7.2.2.3.2 and Section 7.2.2.6, Figure 7-4) indicate trends that reflect proximity to the Midway Valley fault. Recent studies at the Apache Leap site in Arizona have indicated that single-hole and cross-hole tests should yield the same mean permeabilities once heterogeneity and departures from idealized flow geometries are properly taken into account. Therefore, except for the Calico Hills Formation, the single-hole permeabilities better reflect the true permeabilities of the hydrogeologic units in unfaulted areas and can be used to represent the hydrogeologic-unit permeabilities in specific-discharge calculations or in numerical models, provided any effects of faults are accurately taken into account. The geometric-mean permeability estimated for the Calico Hills Formation was probably unduly biased toward that of faulted locations by data from boreholes UE-25 b#1 and UE-25 J-13. In unfaulted areas, the Calico Hills Formation permeability is probably several orders of magnitude less than the

geometric-mean permeability calculated from the single-hole tests. The similarity of geometric-mean permeability values from cross-hole air-permeability testing in the Ghost Dance fault ($k = 14.6 \times 10^{-12}$ m^2) and the maximum permeabilities from cross-hole testing at the C-wells (54.0×10^{-12} m^2) indicate that values of 10.0×10^{-12} to 50.0×10^{-12} m^2 may be appropriate for fault-zone properties in numerical models so long as the modeled width reflects the true width of the fault; otherwise, the permeabilities in the model should be adjusted to preserve the overall transmissivity of the faults (SNL 2007 [DIRS 177394], Section 6.2.4 and Appendix C7). Anisotropy also needs to be considered because a fault that acts as a barrier to perpendicular flow may simultaneously provide a conduit to planar flow. The maximum permeability values that have been calculated for faulted locations at the C-wells and alcoves in the Ghost Dance Fault provide upper bounds on the permeabilities that would be representative of the tuffs at unfaulted locations ($k = 50.0 \times 10^{-12}$ m^2). The expected values of the tuffs are provided by the geometric means calculated from the single-hole tests and are one to several orders of magnitude less than this likely upper bound.

7.2.2.3 Permeability Data from the Yucca Mountain Area

Permeability data from single-hole and cross-hole tests were collected in the Yucca Mountain area from the early 1980s. Test results published up to 1997 were compiled in DTN: SNT05082597001.003 [DIRS 129714]. A statistical analysis of this data set is presented in this section. In addition to permeability data previously available during the development of the SZ site-scale model, additional permeability measurements are now available from the ATC.

7.2.2.3.1 Single-Hole Tests

The statistical analysis required that the test results be grouped by first compiling the permeability estimates for individual hydrogeologic units, where possible, and by considering progressively more general groupings for those cases in which the test interval spanned several hydrogeologic units. For instance, when the test interval was in the Prow Pass tuff, with or without some portion of the adjacent ash fall, the test results were grouped with other permeability estimates for the Prow Pass tuff. If other units within the middle volcanic aquifer (MVA), as defined by Luckey et al. (1996 [DIRS 100465], Figure 7), were also present in the test interval along with the Prow Pass tuff, the test results were considered to represent the MVA. If hydrogeologic units other than those in the MVA were present in the test interval along with the Prow Pass tuff, the permeability estimate for the test was grouped with the most general category, which is mixed tuffs. The mixed-tuff category includes data for all tests that would not fit into a more restrictive category. All tuffs older than the Lithic Ridge tuff are listed as Pre-Lithic Ridge tuffs (“older tuffs”). The other categories were named for the hydrogeologic unit to which they pertain.

There were several instances where several kinds of hydraulic tests (injection, drawdown, or recovery) were conducted in the same depth interval in the same borehole. The results of these tests could have been treated in several different ways. For example, (1) the data for a particular depth interval could have been averaged and primarily the single, average value considered in the statistical summary, in which case the statistical uncertainty could be interpreted as reflecting only the effects of spatial variability; or (2) all of the permeabilities that resulted from testing of the interval could have been used to calculate the summary statistics (this technique was used in this report). By considering multiple measurements from the same test interval, this statistical analysis attempts to reflect the effects of measurement uncertainty as well as the effects of spatial variability.

The base-10 logarithms of the permeabilities were calculated (Section 6.8) and a statistical analysis was performed on the log-transformed values for each category (CRWMS M&O 2000 [DIRS 139582]). The antilogarithms of the statistical parameters for each category were calculated and are listed in Table 6-24. The analysis indicates that the deepest tuffs, which are the Pre-Lithic Ridge tuffs (Pre-Tlr), and the mixed tuff group have the lowest permeabilities, and the Topopah Spring and Prow Pass tuffs have the largest permeabilities. Where they could be calculated, the 95% confidence limits indicate that the mean permeability values are constrained within relatively narrow limits, except for the Pre-Lithic Ridge tuffs.

The results also indicate that the Calico Hills Formation, which is a zeolitized tuff that functions as the upper volcanic confining unit (Luckey et al. 1996 [DIRS 100465], Figure 7), has a higher permeability than both the Bullfrog tuff and the carbonate aquifer. This paradoxical result may reflect the fact that, because it is unsaturated in the western half of Yucca Mountain, the Calico Hills Formation could be hydraulically tested only in the highly faulted eastern half of Yucca Mountain, whereas the other units were also tested in less intensely faulted areas to the west. Fortunately, calibrated effective permeabilities agree that the Calico Hills Volcanic unit has a higher permeability than both the carbonate aquifer and the Bullfrog tuff.

Single-well hydraulic testing of the saturated alluvium in well NC-EWDP-19D of the ATC was conducted between July and November 2000 (SNL 2007 [DIRS 177394], Appendix G). During this testing, a single-well test of the alluvium aquifer to a depth of 247.5 m below land surface was initiated to determine the transmissivity and hydraulic conductivity of the entire alluvium system at the NC-EWDP-19D location. In addition, each of the four intervals in the alluvium in NC-EWDP-19D were isolated and hydraulically tested to obtain transmissivity and associated hydraulic conductivity. This interval-testing program was initiated in an effort to evaluate heterogeneity in hydraulic properties over the thickness of the alluvium at NC-EWDP-19D to help determine the conceptual model of flow in the saturated alluvium south of Yucca Mountain. The results of this testing are presented in Table 7-4.

Table 7-4. Transmissivities, Hydraulic Conductivities, and Permeabilities Determined in the Single-Well Hydraulic Tests Conducted in the Alluvium in NC-EWDP-19D Between July and November 2000

Test Interval (ft below land surface)[a]	*Apparent* Transmissivity of Interval[b] (ft^2/day)	*Apparent* Transmissivity of Total Saturated Alluvium[c] (ft^2/day)	Hydraulic Conductivity Based on Sand Pack Thickness[d] (ft/day)	Hydraulic Conductivity Based on Distance from Water Table[e] (ft/day)	Permeability[f] (m^2)
Combined-Interval Test					
Four combined intervals	223	223	0.5	0.5	0.27×10^{-12}
Isolated-Interval Tests					
#1: 412–437	66	335	2.6	0.77	0.271×10^{-12}
#2: 490–519	7.5	N/A	0.26	0.045	0.0144×10^{-12}
#3: 568–691	223	306	1.89	0.78	0.235×10^{-12}
#4. 717–795	300	300	3.84	0.67	0.242×10^{-12}

Source: SNL 2007 [DIRS 177394], Appendix F.

[a] Depths correspond to upper and lower extent of sand packs.

[b] Transmissivity of the saturated alluvium from the water table to the bottom of the screen being tested was obtained by applying the Neuman (1975 [DIRS 150321]) solution to the drawdown in the interval tested. Ignoring screen #2, which is affected by a local clay layer, these transmissivities increase monotonically as the depth of the screen being tested increases.

[c] Transmissivity from interval tests for the screens #1, #3, and #4 for the entire saturated alluvium thickness tested are calculated by multiplying the transmissivity value in the second column, which is for the interval from the water table to the bottom of the screen being tested, by the ratio of 446 feet (the total saturated alluvium thickness tested) over the depth from the water table to the bottom of the screen being tested. Thus, for screen #1, $66 \times (446/88) = 334.5 \approx 335$ ft^2/day. For screen #3, $223 \times (446/342) = 290.8 \approx 291$ ft^2/day. No corrections are needed for the combined-interval test or for the test on screen #4.

[d] Assumes that interval thickness is the thickness of the interval sand pack. Sand pack (or gravel pack) is the term used for the coarse-grained material that fills the annulus between the slotted pipe (wellscreen) and the borehole wall in well completions. The sand pack generally extends a bit below the bottom and above the top of the slotted pipe to allow for any anomalies in the completion, so it is typically used as the "interval thickness" as opposed to the slotted pipe length. There is generally a bentonite grout plug placed above and below the sand pack to seal the annulus.

[e] Assumes that interval thickness is the distance from the water table to the bottom of the screened interval being pumped. Furthermore, the water table at the ATC is assumed to be 351 ft below land surface, which is the open-hole static water level in NC-EWDP-19D. However, there is a strong upward gradient from the volcanics to the alluvium at this location, and when individual zones in the alluvium are isolated, the static water level drops considerably (for instance, 368 ft below land surface in zone #1, and also in NC-EWDP-19P, which has a piezometer completed only in zone #1).

[f] Multiply the hydraulic conductivity (ft/day) in the fifth column by the factor 3.61×10^{-13} to convert to permeability in m^2.

7.2.2.3.2 Cross-Hole Tests

Permeability data from cross-hole tests were compiled, grouped, and analyzed in a manner similar to the permeability data for the single-hole tests (see Table 6-24). The cross-hole data originate from tests conducted at the C-wells complex. While the permeabilities of the Calico Hills formation are similar for both the single- and cross-hole tests, the permeabilities of the Prow Pass, Bullfrog, Tram tuffs of the Crater Flat group, and the MVA calculated from the cross-hole tests are one to several orders of magnitude greater than the mean permeabilities calculated from the single-hole tests. The differences in the mean permeability values between the single- and cross-hole tests generally have been attributed to the larger volume of rock

affected by the cross-hole tests (Geldon et al. 1997 [DIRS 100397]) that allows a larger number of possible flowpaths, including relatively rare, high-transmissivity flowpaths, to be sampled during the test. Furthermore, combinations of well losses, wellbore formation damage, and scale effects might also serve to increase estimated cross-hole permeabilities. However, some of the increase in permeability attributed to the effects of scale may also be due to the presence of a breccia zone associated with the Midway Valley fault in the Bullfrog and Tram tuffs at boreholes UE-25 c#2 and UE-25 c#3 (Geldon et al. 1997 [DIRS 100397], Figure 3). Thus, some of the difference in the mean permeabilities calculated for the single- and cross-hole tests may be due both to local conditions in the vicinity of the C-wells and to scale.

Another cross-hole hydraulic test was conducted at the ATC in January 2002. During this test, borehole NC-EWDP-19D was pumped in the open-alluvium section, while NC-EWDP-19IM1 and NC-EWDP-19IM2 were used as monitoring wells. NC-EWDP-19IM1 was packed off, isolating each of four intervals in the alluvium section, while NC-EWDP-19IM2 had only one packer inflated, isolating the alluvium section from the intervals below it. Analysis of the drawdown data from NC-EWDP-19IM2 indicated an estimated transmissivity of 307 m^2/day. The transmissivity estimate is approximately an order of magnitude higher than the 27.8-m^2/day value obtained from single-hole testing in NC-EWDP-19D. The differences between single- and cross-hole tests are likely the result of large head losses in the single-hole testing due to the well efficiency of NC-EWDP-19D. The tested interval in NC-EWDP-IM2, from the water table to the bottom of screen #4 is 133.5 m. Therefore, the intrinsic permeability measured in this test is 2.7×10^{-12} m^2.

Cross-hole tests were also conducted in NC-EWDP-22S from December 2004 to January 2005 (SNL 2007 [DIRS 177394], Appendix F). During this test, NC-EWDP-22S was pumped in the open alluvium section while NC-EWDP-22PA and -22PB were monitored. NC-EWDP-22S was screened in four intervals while -22PA and -22PB each had two packed off sections. Analyses of drawdown data yielded transmissivities ranging from 130 to 600 m^2/day. This corresponds to permeabilities between 0.059×10^{-12} and 5.8×10^{-12} m^2.

7.2.2.4 Permeability Data from the Nevada Test Site

Data from the NTS were examined to help constrain permeability estimates for hydrogeologic units that were either not tested or that underwent minimal testing at Yucca Mountain. These permeability data, as well as more qualitative observations concerning the permeability of some of the hydrogeologic units in the site-scale model area, are summarized in the following sections. Additionally, these reports, including those by Blankennagel and Weir (1973 [DIRS 101233]), Winograd and Thordarson (1975 [DIRS 101167]), and Laczniak et al. (1996 [DIRS 103012]), describe the hydrogeologic controls on groundwater movement at the NTS, thereby providing a regional perspective for groundwater flow at Yucca Mountain. Assessments of permeability data from the NTS for the lower carbonate aquifer, the valley fill aquifer, the welded tuff aquifer, and the lava flow aquifer are presented.

7.2.2.4.1 Lower Carbonate Aquifer (Unit 5)

The results of hydraulic tests in the lower carbonate aquifer were reported for eight boreholes by Winograd and Thordarson (1975 [DIRS 101167], Table 3). For two of the boreholes, only transmissivity estimates based on specific capacity were made. Where permeability estimates based on drawdown curves were also available, these permeability estimates are based on specific capacity and were much lower than the estimates based on the drawdown curves. At five boreholes where both drawdown and recovery tests were conducted, the permeabilities estimated from recovery tests were several times higher than those estimated from drawdown tests. Both the drawdown and recovery data exhibited complex responses to pumping that were attributed to test conditions as well as to aquifer properties. These responses were manifested on log-linear plots of time versus drawdown as straight-line segments with distinct breaks in slope. Because they were unable to explain the differences in the results from the drawdown and recovery tests, Winograd and Thordarson (1975 [DIRS 101167], p. C25) advised against the use of the transmissivities estimated from the recovery tests. The transmissivities estimated from drawdown tests in the lower carbonate aquifer are listed for six boreholes in Table 7-5 along with thicknesses of the test intervals and the calculated permeabilities. The permeabilities were calculated from hydraulic conductivity values using a viscosity of 0.001 Pa-s, a density of 1,000 kg/m^3, and a gravitation acceleration of 9.81 m/s^2. These viscosity and density values are appropriate for test temperatures of about 25°C. The actual test temperatures were not reported by Winograd and Thordarson (1975 [DIRS 101167]) although they may have been substantially higher (greater than 50°C) than the temperatures assumed in this calculation, in which case the calculated permeabilities may overestimate the true permeabilities measured by the tests by a factor of 2 to 3. A statistical analysis of the base-10 logarithms of the permeabilities listed in Table 7-5 resulted in an estimated mean permeability for the carbonate aquifer of 0.60×10^{-13} m^2. The 95% lower and upper confidence limits for the mean permeability were 0.139×10^{-12} m^2 and 2.58×10^{-12} m^2, respectively.

Table 7-5. Permeabilities Calculated for the Lower Carbonate Aquifer

Well	Thickness (ft)	Transmissivity[a] (gpd/ft)[b]	Hydraulic Conductivity (gpd/ft^2)	Permeability (m^2)
67-73	281	20,000	71.2	3.44×10^{-12}
67-68	996	39,000	39.2	1.89×10^{-12}
66-75	753	11,000	14.6	0.705×10^{-12}
88-66	872	1,300	1.49	0.0719×10^{-12}
75-73	750	3,800	5.07	0.245×10^{-12}
84-68	205	2,400	11.7	0.565×10^{-12}

Source: Winograd and Thordarson 1975 [DIRS 101167], Table 3.

NOTE: Statistics for the logarithm of permeability (log *k*) are:
Mean = –12.223.
Standard deviation = 0.605.
Median = –12.200.
Lower 95% confidence level for mean = –11.740.
Upper 95% confidence level for mean = –12.708.

[a]These transmissivities were estimated by Winograd and Thordarson (1975 [DIRS 101167], Table 3) from drawdown curves.
[b]gpd is gallons per day.

In addition to providing quantitative estimates of the permeability, Winograd and Thordarson (1975 [DIRS 101167]) made several qualitative observations regarding the distribution of permeability within the carbonate aquifers.

The permeability data for the carbonate aquifer showed no systematic decrease either with depth beneath the top of the aquifer or beneath the land surface (Winograd and Thordarson 1975 [DIRS 101167], p. C20). The inference that groundwater may circulate freely within the entire thickness of the lower carbonate aquifer is not negated by chemical data that indicate no significant increase in the dissolved-solids content to depths of several thousand feet (Winograd and Thordarson (1975 [DIRS 101167], p. C103).

No major caverns were detected during drilling in the lower carbonate aquifer, despite the fact that approximately 4,900 m of the lower carbonate aquifer was penetrated in 26 holes drilled in 10 widely separated areas, including over 1,500 m at 13 holes beneath the Tertiary/pre-Tertiary unconformity, where caverns might be expected to exist (Winograd and Thordarson 1975 [DIRS 101167], p. C19). Drill-stem tests in three holes in the Rock Valley and Yucca Flat indicated negligible to moderate permeability immediately below the unconformity (Winograd and Thordarson 1975 [DIRS 101167], p. C20). Outcrop evidence indicates that klippen, which are the upper plates of low-angle thrust faults and gravity slump faults, have a higher intensity of fracturing and brecciation than rock below the fault planes and may have above-average porosity and permeability (Winograd and Thordarson 1975 [DIRS 101167], pp. C19 to C20). Specific capacity data for five wells penetrating the upper plates of low-angle faults in southern Yucca Flat and the northwestern Amargosa Desert indicated relatively high transmissivities for these plates (Winograd and Thordarson 1975 [DIRS 101167], p. C28).

The presence of hydraulic barriers within the lower carbonate aquifer is indicated in the hydraulic response in two-thirds of the wells pumped, indicating that zones of above-average transmissivity may often not be connected to each other (Winograd and Thordarson 1975 [DIRS 101167], p. C116). However, this observation needs to be reconciled with hydraulic and chemical evidence supporting the existence of a “mega channel” extending over 64 km between southern Frenchman Flat and the discharge area at Ash Meadows (Winograd and Pearson 1976 [DIRS 108882]).

7.2.2.4.2 Valley Fill Aquifer (Units 11, 26, 27, and 28)

The valley fill aquifer, as defined by Winograd and Thordarson (1975 [DIRS 101167], Table 1, p. C37) is composed of alluvial fan, fluvial, fanglomerate, lakebed, and mudflow deposits in depressions created by post-Pliocene block faulting. As defined, the valley fill aquifer of Winograd and Thordarson (1975 [DIRS 101167]) probably includes the Volcanic and Sedimentary Unit – Lower (Unit 11), the Older Alluvial Aquifer (Unit 26), the Young Alluvial Confining Unit (Unit 27), and the Young Alluvial Aquifer (Unit 28).

Transmissivity estimates for the valley-fill aquifer were made at six boreholes in Emigrant Valley, Yucca Flat, and Frenchmen Flat (Winograd and Thordarson 1975 [DIRS 101167], Table 3). For two of the boreholes, only transmissivity estimates based on specific capacity data were available. However, these estimates are considered unreliable because of the lack of agreement with transmissivity estimates based on drawdown or recovery curves at boreholes in

which both types of estimates were made. The transmissivity estimates made from drawdown and recovery curves were consistent at wells where both types of tests were conducted, in which case the transmissivity values from the drawdown and recovery curves were averaged to produce the transmissivity estimates listed in Table 7-6. Values used for the viscosity, density, and gravity terms in the expression for permeability are the same as those used for the lower carbonate aquifer. Based on a statistical analysis of the logarithm of the permeabilities listed in Table 7-5, the mean permeability of the valley fill is 1.57×10^{-12} m^2, and the 95% lower and upper confidence limits for the mean permeability are 0.095×10^{-12} and 26.0×10^{-11} m^2, respectively. The relatively high mean permeability calculated for the valley fill is probably more reflective of the permeability of the Young Alluvial Aquifer (Unit 20) and, possibly, the Volcanic and Sedimentary Unit – Lower (Unit 11) than of the Young Alluvial Confining Unit (Unit 27). Calibrated effective permeabilities for these units ranged from 0.0091 to 0.91×10^{-11} m^2.

Table 7-6. Permeability Estimates for the Valley Fill Aquifer

Well	Thickness (ft)	Transmissivity (gpd/ft)	Hydraulic Conductivity (gpd/ft^2)	Permeability (m^2)
74-70 [b]	511	2,200 [a]	4.31	0.208×10^{-12}
74-70 [a]	217	9,350 [b]	43.1	2.08×10^{-12}
83-68	264	12,700 [b]	48.1	2.32×10^{-12}
91-74	264	33,500 [c]	126.9	6.12×10^{-12}

Source: Winograd and Thordarson 1975 [DIRS 101167], Table 3.

NOTE: Permeability estimates based on transmissivity data from Winograd and Thordarson 1975 [DIRS 101167], Table 3.
Statistics for the logarithm of permeability (log *k*) are:
Mean = –11.803.
Standard deviation = 0.623.
Median = –11.658.
Lower 95% confidence level for mean = –12.413.
Upper 95% confidence level for mean = –11.193.

[a] Average is the arithmetic sum of the results of one drawdown and two recovery tests.
[b] Average is the arithmetic sum of the results of one drawdown and one recovery test.
[c] Representative Value is the result of one recovery test.
gpd = gallons per day.

In addition to providing the quantitative estimates of the permeability of the valley fill, Winograd and Thordarson (1975 [DIRS 101167]) also made numerous observations regarding the permeability of the valley fill at particular locations in the area of the NTS. Of special interest to this report are those observations made for the valley fill in the Amargosa Desert. Winograd and Thordarson (1975 [DIRS 101167], pp. C84 to C85) noted that hydraulic head contours south of Amargosa Valley (formerly called Lathrop Wells) probably reflect the effects of upward leakage from the lower carbonate aquifer into poorly permeable valley fill along the Gravity Fault and associated faults and of the drainage of this water to more permeable sediments farther west. Immediately west of the Gravity fault, gravity data indicate that downward displacement of the pre-Tertiary rocks west of the fault is 152.4 to 457.2 m at a location one mile east of Amargosa Valley and 365.8 to 670.6 m at a point 1.6 km southeast of the inferred intersection of the Specter Range Thrust fault and the Gravity fault. The low permeability of the valley fill immediately west of the Gravity fault was indicated by drillers' logs that showed valley fill in this area to be mainly clay. Winograd and Thordarson (1975 [DIRS 101167], p. C85) argued

that the discharge across the Gravity fault near Amargosa Valley was probably small because only the lower-most part of the lower carbonate aquifer is present in the area and the lower clastic aquitard, which underlies the carbonate aquifer at shallow depths, would probably not transmit much water.

7.2.2.4.3 Welded Tuff Aquifer (Units 19 and 20)

The welded tuff aquifer corresponds to the Timber Mountain and Paintbrush Volcanic Aquifer units (Units 19 and 20) of Table 6-2. Results of hydraulic tests conducted in the welded tuff aquifer were reported by Winograd and Thordarson (1975 [DIRS 101167], Table 3) for four wells, but only two wells, both in Jackass Flats, had transmissivity estimates based on drawdown curves. Well 74-57 tested the Topopah Spring tuff and well 74-61 tested both the Topopah Spring tuff and the Basalt of Kiwi Mesa. Permeabilities calculated from the drawdown curves at these wells are listed in Table 7-7. The geometric-mean permeability, based on the estimated permeabilities in Table 7-7, is 5.3×10^{-12} m^2. Calibrated effective permeabilities for these units are 0.065 and 0.076×10^{-11} m^2 for the Paintbrush and Timber Mountain Volcanic Aquifers, respectively.

Table 7-7. Permeability Estimates for the Welded Tuff Aquifer

Well	Thickness (ft)	Transmissivity (gpd/ft)	Hydraulic Conductivity (gpd/ft^2)	Permeability (m^2)
74-61	290	28,000	96.6	4.7×10^{-12}
74-57	547	68,000	124.3	6.0×10^{-12}

Source: Winograd and Thordarson 1975 [DIRS 101167], Table 3.

NOTE: Permeability estimates based on transmissivities determined from drawdown curves (Winograd and Thordarson 1975 [DIRS 101167], Table 3). Statistics: The geometric-mean permeability is 5.3×10^{-12} m^2.

gpd = gallons per day.

7.2.2.4.4 Lava Flow Aquifer (Unit 23)

Rhyolitic lavas and welded and nonwelded tuffs fill the Silent Canyon caldera complex, which now lies buried beneath Pahute Mesa by younger tuffs, erupted from the Timber Mountain caldera complex to the south (Blankennagel and Weir 1973 [DIRS 101233], p. 6; Laczniak et al. 1996 [DIRS 103012], p. 36). The permeabilities of the lava flows beneath Pahute Mesa are assumed to be an appropriate analogue for the Lava Flow Aquifer (Unit 23) near Yucca Mountain.

A qualitative comparison of the water-producing attributes of the lavas and tuffs based on the concept of specific capacity (in gal/min/ft of drawdown) indicated that despite considerable overlap in their water-yield potential, the lavas generally were the most transmissive rocks tested, followed by the welded tuffs and, finally, the zeolitized nonwelded tuffs (Blankennagel and Weir 1973 [DIRS 101233], Figure 4). Pumping tests were conducted in 16 boreholes at Pahute Mesa, including 14 where the major water production came from the rhyolitic lava flows (Blankennagel and Weir 1973 [DIRS 101233], Table 3). The borehole names, uncased saturated thickness, measured transmissivities, and calculated hydraulic conductivities and permeabilities associated with these 14 tests are provided in Table 7-8. The geometric-mean permeability of the rhyolitic lava is estimated to be 0.314×10^{-12} m^2, with 95% lower and upper confidence

limits of 0.119×10^{-12} m^2 and 0.825×10^{-12} m^2, respectively. However, these estimates should be viewed as approximate lower bounds because other less permeable rocks (welded and nonwelded tuffs) are present in the test interval, and these less permeable rocks would cause the transmissivity to be lower than the transmissivity that would be expected if only lava had been present. Resistivity logs indicated that nonwelded tuffs could constitute as much as 73% of the upper 2,000 ft of saturated rock at the boreholes listed by Blankennagel and Weir (1973 [DIRS 101233], Table 2). Because most of the water pumped from the lava enters the wells from zones that constitute only 3% to 10% of the total saturated thickness (Blankennagel and Weir 1973 [DIRS 101233], p. 11), permeabilities in the lava may be locally much higher than the calculated mean value. Calibrated effective permeability for the Lava Flow Unit is 0.088×10^{-11} m^2.

Table 7-8. Permeabilities of the Lava Flow Aquifer

Well	Uncased, Saturated Thickness (ft)[a]	Transmissivity (gpd/ft)[b]	Hydraulic Conductivity (gpd/ft^2)[b]	Permeability (m^2)
UE-18r	3,375	23,000	6.82	0.328×10^{-12}
TW-8	4,422	185,000	41.8	2.01×10^{-12}
UE19b-1	2,310	56,000	24.2	1.17×10^{-12}
UE19c	2,099	12,000	5.72	0.275×10^{-12}
UE-19d	5,129	20,000	3.90	0.188×10^{-12}
UE-19fs	2,214	11,000	4.97	0.239×10^{-12}
UE-19gs	1,858	30,000	16.1	0.777×10^{-12}
UE-19h	1,383	140,000	101.0	4.87×10^{-12}
UE-19l	5,104	1,400	0.274	0.0132×10^{-12}
U-20a-2	2,434	18,000	7.40	3.56×10^{-13}
UE-20d	2,047	44,000	21.5	1.03×10^{-12}
UE-20e-1	4,573	8,300	1.82	0.873×10^{-12}
UE-20f	9,230	1,000	0.108	0.00521×10^{-12}
UE-20h	4,701	11,000	2.34	0.113×10^{-12}

Source: Blankennagel and Weir 1973 [DIRS 101233], Table 3.

NOTE: Statistics for the logarithm of permeability (log k) are:
Mean = –12.503
Standard deviation = 0.801
Median = –12.466
Lower 95% confidence level for mean = –12.923
Upper 95% confidence level for mean = –12.084

[a] Uncased, saturated thickness was calculated as the depth of the well minus the depth to water or casing, whichever was greater. The depth to water was used for TW-8, where the casing was perforated.
[b] gpd = gallons per day.

7.2.2.5 Inferences About Permeability from Regional Observations

In addition to the permeability values from the NTS summarized in the previous section, Winograd and Thordarson (1975 [DIRS 101167]) made numerous qualitative evaluations of the relative magnitude of permeability for different hydrogeologic units. These evaluations were based on examination of cores containing fractures and mineral infilling, the geologic setting and the magnitude of discharge of springs in the region, and the correspondence between changes in hydraulic gradients and the underlying hydrogeologic unit. Sections 7.2.2.5.1 through 7.2.2.5.3 focus on qualitative assessments of hydrogeologic units that have little actual test data and for which the qualitative evaluations, thus, assume relatively more importance.

7.2.2.5.1 Lower Clastic Aquitard (Units 3 and 4)

The Lower Clastic Aquitard of Winograd and Thordarson (1975 [DIRS 101167], Table 1) corresponds to the Crystalline and Lower Clastic Confining Units unit (Units 3 and 4) of Table 6-2. According to Winograd and Thordarson (1975 [DIRS 101167], p. C43), the large-scale transmissivity of the lower clastic aquitard is probably controlled by its interstitial permeability, which, based on the hydraulic conductivity of 18 cores (Winograd and Thordarson 1975 [DIRS 101167], Table 4), ranges from $0.000000034 \times 10^{-12}$ m^2 to $0.0000048 \times 10^{-12}$ m^2 and has a median value of $0.000000097 \times 10^{-12}$ m^2. Although the lower clastic aquitard is highly fractured, Winograd and Thordarson (1975 [DIRS 101167], p. C43) argued that fractures probably do not augment the interstitial permeability of the unit on a regional scale to the same degree as in the lower carbonate aquifer because:

- The argillaceous formations within the unit have a tendency to deform plastically, that is, by folding, rather than by fracturing. Thus, fracture continuity across the lower clastic aquitard is disrupted by the argillaceous layers

- Micaceous partings and argillaceous laminae tend to seal the fractures in the brittle quartzite parts of the unit, reducing or eliminating the ability of the fractures to transmit water

- The clastic rocks that constitute the unit have a low solubility; therefore, solution channels, which can further enhance permeability along fractures in carbonate rocks, are not likely to be present in this unit.

The low permeability of the lower clastic aquitard compared to the carbonate rocks also was indicated by the observation that, in the Spring Mountains, the total discharge issuing from the lower clastic aquitard is only a small fraction of the total discharge of the springs in the lower carbonate aquifer (Winograd and Thordarson 1975 [DIRS 101167], pp. C42 to C43, C53). The comparatively low permeability of the clastic aquitard also is indicated by a head drop across the lower clastic aquitard of 610 m over a distance of less than 12.8 km (an apparent hydraulic gradient of 0.0476 m/m) in the hills northeast of Yucca Flat (Winograd and Thordarson 1975 [DIRS 101167], Plate 1). In contrast, the hydraulic gradient in the carbonate aquifer ranges from 0.00112 m/m or less along the axis of the potentiometric trough in Yucca Flat to 0.0038 m/m) along the flanks of the trough (Winograd and Thordarson 1975 [DIRS 101167], p. C71). The calibrated effective permeability of these units are the second and third lowest of all calibrated

values at 0.000060×10^{-11} and 0.000066×10^{-11} m^2 for the Crystalline and Lower Clastic Confining Units, respectively.

7.2.2.5.2 Upper Clastic Aquitard (Unit 6)

The upper clastic aquitard is equivalent to the Upper Clastic Confining Unit (Unit 6) of Table 6-2. The upper clastic aquitard corresponds to the Eleana formation, which consists of argillite, quartzite, conglomerate, and limestone (Winograd and Thordarson 1975 [DIRS 101167], Table 1). The upper two-thirds of the unit consists mainly of argillite, whereas the lower one-third of the unit is principally quartzite (Winograd and Thordarson 1975 [DIRS 101167], p. C118). Winograd and Thordarson (1975 [DIRS 101167], p. C43) argued that fractures were unlikely to remain open in the rock at depth because of the plastic deformation behavior of the rock, which is evidenced by tight folds, and the fact that the formation serves as a glide plane for several thrust faults at the NTS. No core-scale permeability measurements exist, but based on analogy with the lower clastic aquitard, its interstitial permeability probably is less than 0.000048×10^{-12} m^2 (Winograd and Thordarson 1975 [DIRS 101167], p. C43). In the hills northwest of Yucca Flat, an approximately 610-m drop in hydraulic head in the pre-Tertiary rocks over a distance of less than 16 km (an apparent hydraulic gradient of 0.038 m/m) suggests a comparatively low regional permeability for the upper clastic aquitard. However, because land-surface elevation changes abruptly over this same distance and because water table elevations often mimic ground-surface elevations, it is not possible to isolate the effects of permeability from the effects of topography on the head gradient in this area. The calibrated effective permeability for the Upper Clastic Confining Unit is 0.00018×10^{-12} m^2.

7.2.2.5.3 Faults

A summary of the possible effects of faults on groundwater movement in the Death Valley region is presented by Faunt (1997 [DIRS 100146], p. 30). The transmissivity of faults was described to be a function of:

- The orientation of the fault relative to the minimum horizontal stress in the region
- The amount and type of fill material in the fault
- The relative transmissivities of hydrogeologic units juxtaposed by offset across the fault
- The solubility and deformation behavior of the rock adjacent to the fault
- Recent seismic history.

7.2.2.5.3.1 Orientation of Faults Relative to the Minimum Horizontal Stress in the Region

In the vicinity of Yucca Mountain, the mean azimuth of the minimum horizontal stress is 306 ± 11 degrees (Faunt 1997 [DIRS 100146], Table 4-4), so that faults with traces oriented north-northeast are expected to be more open and permeable than faults with traces oriented in directions that place them in either a shear or a compressive state. Faults oriented northwest, or perpendicular to the maximum horizontal stress direction, would be expected to be least transmissive, all other factors being equal. One example cited by Faunt (1997 [DIRS 100146], pp. 34 to 35) to illustrate the northeast-southwest trending structures that may have relatively high transmissivity is the "mega channel" formed in the Spotted Range-Mine Mountain shear zone between Frenchman Flat and Ash Meadows. The presence of a highly transmissive zone in the carbonate aquifer was indicated by a potentiometric trough in this area and relatively young

^{14}C ages of groundwater discharging from springs at the distal end of the trough (Winograd and Pearson 1976 [DIRS 108882]).

7.2.2.5.3.2 Amount and Type of Infilling Material in the Fault

Fine-grained gouge or clayey infilling material can cause faults to become poorly transmissive, even if their orientation relative to the stress field indicates they have the potential to be highly transmissive. The effects of deformation behavior, solubility, and infilling material in the clastic aquitards and carbonate aquifer were discussed in Sections 7.2.2.5.1 and 7.2.2.5.2. Solution channels along faults in the carbonate rock have the potential to further enhance the transmissivity of faults in this unit.

7.2.2.5.3.3 Relative Transmissivities of Hydrogeologic Units Juxtaposed by Offset Across the Fault

Where faults juxtapose hydrogeologic units with contrasting permeabilities, the hydrologic effects caused by juxtaposition may be difficult to isolate from the effects of the fault properties themselves. As indicated by Faunt (1997 [DIRS 100146], Figure 16), an increase in the local head gradient compared to the regional gradient can occur across a fault if:

- The fault is closed, thereby blocking flow
- The fault is open, thereby redirecting flow
- The permeability of the material downgradient of the fault is low compared to the upgradient material, so that flow across the fault is blocked
- The permeability of the material downgradient of the fault is high compared to the upgradient material, so that flow can drain away from the fault faster than it can be delivered by the upgradient material.

Evidence that springs in Ash Meadows are caused by the juxtaposition of poorly permeable sediments and rocks downgradient of the carbonate aquifer across the Gravity fault was presented by Winograd and Thordarson (1975 [DIRS 101167], p. C82). Hydraulic data in southern Indian Springs Valley were interpreted by Winograd and Thordarson (1975 [DIRS 101167], pp. C67 to C68) to indicate the presence of two hydraulic barriers related to the Las Vegas shear zone: (1) a northern barrier caused by the juxtaposition of the lower clastic aquitard and lower carbonate aquifer; and (2) a southern barrier, which was attributed to the presence of gouge along a major fault zone.

7.2.2.5.3.4 Recent Seismic History

The seismic history of the faults may indicate which faults have undergone recent movement. Recent movement on a fault may serve to break calcite or silica cement or other material that may have closed the fault. A map showing which faults or fault segments near Yucca Mountain have undergone recent movement was developed by Simonds et al. (1995 [DIRS 101929]). Of the faults that have been mapped near the repository area, only the Solitario Canyon fault and short segments of the Bow Ridge Fault near Exile Hill show evidence of late Quaternary (or more recent) movement.

7.2.2.6 Comparing Permeability Data to Calibrated Permeability Values

To check if the calibrated effective permeabilities are reasonable, the logarithms of permeabilities estimated during calibration of the model are compared to the logarithms of permeability estimated from pump-test data near Yucca Mountain and elsewhere at the NTS in Figure 7-4. Where they could be estimated, the 95% confidence limits for the mean logarithm of the permeability data error bars also are shown. For the Calico Hills Volcanic Unit, the Prow Pass, Bullfrog, and Tram tuffs, and the MVA permeabilities are shown for both the single- and cross-hole tests at the C-wells complex. As shown in Figure 7-4, most of the calibrated permeabilities fall within the 95% confidence interval on the mean measured permeability for single- and cross-hole tests or are within a factor of two of these ranges (within 50%). Therefore, with the exception of the lower clastic aquitard and the welded tuff, which are far from the flowpaths, the validation criterion for permeability is satisfied.

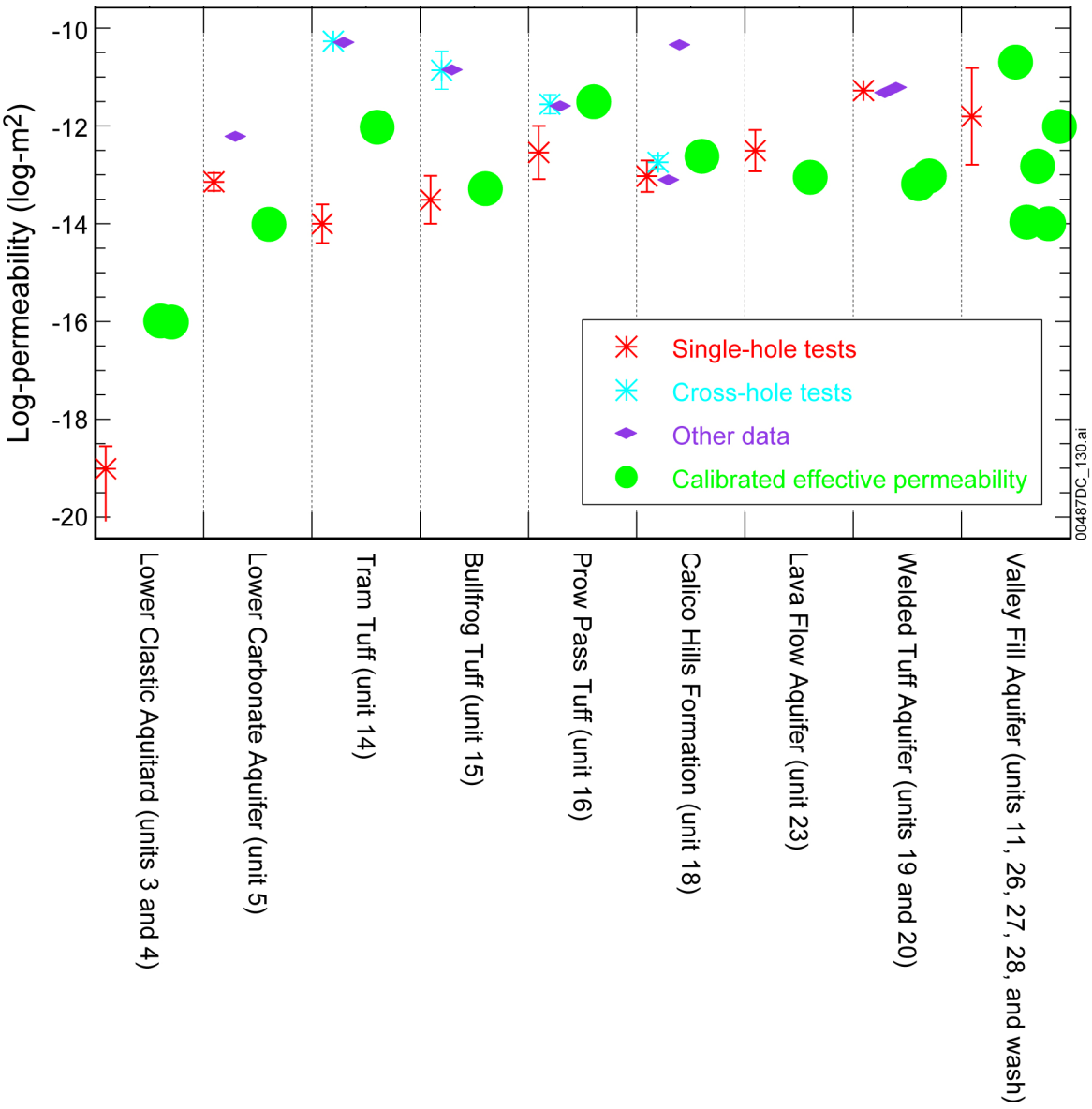

Source: DTN: SNT05082597001.003 [DIRS 129714].

NOTE: Bars on single- and cross-holes tests represents the 95% confidence interval on the mean.

Figure 7-4. Logarithms of Effective Permeabilities Estimated During Model Calibration Compared to Logarithms of Permeability Determined from Pump-Test Data

Calibrated effective permeabilities for the lower clastic aquitard are higher than those discussed in Section 7.2.2.5.1; however, the calibrated values are among the lowest in the model and consistent with the current understanding of the geology. Considering its depth below the surface and associated depth decay, it is perhaps surprising that the Lower Carbonate Aquifer (Section 7.2.2.4.1) permeabilities based on transmissivity measurements are among the highest in the model domain. The calibrated effective permeability for the Lower Carbonate Aquifer was nevertheless within the 95% uncertainty interval. Despite this lower calibrated effective

permeability, the Lower Carbonate Aquifer remained the primary water bearing unit in the model.

Overall, the calibrated effective permeabilities show trends consistent with permeability data from Yucca Mountain and elsewhere at the NTS. The calibrated effective permeability of the three Crater Flat tuffs and Calico Hills formation are all within the values measured in the field. The relatively high permeability estimated for the Tram tuff from the cross-hole tests may be at least partially attributable to local conditions at the site of these tests. A breccia zone is present in the Tram tuff at boreholes UE-25 c#2 and UE-25 c#3 (Geldon et al. 1997 [DIRS 100397], Figure 3) that may have contributed to a local enhancement in the permeability of the Tram tuff.

Calibrated effective permeabilities for units corresponding to the Lava Flow Aquifer and the valley fill aquifer are within the range of measured permeabilities. The calibrated effective permeabilities of units corresponding to the Welded Tuff Aquifer are more than an order of magnitude lower than field estimates, but no confidence intervals are available and calibrated values would probably fall within these limits if they were available.

7.2.3 Specific Discharge

Although the calibrated permeabilities of any geologic unit or feature in the SZ site-scale flow model indirectly influence the simulated specific discharge, those geologic units along the flowpath from the repository to the compliance boundary directly determine the simulated specific discharge. Particle tracking using the SZ site-scale model (see Section 6.5.2.4) indicates that fluid particles migrating from the repository generally enter the SZ in the Crater Flat units (see Figure 6-22). Because of the high permeabilities of these units and the small hydraulic gradient, the particles remain in those units until reaching their southern ends. At this point, flow generally enters the alluvial portion of the flow system after briefly transitioning through the Paintbrush Volcanic Aquifer. The flowpath through the alluvial deposits is represented in the SZ site-scale model by the Lower Fortymile Wash alluvium. Thus, those calibrated permeabilities that most directly control the simulation of specific discharge by the SZ site-scale model are those for the Crater Flat units and the Lower Fortymile Wash alluvia.

The 18-km compliance boundary shown on Figure 6-17 and discussed throughout other documents (SNL 2007 [DIRS 177392]) are strongly influenced by groundwater flow in alluvium. Estimates of specific discharge in the SZ were recently obtained from field-testing at the ATC (SNL 2007 [DIRS 177394], Section 6.5.5). The ATC is located approximately 18 km from Yucca Mountain at the boundary of the accessible environment as specified at 10 CFR 63.302 [DIRS 176544]. The specific discharge from the repository to the 18-km compliance boundary was 0.55 m/yr (average across all flowpath lengths divided by travel times), although much of the time along this flowpath is spent in the slower flowing volcanic units indicating that the specific discharge in the alluvial material is higher than in the volcanics. The technique used to estimate specific discharge at locations within the SZ site-scale flow model corresponding to the locations where measurements are available (UE-25 c#3, NC-EWDP-22S, and NC-EWDP-19P) was to isolate a cubic volume within 1,000 m of the well location extended to 10 m above and below the entire open interval and to calculate the average specific discharge across all flowing nodes. The ATC testing was performed in the alluvium aquifer and estimates of groundwater specific discharge at the ATC range from 0.5 to 12 m/yr.

For a discussion of flow porosity in alluvium see *Saturated Zone In-Situ Testing* (SNL 2007 [DIRS 177394], Section 6.4).At the NC-EWDP-22S location the testing specific discharge was estimated with three methods. Based on analyses using the peak arrival analysis the testing estimated values range between 0.5 and 1.2 m/yr. Based on the high-recovery analysis, the testing estimated values range between 2.2 and 5.4 m/yr). Based on the analysis of hydraulic head/conductivity data the testing estimated values range between 3 and 12 m/yr). The testing estimate is about 7.3 m/yr at NC-EWDP-19D. Model-simulated specific discharge at NC-EWDP-22S and -19P are 21.0 and 11.7 m/yr, respectively. These relatively high values correspond to the high effective permeability assigned to the Lower Fortymile Wash Alluvium model unit, but it is still within the factor of 3 specified in the TWP (see Section 7.2). Although there were no specific discharge measurements from the C-wells tests, the average modeled specific discharge at nodes surrounding the C-wells was 1.75 m/yr.

The model-simulated specific discharge at the NC-EWDP-22S location is higher than the test-derived values. At NC-EWDP-19D, the model-simulated value is slightly higher than the testing values. Several points could be made to explain this:

- Testing estimates come from a methodology that involves several assumptions that have never been "validated" in a situation where the actual specific discharge or seepage velocity is known. Thus, there may be unknown biases associated with the method that result in low estimates (alternatively, it could be argued that these biases might be in the other direction, yielding high estimates).

- Testing estimates are obtained over an extremely small scale relative to the flow-model scale. The discrepancies could easily be due to the fact that the few cubic meters interrogated in the tracer tests happen to be in a zone of lower specific discharge (due to slightly lower permeability) than the surrounding alluvium. Also, the measurements were made over only a 30-m (100-ft) interval of a 200-m (650-ft) -thick section of saturated alluvium, whereas the flow model integrates specific discharge over a significantly larger flow area. A somewhat more permeable layer above or below the test interval could easily account for the discrepancy. If one has a conceptual model that flow in the alluvium is focused into ancestral Fortymile Wash channels (as is commonly observed in this type of environment), then it is unlikely that the test interval would have intersected such a channel.

- The fact that the head and hydraulic conductivity estimates are closer to the modeled specific discharge is not surprising given that the hydraulic conductivity estimates were obtained from hydraulic tests that effectively interrogate a larger volume than the tracer tests. Also, they are partly based on heads along Fortymile Wash to which the flow model is calibrated.

- Finally, the zone of enhanced permeability along Fortymile Wash in the model may be partly responsible for an elevated estimate of specific discharge in the model. Flow will naturally channel into such a zone and the specific discharge can be expected to be higher in such a zone than in surrounding media. This again gets at the scale issue: if there is in fact such a zone, is it relatively homogeneous, or does it have significant heterogeneity within it that could account for the discrepancies?

The simulated average specific discharge across the 5-km boundary ranges from 0.35 to 0.38 m/yr for differing values of horizontal anisotropy in permeability ranging from 20 to 0.05 (0.36 m/yr for the expected horizontal anisotropy values of 5:1 N-S to E-W with end members of the 100-particle distribution of 0.11 to 0.66 m/yr). This compares to the 0.6 m/yr derived by the Expert Elicitation Panel (CRWMS M&O 1998 [DIRS 100353], Section 3.2) and is also within their range, which actually spans nearly five orders of magnitude. The data from ATC field testing yielded specific discharge estimates ranging from 1.2 to 9.4 m/yr while testing at NC-EWDP-22S ranged from 0.47 to 5.4 m/yr. A distribution of specific discharge multipliers was developed (SNL 2007 [DIRS 177390], Section 6.5.2.1) that ranged from 1/30th to 10 times the nominal value. Recently, that range was reduced to 1/8.93 and 8.93 times nominal specific discharge (SNL 2007 [DIRS 177390], Section 6.5.2). In addition to a distribution in specific discharge, uncertainty in effective porosity (variable effective porosity in conjunction with specific discharge can result in highly variable flow velocities through the SZ) is implemented through the use of a truncated normal distribution in the SZ transport abstraction model (SNL 2007 [DIRS 177390], Section 6.5.2.3). The details of the uncertainty distributions of specific discharge multiplier and effective porosity in the alluvium and their associated sampling techniques are contained in the SZ flow and transport abstraction model (SNL 2007 [DIRS 177390], Sections 6.5.2.1 and 6.5.2.3).

7.2.4 Comparison of Hydrochemical Data Trends with Calculated Particle Pathways

Groundwater flowpaths and mixing zones were identified in Appendices A and B in the analyses of the areal distributions of measured and calculated geochemical and isotopic parameters, scatter plots, and inverse mixing and reaction models Flowpaths of tracer particles were calculated with the SZ site-scale flow model. The particles were started below the repository footprint and allowed to transport downstream to the model boundary. These flow pathways are compared to flowpaths deduced from hydrochemical data shown in Figure 7-5. These flowpaths must be evaluated in the context of the hydraulic gradient while considering the possibility that flowpaths can be oblique to the potentiometric gradient because of anisotropy in permeability. Theses flowpaths were drawn by first using chemical and isotopic constituents generally considered to behave conservatively in groundwater such as chloride (Cl^-) and sulfate (SO_4^{2-}) ions. However, because no single chemical or isotopic species varies sufficiently to determine flowpaths everywhere in the study area, multiple lines of evidence were used to construct the flowpaths. This evidence includes the areal distribution of chemical and isotopic species, sources of recharge, groundwater ages and evaluation of mixing/groundwater evolution through scatter plots, and inverse mixing and reaction models as presented in Appendices A and B. The derivation of flow pathways from hydrochemical data is developed in detail in Appendices A and B and summarized in Sections B6.6 and B7.

Of particular interest are the Flow Paths 2 and 7 from this analysis. As shown in Figure 7-5, Flow Path 7 originates in the vicinity of the repository footprint and overlaps the model-calculated flowpaths. Flow Path 2 is also of interest, although it originates northeast of the repository, because it closely bounds Flow Path 7 to the east. Although flow pathways derived from hydrochemical data do not originate in the same location as particle tracks derived from the site-scale model, the paths converge east and south of the repository.

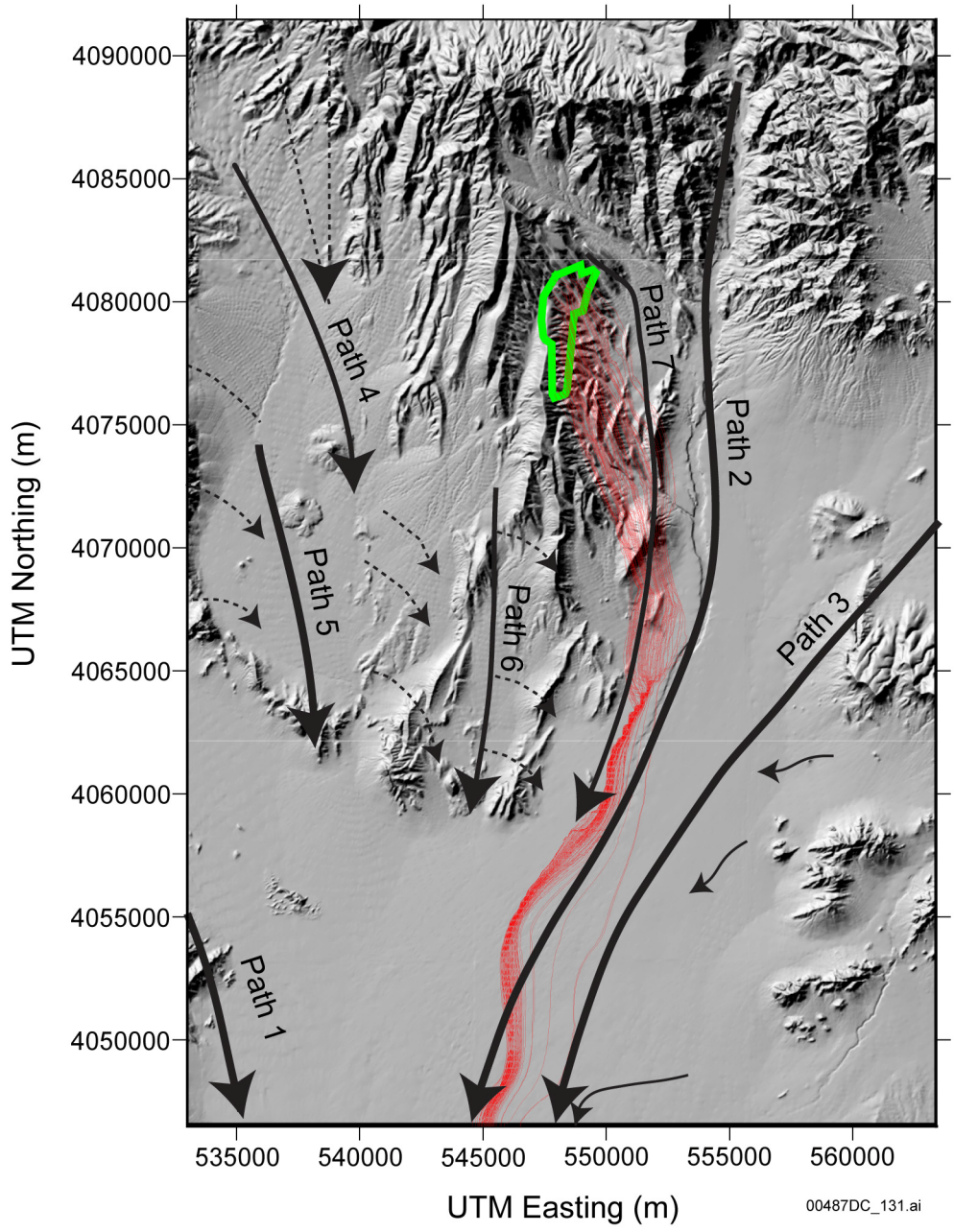

Source: Appendix B, Figure B6-15.

NOTE: Solid lines indicate a relatively high degree of confidence in the interpretations; dashed flow paths indicate relatively less confidence. Thin solid lines represent Path 8. Flowpaths inferred from hydrochemistry data are in black and flowpaths calculated for tracer particles starting at the inferred repository footprint are in red.

UTM = Universal Transverse Mercator.

Figure 7-5. Transport Pathways Deduced from Hydrochemistry Data Compared to Particle Pathways Calculated for the SZ Site-Scale Transport Model

7.3 VALIDATION SUMMARY

The SZ site-scale flow model has met the established validation criteria. A comparison of the simulated and observed water levels from the newly installed NC-EWDP Phase V wells demonstrates that the SZ site-scale flow model can reliably simulate the water levels and gradients along the flowpath from the repository. An analysis of the impact of the differences between observed and simulated hydraulic gradients on the flowpaths from the repository has identified only a minimal impact on the specific discharge that meets the validation criteria established for this comparison.

A comparison of the permeability measurements from the ATC with the calibrated effective permeability values for the valley fill aquifer has similarly indicated agreement between calibrated and measured values. An analysis of the impact of differences between calibrated and measured permeability on the flowpaths from the repository has demonstrated only a minimal impact on the specific discharge, which easily meets the validation criteria established for this comparison.

The comparison between the flowpaths simulated by the SZ site-scale flow model and those indicated by hydrochemical analyses has demonstrated close agreement between these flowpaths, with the flowpaths derived from hydrochemical analysis generally enveloping those simulated by the SZ site-scale flow model.

The SZ site-scale flow model has been validated by applying acceptance criteria based on an evaluation of the model's relative importance to the potential performance of the repository system. Activities for confidence building during model development have been satisfied (Sections 7.1.1 and 7.1.2). Also, all post-development model validation requirements defined in the TWP (BSC 2006 [DIRS 177375], Section 2.2) have been fulfilled (with justification for any changes in the validation criteria), including corroboration of model results with hydrochemical and water-level data that were not used in the model development (Sections 7.2.1, 7.2.3, and 7.2.4). The model development activities and the post-development model validation activities describe the scientific basis for the SZ site-scale flow model. No future activities are needed for model validation. The model validation activities establish that the SZ site-scale flow model is adequate and sufficiently accurate for the stated and intended purpose.

8. CONCLUSIONS

The SZ site-scale flow model is the culmination of enormous efforts incorporating volumes of geologic, hydrologic-testing, and geochemical data into a coherent representation of flow through the SZ near Yucca Mountain. This model is based upon a three-dimensional finite-element mesh with 250×250 m^2 horizontal elements that grid convergence studies have shown to represent the hydrogeologic framework adequately without introducing significant numerical error. Additionally, the model's vertical resolution varies from 10 to 600 m with finest resolution near the water table in the area under Yucca Mountain. This model is calibrated to and reproduces two important data sets: the observed potentiometric surface (water-level data) and boundary fluxes obtained from the SZ regional-scale flow model. In addition, the SZ site-scale flow model matches other data quantitatively and qualitatively. These data include permeability values derived from single- and multiple-well tests, hydrochemical data, and those specific discharges estimated from the Expert Elicitation Panel (CRWMS M&O 1998 [DIRS 100353], Section 3.2) and derived through field testing.

The SZ site-scale flow model matches much of the existing SZ-related data, particularly with respect to the inferred fluid pathways below the repository area. The hydrochemical data were used as a quality check for flowpath direction. The SZ model produced flowpaths from the repository area that agree with those inferred from geochemical information. However, there was a bias in the calibration, notably in the small-gradient area where the calibrated heads were consistently 2 to 5 m higher than the observations. More importantly, however, the gradient was accurately represented despite the bias.

When using the SZ site-scale flow model for TSPA calculations, three limitations must be noted:

- Changes to calibration parameter values. Some calibration parameters can be varied over a moderate range, and the overall calibration is not adversely affected. For example, calibration was performed assuming a single set of anisotropic horizontal permeabilities, while the performance assessment model runs incorporate a range of anisotropic permeabilities. Incorporating anisotropy resulted in a better calibration than isotropic conditions, but model runs using the limits to the distribution (0.05 and 20) yielded weighted RMSEs of 0.82 and 0.83 m, which also certainly maintain calibration. If anisotropies outside this range are used, an assessment on calibration should be made.

- Usable flowpath distances. The continuum approach used for the SZ site-scale flow model requires large grid blocks that effectively average fracture and rock matrix properties. To produce meaningful results, the flowpath should be long compared to the grid block size.

- Overall model recharge fluxes. Because the SZ site-scale flow model is linear, recharge fluxes may be changed to reflect uncertainty in specific discharge, so long as the boundary fluxes and permeabilities are changed proportionally.

8.1 SUMMARY OF MODELING ACTIVITIES

The SZ site-scale flow model was developed in several stages. First, the hydrogeology of a region around Yucca Mountain was numerically characterized by the DVRFS model (Section 6.3). Second, a detailed conceptual model of flow processes was developed for a smaller region (i.e., the site-scale) appropriate for TSPA calculations (Section 6.4). Third, a numerical model of groundwater flow was developed and calibrated (i.e., the SZ site-scale flow model, Section 6.4.2). Fourth, a series of validation activities was completed to provide confidence in the SZ site-scale flow model and its output (Section 7). Finally, results of this model were presented (Section 6.5.2) and the associated uncertainties were discussed (Section 6.7).

8.1.1 Saturated Zone Flow Characterization

Much information is available about the regional-scale hydrogeology at Yucca Mountain, both from site characterization activities as well as from numerous hydrogeologic studies that have been conducted at the NTS. Specifically, sufficient data are available to describe the stratigraphy, structure, and hydraulic properties of component media, recharge and discharge regions, and groundwater flowpaths.

The climate in the Yucca Mountain area is arid and the water table varies from hundreds of meters below ground surface in the northern part of the model to tens of meters below ground surface in the southern part of the model. Natural recharge to the saturated zone is from precipitation percolating through the unsaturated zone. Recharge occurs primarily in mountainous areas where there is more snow and rainfall (i.e., Yucca Mountain, including regions of higher elevation to the north and northeast, and the Spring Mountains 50 km southeast of Yucca Mountain). Estimates of recharge rates at the regional scale are based on empirical relationships and the SZ regional-scale model ensures equal SZ recharge and discharge. Flowpaths in the saturated zone are well characterized at the regional scale because numerous water-level measurements are available.

The fluxes from the SZ regional-scale flow model were used as targets because this model represents a calibrated water balance of the Death Valley hydrologic system with fluxes constrained by data from spring flows and infiltration rates. Boundary fluxes can help link the SZ site-scale flow model to other global-water-balance data, if necessary. The SZ site-scale flow model reasonably matched net flux data from the SZ regional-scale flow model.

In the area near Yucca Mountain, water-level measurements, hydraulic testing in wells, and geochemical analyses provide additional information about groundwater flow in the SZ. Water-level measurements indicate considerable differences in the magnitude of the hydraulic gradient between areas to the north (large hydraulic gradient), to the west (moderate hydraulic gradient), and to the southeast (small hydraulic gradient) of Yucca Mountain. The hydraulic gradient drives flow from the repository to the south and southeast. A vertical, upward hydraulic gradient from the underlying carbonate aquifer and the deeper volcanic units is also observed in some wells immediately downgradient of Yucca Mountain. Data on groundwater chemistry indicate significant spatial variability in geochemical and isotopic composition that results from differences in flowpaths, recharge locations, and groundwater age.

Because the performance of the Yucca Mountain repository is evaluated over thousands of years, the possible impacts of a future wetter climate must be considered. The general locations of areas of recharge and discharge depend primarily on the topography of the land surface. Modeling studies suggest that increased recharge would result in a higher water table and steeper hydraulic gradients. Field mapping of zeolite and paleospring deposits has confirmed that a higher water table existed during past, wetter climates and supports numerical simulations of the possible impacts of climate change. Consequently, wetter climates in the future are expected to result in faster groundwater flow rates along present-day flowpaths. The impacts of an elevated water table are discussed in the SZ transport model report (SNL 2007 [DIRS 177392], Section 6.6 and Appendix E1).

As groundwater in the Death Valley system moves from recharge to discharge areas, flow rates and paths depend largely on the hydraulic properties of the media along the flowpaths. Geologic studies have identified the important rock types and their spatial distribution. The rock types that play the largest role in regional hydrogeology are Paleozoic carbonates, Quaternary-Tertiary volcanic rocks, and Quaternary-Tertiary sediments and volcanic tuffs that fill structural depressions (referred to as valley-fill material in portions of this report). Relatively shallow flow occurs in the volcanic rocks and valley fill (primarily alluvium), and deeper flow occurs in the regionally extensive carbonate aquifer. Along the inferred shallow flowpath, groundwater flowpaths originate in volcanic rocks near the repository site and continue into younger valley-fill deposits at greater distances.

The permeabilities of the volcanic rocks near Yucca Mountain are increased by the presence of fractures. An extensive suite of field observations, interpretations of borehole logs, boreholes hydrologic tests, lab-scale tests, and field tracer tests (C-wells complex) confirms that fractures dominate groundwater flow in the volcanic rocks. However, flow in the alluvium occurs through the primary porosity of these sediments.

8.1.2 Conceptual Model of SZ Site-Scale Flow

The SZ site-scale conceptual model is a synthesis of what is known about flow processes at the scale required for TSPA calculations. This knowledge builds upon, and is consistent with, information collected across the regional scale, but it is more detailed because a higher density of data is available at the site-scale.

Information from geologic maps and cross sections, borehole data, fault-trace maps, and geophysical data were used to construct the HFM, a three-dimensional interpretation of the hydrostratigraphy and geologic structure of the SZ site-scale flow model. Rock stratigraphies within the framework model are grouped into 27 hydrogeologic units that are classified as having either relatively large permeability (aquifers) or relatively small permeability (confining units). The framework model specifies the position and geometry of these hydrogeologic units. In addition, the framework model identifies major faults that affect groundwater flow.

The source of most of the groundwater flow in the SZ site-scale flow model is lateral flow through the western, northern, and eastern boundaries. A small portion (approximately 10%) of the total flux through the SZ site-scale flow model is from precipitation and surface runoff infiltrating along Fortymile Wash. Outflow from the site-scale region is chiefly through the

southern boundary although there is some local outward flow on the eastern boundary. A small amount of water is removed by pumping wells located in the Amargosa Valley near the southern boundary of the model domain. As groundwater moves away from the repository, it first flows through a series of welded and nonwelded volcanic tuffs with relatively low specific discharge. These flowpaths eventually pass into alluvium where the specific discharge is greatest.

8.1.3 Mathematical Model and Numerical Approach

The mathematical basis (Section 6.4.1) and associated numerical approaches of the SZ site-scale flow model is designed to assist in quantifying the uncertainty in the rate and mass transport of radionuclides. In so doing, parameters such as effective permeability of rocks in the geologic framework model must be represented accurately. An automated parameter estimation approach is used to obtain the distribution of rock permeabilities yielding hydraulic heads that best matched measured values, as well as lateral-flow rates across model boundaries that are compatible with results from the SZ regional-scale flow model.

Calculations of groundwater flow (the flow field) are made under steady-state assumptions. The approach of not explicitly representing fractures in the volcanic rocks is reasonable at the scale required for the TSPA (tens of kilometers), but is less accurate at length scales shorter than the dimensions of model grid blocks (less than 250 m).

8.1.4 Model Validation and Confidence Building

Model development activities have been performed with confidence building criteria to ensure the scientific basis for the model (Section 7.1.1 and 7.1.2). Additional confidence in the results of the SZ site-scale flow model was built by comparing: (1) calculated to observed hydraulic heads and associated hydraulic gradients (Section 7.2.1); and (2) calibrated to measured permeabilities and therefore specific discharge (Section 7.2.2). In addition, it was confirmed that the flowpaths leaving the region of the repository are consistent with those inferred from independent water-chemistry data.

8.2 OUTPUTS

The primary technical output from this model (Section 6.5) comprises the SZ site-scale flow model and associated input and output files for current and future wetter climatic conditions. Output from the SZ site-scale flow model is used directly in SZ transport and abstractions models that yield radionuclide breakthrough curves. Specifically, the output from the SZ site-scale flow model can be used to simulate flowpaths from the water table beneath the repository horizon to the accessible environment and to estimate corresponding specific discharges. The computer files associated with the SZ site-scale flow model are archived in Output DTN: SN0612T0510106.004.

Additional technical outputs from this model report are listed in Table 8-1, but are considered intermediate outputs insofar as they were developed in this report to support the development, calibration, or validation of the primary technical output.

Table 8-1. Output Data

DTN	Intermediary?	Description
LA0612RR150304.001	Yes	NC-EWDP UTM coordinates
LA0612RR150304.002	Yes	Underground Testing Area geochemical data
LA0612RR150304.003	Yes	NC-EWDP geochemical data
LA0612RR150304.004	Yes	Hydrochemical flowpaths
LA0612RR150304.005	Yes	Uranium activity ratios for groundwaters
LA0612TM831231.001	No	LaGriT HFM2006 surfaces
MO0611SCALEFLW.000	No	Potentiometric surface
SN0610T0510106.001	Yes	NC-EWDP well location and water-level data
SN0612T0510106.003	Yes	Infiltration data
SN0612T0510106.004	No	SZ site-scale flow model output
SN0702T0510106.006	No	FEHM model of water table rise
SN0702T0510106.007	Yes	NC-EWDP well data used for SZ flow model potentiometric surface, calibration and validation
SN0704T0510106.008	No	Water-level and particle-track output from the calibrated model
SN0705T0510106.009	Yes	PEST v11.1 analyses

8.3 OUTPUT UNCERTAINTY

This section describes remaining uncertainties associated with the nominal flow field. Specifically, the section recommends how the uncertainty in metrics associated with model outputs (specific discharge and flowpaths) should be considered.

8.3.1 Specific Discharge Uncertainty Range

Because uncertainty in permeability translates into uncertainty in specific discharge (given a constant head gradient), insight gained when investigating permeability values during calibration has relevance to specific discharge estimates. Also, recall that for linear models such as this, calibration to hydraulic heads is preserved when scaling the fluxes, recharge, and permeabilities proportionally. The 95% confidence interval for calibrated permeabilities (Output DTN: SN0612T0510106.004, *sz_site_2006.rec*) typically spans 3 or more orders of magnitude. While this range could yield major changes in specific discharge in a homogeneous system, no single change in permeability by up to an order of magnitude yielded even a factor of 2 change in specific discharge because surrounding permeability values strongly impact the flow into/out of the altered unit. It can be concluded that even if calibrated permeabilities are in error by more than an order of magnitude for any given unit, the specific discharge output from the model will remain within the uncertainty limits developed elsewhere for use in TSPA (e.g., 1/8.93 to 8.93 times nominal value (SNL 2007 [DIRS 177390], Section 6.5.2.1)). Experience with the calibrated SZ site-scale flow model indicates that the range of specific discharges used for TSPA is large enough to encapsulate all the uncertainties assumed during the development and calibration of this model.

The specific discharge from the repository to the 18-km compliance boundary is 0.55 m/yr, although much of the distance along this flowpath is in the slower flowing volcanic units indicating that the specific discharge in the alluvial material is higher than in the volcanics. The technique used to estimate specific discharge at locations within the SZ site-scale flow model alluvial material corresponding to the locations where measurements are available (NC-EWDP-22S, and NC-EWDP-19P) was to isolate a cubic volume within 1,000 m of the well location extending 10 m above and below the entire open interval and to calculate the average specific discharge across all flowing nodes. Measured groundwater specific discharges from alluvial pump tests range from 0.47 to 9.4 m/yr (SNL 2007 [DIRS 177394], Tables 6.5-5 and 6.5-6). For the expected flow porosity in the alluvium of 0.18 (SNL 2007 [DIRS 177394], Section 6.4), the field-test-derived specific discharges ranged from 0.89 m/yr at NC-EWDP-22S to 7.3 m/yr at NC-EWDP-19P. Model-simulated specific discharges at NC-EWDP-22S and -19P are 20.97 and 11.75 m/yr, respectively. These relatively high modeled values correspond to the high effective permeability assigned to the model unit for the Lower Fortymile Wash alluvium, but they are still within the factor of 3 of the upper end of test-derived expected value (7.3 m/yr) and therefore meet the validation criterion established by the TWP (BSC 2006 [DIRS 177375, Section 2.2.2.1). Comparatively little sensitivity was seen to horizontal anisotropy in the volcanics; the modeled average specific discharge across the 5-km boundary ranges from 0.35 to 0.38 m/yr for values of N-S to E-W horizontal anisotropy in permeability of 0.05 to 20, respectively (SNL 2007 [DIRS 177394], Section 6.2.6). Although there were no specific discharge measurements from the C-wells tests, the modeled value was estimated at 1.75 m/yr within 1,000 m of the C-wells. Finally, the nonlinear maximum calibrated specific discharge estimated across the 5-km boundary downgradient from the repository is 1.60 m/yr (Section 6.7.2 and Appendix I), which is just less than 3 times the maximum value of 0.66 m/yr. This combination of permeabilities was specifically selected to maximize specific discharge, which is still well within the range established by the specific discharge multiplier used in SZ abstraction models (SNL 2007 [DIRS 177390], Section 6.5.2.1). That is, an uncertainty distribution in specific discharge is constructed where the nominal specific discharge is multiplied by 1/8.93 and 8.93 (BSC 2007 [DIRS 177390], Section 6.5.2). The details of the uncertainty distributions of specific discharge and effective porosity in the alluvium and their associated sampling techniques are outlined in the SZ abstraction model (SNL 2007 [DIRS 177390], Section 6.5.2.1 and 6.5.2.3).

8.3.2 Flowpaths Uncertainty

The flowpaths from the water table beneath the repository to the accessible environment directly affect breakthrough curves and associated radionuclide transport times (recall that flowpath length is used to calculate specific discharge). Because the flowpaths are close to the water table and transition from the volcanic tuffs to the alluvium, flowpath uncertainty directly affects the length of flow in the volcanic tuffs and in the alluvium.

Uncertainty in flowpaths is affected by anisotropy in hydraulic properties of the volcanic tuffs. Large-scale anisotropy and heterogeneity were implemented in the SZ site-scale flow model through direct incorporation of known hydraulic features, faults, and fractures (see Section 6.7.10). Horizontal anisotropy in the volcanic units was derived from analysis of hydraulic testing at the C-wells (SNL 2007 [DIRS 177394], Section 6.2.6 and Appendix C6). This scientific analysis report also recommends an uncertainty range in anisotropy that should be

used in the SZ site-scale flow model to account for uncertainty in the flowpaths and this parameter was carried forward through to SZ abstraction modeling (SNL 2007 [DIRS 177390], Section 6.5.2.10). For isotropic permeability, average flowpath length to the 18-km compliance boundary is approximately 22.9 km. For anisotropy ratios of 20:1 and 0.05:1 (N-S:E-W), average flowpath lengths are 29.7 and 22.8 km, respectively. This is an acceptable range of variability in model results in light of the bounds established by geochemical analyses (Figure 7-5). Also, recall that 5 km of this difference can be attributed solely to the random initial distribution of particles below the repository.

The model is adequate for its intended use of providing flow-field simulations as input to the SZ site-scale transport model necessary to generate radionuclide breakthrough curves.

8.4 HOW THE APPLICABLE ACCEPTANCE CRITERIA ARE ADDRESSED

This section describes how the acceptance criteria in the YMRP (NRC 2003 [DIRS 163274], Section 2.2.1.3.8.3), *Flowpaths in the Saturated Zone*, are addressed by this report.

Acceptance Criteria from Section 2.2.1.3.8.3, *Flowpaths in the Saturated Zone*

Acceptance Criterion 1: *System Description and Model Integration Are Adequate.*

Subcriterion (1): Section 1 explains that this model generates SZ velocity fields which are used as inputs for the model of transport in the SZ and are abstracted in the TSPA. The important physical phenomena are adequately incorporated in the SZ abstraction process as described in the following subsections: hydraulic gradients (Section 6.3.1.4); vertical gradients (Section 6.3.1.5); lateral boundary conditions (Section 6.3.1.6); Recharge (Section 6.3.1.7); Discharge (Section 6.3.1.8); heterogeneity (Section 6.3.1.9); faults (Section 6.3.1.10); and groundwater flow processes (Section 6.3.2.). The discussion of groundwater table rise in Section 6.6.4 uses consistent and appropriate assumptions about climate change.

Subcriterion (2): Aspects of hydrology, geology and geochemistry that may affect flowpaths in the SZ are described adequately in Section 6.3 and Appendices A and B.

Subcriterion (4): Section 6.3.1.7 states that the recharge to the flow model was derived from three sources: regional-scale SZ model (Belcher 2004 [DIRS 173179]), 2003 UZ flow model (BSC 2004 [DIRS 169861]), and Fortymile Wash data (Savard 1998 [DIRS 102213]). Recharge from the UZ site-scale model (percolation flux) was taken as the flow through the base of that model, the domain of which includes approximately 40 km^2 (19.3 mi^2) that encompasses an area only slightly larger than the footprint of Yucca Mountain, a small fraction of the SZ model domain. The SZ site-scale flow model uses appropriate recharge values from flow in the unsaturated zone.

Subcriterion (5): Section 6.2 provides a road map to sections and FEPs document where sufficient data and technical bases to assess the degree to which FEPs have been included in the flowpaths.

Subcriterion (6): Flowpaths in the SZ are adequately delineated, considering site conditions, as described in Section 6.5.2.3 and Appendices A and B. Section 6.5 shows how the flow model that was developed generates flow fields that simulate radionuclide transport in saturated porous rock and alluvium.

Subcriterion (7): The effects of climate on specific discharge flowpaths are evaluated in Section 6.6.4. Saturated zone modeling analyses considered in this report indicate that a rise in the water table will cause some of the flow paths from below the repository to the accessible environment to be in units with lower values of permeability than the ones saturated by the present-day water-table conditions. Furthermore, the approach used to estimate water-table rise to the north of the repository has little impact on the simulated flow system down gradient of Yucca Mountain in the SZ site-scale flow model. Results are presented in a data package (DTN: SN0702T0510106.006) for use by downstream users.

Subcriterion (8): Section 6.4.3.10 explains how the linear approximation of the temperature gradient captures the effect of geothermal heat flux on groundwater viscosity.

Subcriterion (9): The impact of the expected water table rise on potentiometric heads and flow directions, and consequently on repository performance, is adequately considered in Section 6.6.4.

Subcriterion (10): This report was prepared in accordance with the *Quality Assurance Requirements and Description* (QARD) (DOE 2006 [DIRS 177092], DOE/RW-0333P, Rev. 18), which commits to U.S. Nuclear Regulatory Commission guidance. Compliance with the QARD was determined through multiple reviews.

Acceptance Criterion 2: *Data Are Sufficient for Model Justification.*

Subcriterion (1): Sections 6.3, 6.4, and Appendices A and B identify the geological, hydrological, and geochemical information used in this model to evaluate flowpaths in the SZ and adequately justifies those values by identifying their reliable sources. Section 6.4.3 adequately describes how the data were used, interpreted, and appropriately synthesized into parameters by explaining how water level and head distributions, definitions of the hydrogeologic units, the distribution of recharge flux and lateral fluxes into the model domain, feature and fault distribution, temperature profiles in wells, and boundary conditions were incorporated into the SZ site-scale flow model. Section 6.4.3.1 describes the development of the hydrogeologic framework, which, with the known features of the site is used to design a grid for flow modeling. Section 6.4.3.2 describes the generation of the grid, which enables the data to be assigned to hydrogeologic units and features, recharge fluxes, hydrogeologic properties, and boundary conditions at node points. Section 6.4.3.3 describes the use of hydrogeologic properties, Section 6.4.3.7 describes the representation of features, Section 6.4.3.8 describes the use of the boundary conditions described in Section 6.3.1.6, Section 6.4.3.9 describes recharge, and Section 6.4.3.10 describes how the hydrogeologic properties are specified for each node in the computational grid. Section 7.2.2.4 describes the permeability data obtained at the NTS, including the lower carbonate aquifer (Section 7.2.2.4.1), the valley fill aquifer (Section 7.2.2.4.2), the welded tuff aquifer (Section 7.2.2.4.3), and the lava flow aquifer (Section 7.2.4.4).

Subcriterion (2): The sufficiency of the data collected on the natural system to establish boundary conditions on flowpaths in the SZ is demonstrated in Section 6.3.1. Section 6.3.1 describes the hydrogeologic setting of the SZ flow system near Yucca Mountain. Section 6.3.1.1 relates the geologic features to flow in the SZ. Section 6.3.1.2 describes the HFM that includes faults, zones of hydrothermal alteration, and other features that affect flow in the SZ. Section 6.3.1.3 uses the potentiometric surface map to determine the general direction of groundwater flow. Section 6.3.1.4 describes the hydraulic gradients and Section 6.3.1.5 describes the vertical gradients. Section 6.3.1.6 explains how the boundary conditions are derived from regional water level and head data form fixed-head boundary conditions on the lateral sides of the model. Section 6.3.1.7 describes the three components of recharge and Section 6.3.1.8 reports that no natural discharge is observed. Section 6.3.1.9 describes the observed physical and chemical heterogeneity of the rocks and water in the SZ. Section 6.3.1.10 describes the role of faults. Initial conditions are not included in the model because it is a steady-state model.

Subcriterion (3): The appropriateness of the techniques used to obtain the SZ geologic, hydrologic, and geochemical data used in this model is established in the reliable sources of the data listed in Section 4.1. Section 7.2.2.3 describes the acquisition of data on permeability from single-hole tests (Section 7.2.2.3.1) and cross-hole tests (Section 7.2.2.3.2). The HFM report discusses the acquisition of data related to hydrogeology (SNL 2007 [DIRS 174109]). Appendices A and B discusses the acquisition of data related to geochemistry.

Subcriterion (4): Section 6.4 provides sufficient information to substantiate that the mathematical groundwater modeling approach and computational model are applicable to site conditions. Section 6.4.1 discusses the equations from the basic laws of flow that were applied and Section 6.4.2 describes the computational model used to solve those equations. Section 6.4.3 describes the inputs from data about the site, including the HFM (Section 6.4.3.1), grid generation (Section 6.4.3.2), hydrogeologic properties (Section 6.4.3.3), discrete features and regions (Section 6.4.3.7), boundary conditions (Section 6.4.3.8), and recharge (Section 6.4.3.9).

Section 6.5.1 provides sufficient information to substantiate that the mathematical groundwater model is calibrated. Section 6.5.1.1 describes the calibration process. Section 6.5.1.2 describes the parameter optimization procedure, Section 6.5.1.3 describes the calibration targets, and calibration parameters. Section 6.5.2 describes the calibration results for water levels (Section 6.5.2.1), fluxes (Section 6.5.2.2), flowpaths (Section 6.5.2.3), and specific discharge (Section 6.5.2.4).

Acceptance Criterion 3: ***Data Uncertainty Is Characterized and Propagated Through the Model Abstraction.***

Subcriterion (1): Section 6.5.1 explains how calibration is used to optimize the values of important model parameters in a way that is technically defensible, reasonably accounts for uncertainties and variabilities.

Subcriterion (2): The effect of climate on flowpaths is evaluated adequately in Section 6.6.4. Saturated zone modeling analyses considered in this report indicate that a rise in the water table will cause some of the flow paths from below the repository to the accessible environment to be in units with lower values of permeability than the ones saturated by the present-day water-table conditions. Furthermore, the approach used to estimate water-table rise to the north of the repository has little impact on the simulated flow system down gradient of Yucca Mountain in the SZ site-scale flow model. Results are presented in a data package (DTN: SN0702T0510106.006) for use by downstream users.

Subcriterion (3): Section 6.5.1 and 6.7 show how uncertainty has been adequately represented in the development of parameters for the model.

Subcriterion (4): The SZ flow Expert Elicitation Panel was conducted in accordance with instructions by Kotra et al. (1996 [DIRS 100909]) and addressed the following issues:

- Appropriateness of the horizontal to vertical anisotropy ratio of 10:1 (Section 6.6.1)
- Estimates of discharge from the volcanic aquifer (Section 6.7)
- Semiperched water as an explanation for the observed LHG (Section 6.3.1.4)
- Specific discharge near Yucca Mountain (Sections 6.5.1.3, 6.5.2.4, and 8).

Acceptance Criterion 4: ***Model Uncertainty Is Characterized and Propagated Through the Model Abstraction.***

Subcriterion (1): Several ACMs are identified in Sections 6.6.1 through 6.6.4. They are: (1) vertical anisotropies in hydraulic properties, with and without vertical anisotropy and varied horizontal anisotropy ratios (Section 6.6.1); (2) models for the LHG north of Yucca Mountain and variable anisotropy in the Solitario Canyon Fault (Section 6.6.2); and (3) water-table rise resulting from climate change (Section 6.6.4).

ACMs for vertical and horizontal anisotropies were considered (Section 6.6.1). The vertical anisotropy from expert elicitation is only a rule of thumb and removal of the vertical anisotropy from model calibration can affect the difference between the measured and computed heads. Horizontal anisotropy will be included in the TSPA analysis (Section 6). As discussed in Section 6.6.2, the LHG ACM and Solitario Canyon Fault ACM could significantly affect model results, so it is important to represent these features accurately in the conceptual model (i.e., they must be present in some fashion). Section 6.6.4 explains how the change in SZ flowpaths resulting from a rise in the water table need not be included in the TSPA because the use of scaling factors conservatively accounts for the impact of climate changes on SZ flow.

Subcriterion (2): Conceptual model uncertainties are adequately defined and documented in Sections 6.4 and 6.7 and Appendices H and I. These sections also include the proper assessment of the effects on conclusions regarding performance. Section 6.7 addresses uncertainty in the flowpaths due to alternative conceptualizations and model calibration.

Uncertainty in the quantification of specific discharge is discussed in Sections 6.7 and Appendix H. A nonlinear analysis is presented in Section 6.7.2 and Appendix I. There is general consistency between the specific discharge simulated by the model and the median of values of uncertainty ranges estimated by the SZ expert panel from testing data. Uncertainty in specific discharge is propagated forward to the TSPA.

Uncertainty in the hydrologic contacts is discussed in Section 6.7.3 and shown to have moderate effects in some cases. Accordingly, this uncertainty was determined not to warrant propagation to the TSPA. Additional uncertainties due to limitation in site data, conceptualization of the LHG, and representation of potentially perched water-level measurements, and fault conceptualizations are discussed in Sections 6.7.4 through 6.7.8. None of these uncertainties warrants propagation to TSPA.

Uncertainty due to scaling is discussed in Section 6.7.9 where it is concluded that such uncertainty does not significantly affect flow modeling.

Subcriterion (3): The conceptual model uncertainty considered in this report is consistent with available site characterization data and field measurements. The genesis of the conceptual model is discussed in Section 6.3. Alternative conceptual models are considered in Section 6.6. A thorough description of uncertainty, especially uncertainty associated with specific discharge estimates, is given in Section 6.7. Furthermore, an introduction on predictive variance uncertainty minimization and quantification is given in Appendix H. An extension of this theory to nonlinear predictive variance is outlined in Appendix I.

Subcriterion (4): Alternative modeling approaches are appropriate and consistent with available data and current scientific knowledge, and appropriately consider their results and limitations, using analyses that are sensitive to the processes modeled, as discussed above.

Acceptance Criteria from Section 2.2.1.1.3, *System Description and Demonstration of Multiple Barriers*

Acceptance Criterion 3: *Technical Basis for Barrier Capability is Adequately Presented.*

When considered together, reports associated with the saturated zone including this report, *Site-Scale Saturated Zone Transport* (SNL 2007 [DIRS 177392]), and *Saturated Zone Flow and Transport Model Abstraction* (SNL 2007 [DIRS 177390]) constitute an adequate description (including thorough discussions of uncertainty) of the saturated zone as a natural barrier to radionuclide release.

INTENTIONALLY LEFT BLANK

9. INPUTS AND REFERENCES

The following is a list of the references cited in this document. Column 1 contains the unique six-digit numerical identifiers (the Document Input Reference System numbers), which are placed in the text following the reference callout (e.g., Ahlers et al. 1999 [DIRS 109715]). The purpose of these numbers is to assist in locating a specific reference. Multiple sources by the same author (e.g., SNL 2007) are sorted alphabetically by title.

9.1 DOCUMENTS CITED

109715 Ahlers, C.F.; Finsterle, S.; and Bodvarsson, G.S. 1999. "Characterization and Prediction of Subsurface Pneumatic Response at Yucca Mountain, Nevada." *Journal of Contaminant Hydrology, 38,* (1-3), 47-68. New York, New York: Elsevier. TIC: 244160.

103750 Altman, W.D.; Donnelly, J.P.; and Kennedy, J.E. 1988. *Qualification of Existing Data for High-Level Nuclear Waste Repositories: Generic Technical Position.* NUREG-1298. Washington, D.C.: U.S. Nuclear Regulatory Commission. TIC: 200652.

103597 Altman, W.D.; Donnelly, J.P.; and Kennedy, J.E. 1988. *Peer Review for High-Level Nuclear Waste Repositories: Generic Technical Position.* NUREG-1297. Washington, D.C.: U.S. Nuclear Regulatory Commission. TIC: 200651.

105038 Bear, J. 1979. *Hydraulics of Groundwater.* New York, New York: McGraw-Hill. TIC: 217574.

173179 Belcher, W.R. 2004. *Death Valley Regional Ground-Water Flow System, Nevada and California - Hydrogeologic Framework and Transient Ground-Water Flow Model.* Scientific Investigations Report 2004-5205. Reston, Virginia: U.S. Geological Survey. ACC: MOL.20050323.0070.

104370 Benson, L. and Klieforth, H. 1989. "Stable Isotopes in Precipitation and Ground Water in the Yucca Mountain Region, Southern Nevada: Paleoclimatic Implications." *Aspects of Climate Variability in the Pacific and the Western Americas.* Peterson, D.H., ed.. Geophysical Monograph 55. Pages 41-59. Washington, D.C.: American Geophysical Union. TIC: 224413.

101036 Benson, L.V. and McKinley, P.W. 1985. *Chemical Composition of Ground Water in the Yucca Mountain Area, Nevada, 1971-84.* Open-File Report 85-484. Denver, Colorado: U.S. Geological Survey. ACC: NNA.19900207.0281.

101194 Bish, D.L. 1989. *Evaluation of Past and Future Alterations in Tuff at Yucca Mountain, Nevada, Based on the Clay Mineralogy of Drill Cores USW G-1, G-2, and G-3.* LA-10667-MS. Los Alamos, New Mexico: Los Alamos National Laboratory. ACC: NNA.19890126.0207.

101195 Bish, D.L. and Chipera, S.J. 1989. *Revised Mineralogic Summary of Yucca Mountain, Nevada.* LA-11497-MS. Los Alamos, New Mexico: Los Alamos National Laboratory. ACC: NNA.19891019.0029.

101233 Blankennagel, R.K. and Weir, J.E., Jr. 1973. *Geohydrology of the Eastern Part of Pahute Mesa, Nevada Test Site, Nye County, Nevada.* Professional Paper 712-B. Washington, D.C.: U.S. Geological Survey. TIC: 219642.

179072 Bower, K.M. and Zyvoloski, G. 1997. "A Numerical Model for Thermo-Hydro-Mechanical Coupling in Fractured Rock." *International Journal of Rock Mechanics and Mining Sciences & Geomechanics Abstracts, 34,* (8), 1201-1211. New York, New York: Pergamon. TIC: 259103.

149161 Bower, K.M.; Gable, C.W.; and Zyvoloski, G.A. 2000. *Effect of Grid Resolution on Control Volume Finite Element Groundwater Modeling of Realistic Geology.* LA-UR-001870. Los Alamos, New Mexico: Los Alamos National Laboratory. TIC: 248256.

102004 Broxton, D.E.; Bish, D.L.; and Warren, R.G. 1987. "Distribution and Chemistry of Diagenetic Minerals at Yucca Mountain, Nye County, Nevada." *Clays and Clay Minerals, 35,* (2), 89-110. Long Island City, New York: Pergamon Press. TIC: 203900.

143665 CRWMS M&O 2000. *Total System Performance Assessment for the Site Recommendation*. TDR-WIS-PA-000001 REV 00. Las Vegas, Nevada: CRWMS M&O. ACC: MOL.20001005.0282.

155974 BSC (Bechtel SAIC Company) 2001. *Calibration of the Site-Scale Saturated Zone Flow Model.* MDL-NBS-HS-000011 REV 00 ICN 01. Las Vegas, Nevada: Bechtel SAIC Company. ACC: MOL.20010713.0049.

157132 BSC 2001. *Input and Results of the Base Case Saturated Zone Flow and Transport Model for TSPA.* ANL-NBS-HS-000030 REV 00 ICN 01. Las Vegas, Nevada: Bechtel SAIC Company. ACC: MOL.20011112.0068.

160247 BSC 2002. *Analysis of Geochemical Data for the Unsaturated Zone.* ANL-NBS-HS-000017 REV 00 ICN 02. Las Vegas, Nevada: Bechtel SAIC Company. ACC: MOL.20020314.0051.

170029 BSC 2004. *Geologic Framework Model (GFM2000).* MDL-NBS-GS-000002 REV 02. Las Vegas, Nevada: Bechtel SAIC Company. ACC: DOC.20040827.0008.

170008 BSC 2004. *Hydrogeologic Framework Model for the Saturated Zone Site Scale Flow and Transport Model.* MDL-NBS-HS-000024 REV 00. Las Vegas, Nevada: Bechtel SAIC Company. ACC: DOC.20041118.0001.

170014 BSC 2004. *Probability Distribution for Flowing Interval Spacing.* ANL-NBS-MD-000003 REV 01. Las Vegas, Nevada: Bechtel SAIC Company. ACC: DOC.20040923.0003.

170015 BSC 2004. *Recharge and Lateral Groundwater Flow Boundary Conditions for the Saturated Zone Site-Scale Flow and Transport Model.* ANL-NBS-MD-000010 REV 01. Las Vegas, Nevada: Bechtel SAIC Company. ACC: DOC.20041008.0004.

170037 BSC 2004. *Saturated Zone Site-Scale Flow Model.* MDL-NBS-HS-000011 REV 02. Las Vegas, Nevada: Bechtel SAIC Company. ACC: DOC.20041122.0001.

169861 BSC 2004. *UZ Flow Models and Submodels.* MDL-NBS-HS-000006 REV 02. Las Vegas, Nevada: Bechtel SAIC Company. ACC: DOC.20041101.0004; DOC.20050629.0003.

170009 BSC 2004. *Water-Level Data Analysis for the Saturated Zone Site-Scale Flow and Transport Model.* ANL-NBS-HS-000034 REV 02. Las Vegas, Nevada: Bechtel SAIC Company. ACC: DOC.20041012.0002; DOC.20050214.0002.

169734 BSC 2004. *Yucca Mountain Site Description.* TDR-CRW-GS-000001 REV 02 ICN 01. Two volumes. Las Vegas, Nevada: Bechtel SAIC Company. ACC: DOC.20040504.0008.

179466 SNL 2007. *Total System Performance Assessment Data Input Package for Requirements Analysis for Subsurface Facilities*. TDR-TDIP-PA-000001 REV 00. Las Vegas, Nevada: Sandia National Laboratories.

175539 BSC 2005. *Q-List.* 000-30R-MGR0-00500-000-003. Las Vegas, Nevada: Bechtel SAIC Company. ACC: ENG.20050929.0008.

177375 BSC 2006. *Technical Work Plan for Saturated Zone Flow and Transport Modeling.* TWP-NBS-MD-000006 REV 02. Las Vegas, Nevada: Bechtel SAIC Company. ACC: DOC.20060519.0002.

100106 Buesch, D.C.; Spengler, R.W.; Moyer, T.C.; and Geslin, J.K. 1996. *Proposed Stratigraphic Nomenclature and Macroscopic Identification of Lithostratigraphic Units of the Paintbrush Group Exposed at Yucca Mountain, Nevada.* Open-File Report 94-469. Denver, Colorado: U.S. Geological Survey. ACC: MOL.19970205.0061.

162906 Burke, W.H.; Denison, R.E.; Hetherington, E.A.; Koepnick, R.B.; Nelson, H.F.; and Otto, J.B. 1982. "Variation of Seawater $^{87}Sr/^{86}Sr$ Throughout Phanerozoic Time." *Geology, 10,* 516-519. Boulder, Colorado: Geological Society of America. TIC: 255085.

126814 Campana, M.E. and Byer, R.M., Jr. 1996. "A Conceptual Evaluation of Regional Ground-Water Flow, Southern Nevada-California, USA." *Environmental and Engineering Geoscience, II,* (4), 465-478. Boulder, Colorado: Geological Society of America. TIC: 246651.

162940 Chapman, J.B. and Lyles, B.F. 1993. *Groundwater Chemistry at the Nevada Test Site: Data and Preliminary Interpretations.* DOE/NV/10845-16. Las Vegas, Nevada: U.S. Department of Energy, Nevada Operation Office. ACC: MOL.20031023.0087.

153475 Cheng, H.; Edwards, R.L.; Hoff, J.; Gallup, C.D.; Richards, D.A.; and Asmerom, Y. 2000. "The Half-Lives of Uranium-234 and Thorium-230." *Chemical Geology, 169,* 17-33. Amsterdam, The Netherlands: Elsevier. TIC: 249205.

105079 Chipera, S.J. and Bish, D.L. 1997. "Equilibrium Modeling of Clinoptilolite-Analcime Equilibria at Yucca Mountain, Nevada." *Clays and Clay Minerals, 45,* (2), 226-239. Long Island City, New York: Pergamon Press. TIC: 233948.

100025 Chipera, S.J.; Bish, D.L.; and Carlos, B.A. 1995. "Equilibrium Modeling of the Formation of Zeolites in Fractures at Yucca Mountain, Nevada." *Natural Zeolites '93: Occurrence, Properties, Use, Proceedings of the 4th International Conference on the Occurrence, Properties, and Utilization of Natural Zeolites, June 20-28, 1993, Boise, Idaho.* Ming, D.W. and Mumpton, F.A., eds. Pages 565-577. Brockport, New York: International Committee on Natural Zeolites. TIC: 243086.

101125 Claassen, H.C. 1985. *Sources and Mechanisms of Recharge for Ground Water in the West-Central Amargosa Desert, Nevada—A Geochemical Interpretation.* U.S. Geological Survey Professional Paper 712-F. Washington, D.C.: United States Government Printing Office. TIC: 204574.

105738 Clark, I.D. and Fritz, P. 1997. *Environmental Isotopes in Hydrogeology.* Boca Raton, Florida: Lewis Publishers. TIC: 233503.

178598 Cooley, R.L. and Christensen, S. 2006. "Bias and Uncertainty in Regression-Calibrated Models of Groundwater Flow in Heterogeneous Media." *Advances in Water Resources, 29,* 639-656. New York, New York: Elsevier. TIC: 259000.

178650 Cooley, R.L. 2004. *A Theory for Modeling Ground-Water Flow in Heterogeneous Media*. Professional Paper 1679. Reston, Virginia: U.S. Geological Survey. ACC: MOL.20070108.0003.

101040 Craig, R.W. and Robison, J.H. 1984. *Geohydrology of Rocks Penetrated by Test Well UE-25p#1, Yucca Mountain Area, Nye County, Nevada.* Water-Resources Investigations Report 84-4248. Denver, Colorado: U.S. Geological Survey. ACC: NNA.19890905.0209.

100353 CRWMS M&O 1998. *Saturated Zone Flow and Transport Expert Elicitation Project.* Deliverable SL5X4AM3. Las Vegas, Nevada: CRWMS M&O. ACC: MOL.19980825.0008.

139582 CRWMS M&O 2000. *Calibration of the Site-Scale Saturated Zone Flow Model.* MDL-NBS-HS-000011 REV 00. Las Vegas, Nevada: CRWMS M&O. ACC: MOL.20000825.0122.

153246 CRWMS M&O 2000. *Total System Performance Assessment for the Site Recommendation.* TDR-WIS-PA-000001 REV 00 ICN 01. Las Vegas, Nevada: CRWMS M&O. ACC: MOL.20001220.0045.

101043 Czarnecki, J.B. 1984. *Simulated Effects of Increased Recharge on the Ground-Water Flow System of Yucca Mountain and Vicinity, Nevada-California.* Water-Resources Investigations Report 84-4344. Denver, Colorado: U.S. Geological Survey. ACC: HQS.19880517.1750.

160149 Czarnecki, J.B. 1985. *Simulated Effects of Increased Recharge on the Ground-Water Flow System of Yucca Mountain and Vicinity, Nevada-California.* Water-Resources Investigations Report 84-4344. Denver, Colorado: U.S. Geological Survey. TIC: 203222.

100377 Czarnecki, J.B.; Faunt, C.C.; Gable, C.W.; and Zyvoloski, G.A. 1997. *Hydrogeology and Preliminary Calibration of a Preliminary Three-Dimensional Finite-Element Ground-Water Flow Model of the Site Saturated Zone, Yucca Mountain, Nevada.* Administrative Report. Denver, Colorado: U.S. Geological Survey. ACC: MOL.19980204.0519.

100131 D'Agnese, F.A.; Faunt, C.C.; Turner, A.K.; and Hill, M.C. 1997. *Hydrogeologic Evaluation and Numerical Simulation of the Death Valley Regional Ground-Water Flow System, Nevada and California.* Water-Resources Investigations Report 96-4300. Denver, Colorado: U.S. Geological Survey. ACC: MOL.19980306.0253.

120425 D'Agnese, F.A.; O'Brien, G.M.; Faunt, C.C.; and San Juan, C.A. 1999. *Simulated Effects of Climate Change on the Death Valley Regional Ground-Water Flow System, Nevada and California.* Water-Resources Investigations Report 98-4041. Denver, Colorado: U.S. Geological Survey. TIC: 243555.

158876 D'Agnese, F.A.; O'Brien, G.M.; Faunt, C.C.; Belcher, W.R.; and San Juan, C. 2002. *A Three-Dimensional Numerical Model of Predevelopment Conditions in the Death Valley Regional Ground-Water Flow System, Nevada and California.* Water-Resources Investigations Report 02-4102. Denver, Colorado: U.S. Geological Survey. TIC: 253754.

162939 Davisson, M.L.; Kenneally, J.M.; Smith, D.K.; Hudson, G.B.; Nimz, G.J.; and Rego, J.H. 1994. *Preliminary Report on the Isotope Hydrology Investigations at the Nevada Test Site: Hydrologic Resources Management Program, FY 1992-1993.* UCRL-ID-116122. Livermore, California: Lawrence Livermore National Laboratory, Nuclear Chemistry Division. TIC: 210954.

100027 Day, W.C.; Dickerson, R.P.; Potter, C.J.; Sweetkind, D.S.; San Juan, C.A.; Drake, R.M., II; and Fridrich, C.J. 1998. *Bedrock Geologic Map of the Yucca Mountain Area, Nye County, Nevada.* Geologic Investigations Series I-2627. Denver, Colorado: U.S. Geological Survey. ACC: MOL.19981014.0301.

101557 Day, W.C.; Potter, C.J.; Sweetkind, D.S.; Dickerson, R.P.; and San Juan, C.A. 1998. *Bedrock Geologic Map of the Central Block Area, Yucca Mountain, Nye County, Nevada.* Miscellaneous Investigations Series Map I-2601. Washington, D.C.: U.S. Geological Survey. ACC: MOL.19980611.0339.

100439 de Marsily, G. 1986. *Quantitative Hydrogeology: Groundwater Hydrology for Engineers.* San Diego, California: Academic Press. TIC: 208450.

105384 Dettinger, M.D. 1989. "Reconnaissance Estimates of Natural Recharge to Desert Basins in Nevada, U.S.A., by Using Chloride-Balance Calculations." *Journal of Hydrology, 106,* 55-78. Amsterdam, The Netherlands: Elsevier. TIC: 236967.

154690 Dettinger, M.D. 1989. *Distribution of Carbonate-Rock Aquifers in Southern Nevada and the Potential for Their Development, Summary of Findings, 1985-88.* Summary Report No. 1. Carson City, Nevada: State of Nevada. ACC: NNA.19940412.0056.

178613 Doherty, J. 2006. *Addendum to the PEST Manual.* Brisbane, Australia: Watermark Numerical Computing. ACC: MOL.20070111.0003.

118564 Drever, J.I. 1988. *The Geochemistry of Natural Waters.* 2nd Edition. Englewood Cliffs, New Jersey: Prentice-Hall. TIC: 242836.

103415 Dudley, W.W., Jr. and Larson, J.D. 1976. *Effect of Irrigation Pumping on Desert Pupfish Habitats in Ash Meadows, Nye County, Nevada.* Professional Paper 927. Washington, D.C.: U.S. Geological Survey. ACC: MOL.20010724.0312.

163577 Eddebbarh, A.A.; Zyvoloski, G.A.; Robinson, B.A.; Kwicklis, E.M.; Reimus, P.W.; Arnold, B.W.; Corbet, T.; Kuzio, S.P.; and Faunt, C. 2003. "The Saturated Zone at Yucca Mountain: An Overview of the Characterization and Assessment of the Saturated Zone as a Barrier to Potential Radionuclide Migration." *Journal of Contaminant Hydrology, 62-63,* 477-493. New York, New York: Elsevier. TIC: 254205.

100633 Ervin, E.M.; Luckey, R.R.; and Burkhardt, D.J. 1994. *Revised Potentiometric-Surface Map, Yucca Mountain and Vicinity, Nevada.* Water-Resources Investigations Report 93-4000. Denver, Colorado: U.S. Geological Survey. ACC: NNA.19930212.0018.

100146 Faunt, C.C. 1997. *Effect of Faulting on Ground-Water Movement in the Death Valley Region, Nevada and California.* Water-Resources Investigations Report 95-4132. Denver, Colorado: U.S. Geological Survey. ACC: MOL.19980429.0119.

105559 Faure, G. 1986. *Principles of Isotope Geology.* 2nd Edition. New York, New York: John Wiley & Sons. TIC: 237212.

100033 Flint, L.E. 1998. *Characterization of Hydrogeologic Units Using Matrix Properties, Yucca Mountain, Nevada.* Water-Resources Investigations Report 97-4243. Denver, Colorado: U.S. Geological Survey. ACC: MOL.19980429.0512.

109425 Forester, R.M.; Bradbury, J.P.; Carter, C.; Elvidge-Tuma, A.B.; Hemphill, M.L.; Lundstrom, S.C.; Mahan, S.A.; Marshall, B.D.; Neymark, L.A.; Paces, J.B.; Sharpe, S.E.; Whelan, J.F.; and Wigand, P.E. 1999. *The Climatic and Hydrologic History of Southern Nevada During the Late Quaternary.* Open-File Report 98-635. Denver, Colorado: U.S. Geological Survey. TIC: 245717.

144110 Forsyth, P.A. 1989. "A Control Volume Finite Element Method for Local Mesh Refinement." *Proceedings, Tenth. SPE Symposium on Reservoir Simulation, Houston, Texas, February 6-8, 1989.* SPE 18415. Pages 85-96. Richardson, Texas: Society of Petroleum Engineers. TIC: 247068.

101173 Freeze, R.A. and Cherry, J.A. 1979. *Groundwater.* Englewood Cliffs, New Jersey: Prentice-Hall. TIC: 217571.

178611 Freifeld, B.; Doughty, C.; and Finsterle, S. 2006. *Preliminary Estimates of Specific Discharge and Transport Velocities Near Borehole NC-EWDP-24PB.* LBNL-60740. Berkeley, California: Lawrence Berkeley National Laboratory. ACC: MOL.20070111.0001.

100575 Fridrich, C.J.; Dudley, W.W., Jr.; and Stuckless, J.S. 1994. "Hydrogeologic Analysis of the Saturated-Zone Ground-Water System, Under Yucca Mountain, Nevada." *Journal of Hydrology, 154,* 133-168. Amsterdam, The Netherlands: Elsevier. TIC: 224606.

178742 Futa, K.; Marshall, B.D.; and Peterman, Z.E. 2006. "Evidence for Ground-Water Stratification Near Yucca Mountain, Nevada." *Proceedings of the 11th International High-Level Radioactive Waste Management Conference (IHLRWM), April 30 - May 4, 2006, Las Vegas, Nevada.* Pages 301-306. La Grange Park, Illinois: American Nuclear Society. TIC: 258345.

127184 Gascoyne, M. 1992. "Geochemistry of the Actinides and Their Daughters." Chapter 2 of *Uranium-Series Disequilibrium: Applications to Earth, Marine, and Environmental Sciences.* Ivanovich, M. and Harmon, R.S., eds. 2nd Edition. New York, New York: Oxford University Press. TIC: 234680.

129721 Geldon, A.L.; Umari, A.M.A.; Earle, J.D.; Fahy, M.F.; Gemmell, J.M.; and Darnell, J. 1998. *Analysis of a Multiple-Well Interference Test in Miocene Tuffaceous Rocks at the C-Hole Complex, May-June 1995, Yucca Mountain, Nye County, Nevada.* Water-Resources Investigations Report 97-4166. Denver, Colorado: U.S. Geological Survey. TIC: 236724.

100397 Geldon, A.L.; Umari, A.M.A.; Fahy, M.F.; Earle, J.D.; Gemmell, J.M.; and Darnell, J. 1997. *Results of Hydraulic and Conservative Tracer Tests in Miocene Tuffaceous Rocks at the C-Hole Complex, 1995 to 1997, Yucca Mountain, Nye County, Nevada.* Milestone SP23PM3. Las Vegas, Nevada: U.S. Geological Survey. ACC: MOL.19980122.0412.

179104 Gilmore, K. 2006. "RE: Some Problems in Checking." E-mail to from K. Gilmore (Nye County) to C.L. Axness (SNL), July 26, 2006. ACC: LLR.20070228.0142.

155411 Graves, R.P. 1998. *Water Levels in the Yucca Mountain Area, Nevada, 1996.* Open-File Report 98-169. Denver, Colorado: U.S. Geological Survey. ACC: MOL.19981117.0340.

155197 Harbaugh, A.W.; Banta, E.R.; Hill, M.C.; and McDonald, M.G. 2000. *MODFLOW-2000, The U.S. Geological Survey Modular Ground-Water Model—User Guide to Modularization Concepts and the Ground-Water Flow Process.* Open-File Report 00-92. Reston, Virginia: U.S. Geological Survey. TIC: 250197.

178488 Harter, T. and Hopmans, J.W. 2004. "Role of Vadose-Zone Flow Processes in Regional-Scale Hydrology: Review, Opportunities and Challenges." In *Unsaturated-Zone Modeling,* Volume 6, Chapter 6 of *Wageningen UR Frontis Series.* Feddes, R.A.; de Rooij, G.H.; and van Dam, J.C., eds. Boston, Massachusetts: Kluwer Academic Publishers. TIC: 258894.

169681 Hevesi, J.A.; Flint, A.L.; and Flint, L.E. 2003. *Simulation of Net Infiltration and Potential Recharge Using a Distributed-Parameter Watershed Model of the Death Valley Region, Nevada and California.* Water-Resources Investigations Report 03-4090. Sacramento, California: U.S. Geological Survey. ACC: MOL.20031124.0212.

116809 Hevesi, J.A.; Flint, A.L.; and Istok, J.D. 1992. "Precipitation Estimation in Mountainous Terrain Using Multivariate Geostatistics. Part II: Isohyetal Maps." *Journal of Applied Meteorology, 31,* (7), 677-688. Boston, Massachusetts: American Meteorological Society. TIC: 225248.

158753 Hill, M.C.; Banta, E.R.; Harbaugh, A.W.; and Anderman, E.R. 2000. *MODFLOW-2000, The U.S. Geological Survey Modular Ground-Water Model — User Guide to the Observation, Sensitivity, and Parameter-Estimation Processes and Three Post-Processing Programs.* Open-File Report 00-184. Denver, Colorado: U.S. Geological Survey. TIC: 252581.

145088 Ingraham, N.L.; Lyles, B.F.; Jacobson, R.L.; and Hess, J.W. 1991. "Stable Isotopic Study of Precipitation and Spring Discharge in Southern Nevada." *Journal of Hydrology, 125,* 243-258. Amsterdam, The Netherlands: Elsevier. TIC: 238581.

103010 Kilroy, K.C. 1991. *Ground-Water Conditions in Amargosa Desert, Nevada-California, 1952-87.* Water-Resources Investigations Report 89-4101. Carson City, Nevada: U.S. Geological Survey. TIC: 209975.

178599 Kitanidis, P.K. 1996. "On the Geostatistical Approach to the Inverse Problem." *Advances in Water Resources, 19,* (6), 333-342. New York, New York: Elsevier. TIC: 259001.

100909 Kotra, J.P.; Lee, M.P.; Eisenberg, N.A.; and DeWispelare, A.R. 1996. *Branch Technical Position on the Use of Expert Elicitation in the High-Level Radioactive Waste Program.* NUREG-1563. Washington, D.C.: U.S. Nuclear Regulatory Commission. TIC: 226832.

103011 La Camera, R.J. and Locke, G.L. 1997. *Selected Ground-Water Data for Yucca Mountain Region, Southern Nevada and Eastern California, Through December 1996.* Open-File Report 97-821. Carson City, Nevada: U.S. Geological Survey. ACC: MOL.20010724.0311.

181434 LANL (Los Alamos National Laboratory) 2001. *Software Management Report (SMR) for CORPSCON Version 5.11.08*. SDN: 10547-SMR-5.11.08-00. Los Alamos, New Mexico: Los Alamos National Laboratory. ACC: MOL.20011011.0403.

103012 Laczniak, R.J.; Cole, J.C.; Sawyer, D.A.; and Trudeau, D.A. 1996. *Summary of Hydrogeologic Controls on Ground-Water Flow at the Nevada Test Site, Nye County, Nevada.* Water-Resources Investigations 96-4109. Carson City, Nevada: U.S. Geological Survey. TIC: 226157.

100051 Langmuir, D. 1997. *Aqueous Environmental Geochemistry.* Upper Saddle River, New Jersey: Prentice Hall. TIC: 237107.

100153 LeCain, G.D. 1997. *Air-Injection Testing in Vertical Boreholes in Welded and Nonwelded Tuff, Yucca Mountain, Nevada.* Water-Resources Investigations Report 96-4262. Denver, Colorado: U.S. Geological Survey. ACC: MOL.19980310.0148.

144612 LeCain, G.D.; Anna, L.O.; and Fahy, M.F. 2000. *Results from Geothermal Logging, Air and Core-Water Chemistry Sampling, Air-Injection Testing, and Tracer Testing in the Northern Ghost Dance Fault, Yucca Mountain, Nevada, November 1996 to August 1998.* Water-Resources Investigations Report 99-4210. Denver, Colorado: U.S. Geological Survey. TIC: 247708.

100053 Levy, S.S. 1991. "Mineralogic Alteration History and Paleohydrology at Yucca Mountain, Nevada." *High Level Radioactive Waste Management, Proceedings of the Second Annual International Conference, Las Vegas, Nevada, April 28-May 3, 1991. 1,* 477-485. La Grange Park, Illinois: American Nuclear Society. TIC: 204272.

100589 Lichty, R.W. and McKinley, P.W. 1995. *Estimates of Ground-Water Recharge Rates for Two Small Basins in Central Nevada.* Water-Resources Investigations Report 94-4104. Denver, Colorado: U.S. Geological Survey. ACC: MOL.19960924.0524.

101258 Loeven, C. 1993. *A Summary and Discussion of Hydrologic Data from the Calico Hills Nonwelded Hydrogeologic Unit at Yucca Mountain, Nevada.* LA-12376-MS. Los Alamos, New Mexico: Los Alamos National Laboratory. ACC: NNA.19921116.0001.

100465 Luckey, R.R.; Tucci, P.; Faunt, C.C.; Ervin, E.M.; Steinkampf, W.C.; D'Agnese, F.A.; and Patterson, G.L. 1996. *Status of Understanding of the Saturated-Zone Ground-Water Flow System at Yucca Mountain, Nevada, as of 1995.* Water-Resources Investigations Report 96-4077. Denver, Colorado: U.S. Geological Survey. ACC: MOL.19970513.0209.

101142 Marshall, B.D.; Peterman, Z.E.; and Stuckless, J.S. 1993. "Strontium Isotopic Evidence for a Higher Water Table at Yucca Mountain." *High Level Radioactive Waste Management, Proceedings of the Fourth Annual International Conference, Las Vegas, Nevada, April 26-30, 1993. 2,* 1948-1952. La Grange Park, Illinois: American Nuclear Society. TIC: 208542.

116222 McKinley, P.W.; Long, M.P.; and Benson, L.V. 1991. *Chemical Analyses of Water from Selected Wells and Springs in the Yucca Mountain Area, Nevada and Southeastern California.* Open-File Report 90-355. Denver, Colorado: U.S. Geological Survey. ACC: NNA.19901031.0004.

158813 Meijer, A. 2002. "Conceptual Model of the Controls on Natural Water Chemistry at Yucca Mountain, Nevada." *Applied Geochemistry, 17,* (6), 793-805. New York, New York: Elsevier. TIC: 252808.

126847 Merlivat, L. and Jouzel, J. 1979. "Global Climatic Interpretation of the Deuterium-Oxygen 18 Relationship for Precipitation." *Journal of Geophysical Research, 84,* (C8), 5029-5033. Washington, D.C.: American Geophysical Union. TIC: 247773.

178788 Moore, C. 2005. *The Use of Regularized Inversion in Groundwater Model Calibration and Prediction Uncertainty Analysis.* Ph.D. Thesis. Queensland, Australia: The University of Queensland. TIC: 259082.

178402 Moore, C. and Doherty, J. 2005. "Role of the Calibration Process in Reducing Model Predictive Error." *Water Resources Research, 41,* 1-14. Washington, D.C.: American Geophysical Union. TIC: 258856.

178403 Moore, C. and Doherty, J. 2006. "The Cost of Uniqueness in Groundwater Model Calibration." *Advances in Water Resources, 29,* 605-623. New York, New York: Elsevier. TIC: 258857.

150321 Neuman, S.P. 1975. "Analysis of Pumping Test Data from Anisotropic Unconfined Aquifers Considering Delayed Gravity Response." *Water Resources Research, 11,* (2), 329-342. Washington, D.C.: American Geophysical Union. TIC: 222414.

101464 Neuman, S.P. 1990. "Universal Scaling of Hydraulic Conductivities and Dispersivities in Geologic Media." *Water Resources Research, 26,* (8), 1749-1758. Washington, D.C.: American Geophysical Union. TIC: 237977.

147379 Norton, D. and Knapp, R.B. 1977. "Transport Phenomena in Hydrothermal Systems: The Nature of Porosity." *American Journal of Science, 277,* 913-936. New Haven, Connecticut: Yale University, Kline Geology Laboratory. TIC: 247599.

107770 NRC (U.S. Nuclear Regulatory Commission) 1998. "Proposed Rule: 10 CFR Part 63---'Disposal of High-Level Radioactive Wastes in a Proposed Geologic Repository at Yucca Mountain, Nevada'." SECY-98-225. Washington, D.C.: U.S. Nuclear Regulatory Commission. Accessed October 30, 1999. TIC: 240520. URL: http://www.nrc.gov/NRC/COMMISSION/SECYS/1998-225scy.html.

163274 NRC 2003. *Yucca Mountain Review Plan, Final Report.* NUREG-1804, Rev. 2. Washington, D.C.: U.S. Nuclear Regulatory Commission, Office of Nuclear Material Safety and Safeguards. TIC: 254568.

101278 O'Brien, G.M. 1998. *Analysis of Aquifer Tests Conducted in Borehole USW G-2, 1996, Yucca Mountain, Nevada.* Water-Resources Investigations Report 98-4063. Denver, Colorado: U.S. Geological Survey. ACC: MOL.19980904.0095.

149438 Oatfield, W.J. and Czarnecki, J.B. 1989. *Hydrogeologic Inferences from Drillers Logs and from Gravity and Resistivity Surveys in the Amargosa Desert, Southern Nevada.* Open-File Report 89-234. Denver, Colorado: U.S. Geological Survey. TIC: 200468.

100069 Oliver, T. and Root, T. 1997. *Hydrochemical Database for the Yucca Mountain Area, Nye County, Nevada.* Denver, Colorado: U.S. Geological Survey. ACC: MOL.19980302.0367.

145190 Osmond, J.K. and Cowart, J.B. 1992. "Ground Water." Chapter 9 of *Uranium-Series Disequilibrium: Applications to Earth, Marine, and Environmental Sciences.* Ivanovich, M. and Harmon, R.S., eds. 2nd Edition. New York, New York: Oxford University Press. TIC: 234680.

154724 Paces, J.B. and Whelan, J.F. 2001. "Water-Table Fluctuations in the Amargosa Desert, Nye County, Nevada." *"Back to the Future - Managing the Back End of the Nuclear Fuel Cycle to Create a More Secure Energy Future," Proceedings of the 9th International High-Level Radioactive Waste Management Conference (IHLRWM), Las Vegas, Nevada, April 29-May 3, 2001.* La Grange Park, Illinois: American Nuclear Society. TIC: 247873.

158817 Paces, J.B.; Ludwig, K.R.; Peterman, Z.E.; and Neymark, L.A. 2002. "$^{234}U/^{238}U$ Evidence for Local Recharge and Patterns of Ground-Water Flow in the Vicinity of Yucca Mountain, Nevada, USA." *Applied Geochemistry, 17,* (6), 751-779. New York, New York: Elsevier. TIC: 252809.

100072 Paces, J.B.; Ludwig, K.R.; Peterman, Z.E.; Neymark, L.A.; and Kenneally, J.M. 1998. "Anomalous Ground-Water $^{234}U/^{238}U$ Beneath Yucca Mountain: Evidence of Local Recharge?" *High-Level Radioactive Waste Management, Proceedings of the Eighth International Conference, Las Vegas, Nevada, May 11-14, 1998.* Pages 185-188. La Grange Park, Illinois: American Nuclear Society. TIC: 237082.

107408 Paces, J.B.; Neymark, L.A.; Marshall, B.D.; Whelan, J.F.; and Peterman, Z.E. 1998. "Inferences for Yucca Mountain Unsaturated-Zone Hydrology from Secondary Minerals." *High-Level Radioactive Waste Management, Proceedings of the Eighth International Conference, Las Vegas, Nevada, May 11-14, 1998.* Pages 36-39. La Grange Park, Illinois: American Nuclear Society. TIC: 237082.

156507 Paces, J.B.; Neymark, L.A.; Marshall, B.D.; Whelan, J.F.; and Peterman, Z.E. 2001. *Ages and Origins of Calcite and Opal in the Exploratory Studies Facility Tunnel, Yucca Mountain, Nevada.* Water-Resources Investigations Report 01-4049. Denver, Colorado: U.S. Geological Survey. TIC: 251284.

159511 Parkhurst, D.L. and Appelo, C.A.J. 1999. *User's Guide to PHREEQC (Version 2)—A Computer Program for Speciation, Batch-Reaction, One-Dimensional Transport, and Inverse Geochemical Calculations.* Water-Resources Investigations Report 99-4259. Denver, Colorado: U.S. Geological Survey. TIC: 253046.

158824 Patterson, G.L. 1999. "Occurrences of Perched Water in the Vicinity of the Exploratory Studies Facility North Ramp." *Hydrogeology of the Unsaturated Zone, North Ramp Area of the Exploratory Studies Facility, Yucca Mountain, Nevada.* Rousseau, J.P.; Kwicklis, E.M.; and Gillies, D.C., eds. Water-Resources Investigations Report 98-4050. Denver, Colorado: U.S. Geological Survey. ACC: MOL.19990419.0335.

178743 Patterson, G.L. and Striffler, P.S. 2006. "Vertical Variability in Saturated Zone Hydrochemistry Near Yucca Mountain, Nevada." *Proceedings of the 11th International High-Level Radioactive Waste Management Conference (IHLRWM), April 30 - May 4, 2006, Las Vegas, Nevada.* Pages 390-394. La Grange Park, Illinois: American Nuclear Society. TIC: 258345.

179459 Patterson, G.L. and Thomas, J. 2005. "Carbon-14 Groundwater Analysis." *Office of Science and Technology and International OSTI&I: Annual Report 2005*. DOE/RW-0581. Pages 183-184. Washington, D.C.: U.S. Department of Energy, Office of Science and Technology and International. ACC: HQO.20060322.0021.

107402 Patterson, G.L.; Peterman, Z.E.; and Paces, J.B. 1998. "Hydrochemical Evidence for the Existence of Perched Water at USW WT-24, Yucca Mountain, Nevada." *High-Level Radioactive Waste Management, Proceedings of the Eighth International Conference, Las Vegas, Nevada, May 11-14, 1998.* Pages 277-278. La Grange Park, Illinois: American Nuclear Society. TIC: 237082.

101149 Peterman, Z.E. and Stuckless, J.S. 1993. "Isotopic Evidence of Complex Ground-Water Flow at Yucca Mountain, Nevada, USA." *High Level Radioactive Waste Management, Proceedings of the Fourth Annual International Conference, Las Vegas, Nevada, April 26-30, 1993. 2,* 1559-1566. La Grange Park, Illinois: American Nuclear Society. TIC: 208542.

107034 Plummer, M.A.; Phillips, F.M.; Fabryka-Martin, J.; Turin, H.J.; Wigand, P.E.; and Sharma, P. 1997. "Chlorine-36 in Fossil Rat Urine: An Archive of Cosmogenic Nuclide Deposition During the Past 40,000 Years." *Science, 277,* 538-541. Washington, D.C.: American Association for the Advancement of Science. TIC: 237425.

101466 Pollock, D.W. 1988. "Semianalytical Computation of Path Lines for Finite-Difference Models." *Ground Water, 26,* (6), 743-750. Worthington, Ohio: National Water Well Association. TIC: 226464.

103316 Press, W.H.; Teukolsky, S.A.; Vetterling, W.T.; and Flannery, B.P. 1992. *Numerical Recipes in Fortran 77, The Art of Scientific Computing.* Volume 1 of *Fortran Numerical Recipes.* 2nd Edition. Cambridge, United Kingdom: Cambridge University Press. TIC: 243606.

100073 Quade, J. and Cerling, T.E. 1990. "Stable Isotopic Evidence for a Pedogenic Origin of Carbonates in Trench 14 Near Yucca Mountain, Nevada." *Science, 250,* 1549-1552. Washington, D.C.: American Association for the Advancement of Science. TIC: 222617.

154688 Rasmussen, T.C.; Evans, D.D.; Sheets, P.J.; and Blanford, J.H. 1993. "Permeability of Apache Leap Tuff: Borehole and Core Measurements Using Water and Air." *Water Resources Research, 29,* (7), 1997-2006. Washington, D.C.: American Geophysical Union. TIC: 245278.

101284 Rice, W.A. 1984. *Preliminary Two-Dimensional Regional Hydrologic Model of the Nevada Test Site and Vicinity.* SAND83-7466. Albuquerque, New Mexico: Sandia National Laboratories. ACC: NNA.19900810.0286.

165986 Robledo, A.R.; Ryder, P.L.; Fenelon, J.M.; and Paillet, F.L. 1998. *Geohydrology of Monitoring Wells Drilled in Oasis Valley near Beatty, Nye County, Nevada, 1997.* Water-Resources Investigations Report 98-4184. Carson City, Nevada: U.S. Geological Survey. ACC: MOL.20031027.0156.

162938 Rose, T.P.; Benedict, F.C., Jr.; Thomas, J.M.; Sicke, W.S.; Hershey, R.L.; Paces, J.B.; Farnham, I.M.; and Peterman, Z.E. 2002. *Preliminary, Geochemical Data Analysis and Interpretation of the Pahute Mesa-Oasis Valley Groundwater Flow System, Nye County, Nevada.* Las Vegas, Nevada: U.S. Department of Energy, Nevada Operations Office. ACC: MOL.20031208.0200.

144725 Rose, T.P.; Kenneally, J.M.; Smith, D.K.; Davisson, M.L.; Hudson, G.B.; and Rego, J.H. 1997. *Chemical and Isotopic Data for Groundwater in Southern Nevada.* UCRL-ID-128000. Livermore, California: Lawrence Livermore National Laboratory. TIC: 243649.

102097 Rousseau, J.P.; Kwicklis, E.M.; and Gillies, D.C., eds. 1999. *Hydrogeology of the Unsaturated Zone, North Ramp Area of the Exploratory Studies Facility, Yucca Mountain, Nevada.* Water-Resources Investigations Report 98-4050. Denver, Colorado: U.S. Geological Survey. ACC: MOL.19990419.0335.

100644 Sass, J.H.; Lachenbruch, A.H.; Dudley, W.W., Jr.; Priest, S.S.; and Munroe, R.J. 1988. *Temperature, Thermal Conductivity, and Heat Flow Near Yucca Mountain, Nevada: Some Tectonic and Hydrologic Implications.* Open-File Report 87-649. Denver, Colorado: U.S. Geological Survey. TIC: 203195.

102213 Savard, C.S. 1998. *Estimated Ground-Water Recharge from Streamflow in Fortymile Wash Near Yucca Mountain, Nevada.* Water-Resources Investigations Report 97-4273. Denver, Colorado: U.S. Geological Survey. TIC: 236848.

100075 Sawyer, D.A.; Fleck, R.J.; Lanphere, M.A.; Warren, R.G.; Broxton, D.E.; and Hudson, M.R. 1994. "Episodic Caldera Volcanism in the Miocene Southwestern Nevada Volcanic Field: Revised Stratigraphic Framework, $^{40}Ar/^{39}Ar$ Geochronology, and Implications for Magmatism and Extension." *Geological Society of America Bulletin, 106,* (10), 1304-1318. Boulder, Colorado: Geological Society of America. TIC: 222523.

161591 Sharpe, S. 2003. *Future Climate Analysis—10,000 Years to 1,000,000 Years After Present.* MOD-01-001 REV 01. Reno, Nevada: Desert Research Institute. ACC: MOL.20030407.0055.

101929 Simonds, F.W.; Whitney, J.W.; Fox, K.F.; Ramelli, A.R.; Yount, J.C.; Carr, M.D.; Menges, C.M.; Dickerson, R.P.; and Scott, R.B. 1995. *Map Showing Fault Activity in the Yucca Mountain Area, Nye County, Nevada.* Miscellaneous Investigations Series Map I-2520. Denver, Colorado: U.S. Geological Survey. TIC: 232483.

150228 Slate, J.L.; Berry, M.E.; Rowley, P.D.; Fridrich, C.J.; Morgan, K.S.; Workman, J.B.; Young, O.D.; Dixon, G.L.; Williams, V.S.; McKee, E.H.; Ponce, D.A.; Hildenbrand, T.G.; Swadley, W C; Lundstrom, S.C.; Ekren, E.B.; Warren, R.G.; Cole, J.C.; Fleck, R.J.; Lanphere, M.A.; Sawyer, D.A.; Minor, S.A.; Grunwald, D.J.; Laczniak, R.J.; Menges, C.M.; Yount, J.C.; Jayko, A.S.; Mankinen, E.A.; Davidson, J.G.; Morin, R.L.; and Blakely, R.J. 2000. *Digital Geologic Map of the Nevada Test Site and Vicinity, Nye, Lincoln and Clark Counties, Nevada, and Inyo County, California, Revision 4; Digital Aeromagnetic Map of the Nevada Test Site and Vicinity, Nye, Lincoln, and Clark Counties, Nevada, and Inyo County, California; and Digital Isostatic Gravity Map of the Nevada Test Site and Vicinity, Nye, Lincoln, and Clark Counties, Nevada, and Inyo County, California.* Open-File Report 99-554—A, —B, and —C. Denver, Colorado: U.S. Geological Survey. TIC: 248049; 251985; 251981.

174109 SNL 2007. *Hydrogeologic Framework Model for the Saturated Zone Site Scale Flow and Transport Model.* MDL-NBS-HS-000024 REV 01. Las Vegas, Nevada: Sandia National Laboratories.

177390 SNL 2007. *Saturated Zone Flow and Transport Model Abstraction.* MDL-NBS-HS-000021 REV 04. Las Vegas, Nevada: Sandia National Laboratories.

177394 SNL 2007. *Saturated Zone In-Situ Testing.* ANL-NBS-HS-000039 REV 02. Las Vegas, Nevada: Sandia National Laboratories. ACC: DOC.20070608.0004.

174294 SNL 2007. *Simulation of Net Infiltration for Present-Day and Potential Future Climates*. MDL-NBS-HS-000023 REV 01. Las Vegas, Nevada: Sandia National Laboratories.

177392 SNL 2007. *Site-Scale Saturated Zone Transport.* MDL-NBS-HS-000010 REV 03. Las Vegas, Nevada: Sandia National Laboratories.

178871 SNL 2007. *Total System Performance Assessment Model /Analysis for the License Application*. MDL-WIS-PA-000005 REV 00. Las Vegas, Nevada: Sandia National Laboratories.

175177 SNL 2007. *UZ Flow Models and Submodels.* MDL-NBS-HS-000006 REV 03. Las Vegas, Nevada: Sandia National Laboratories.

158818 Steinkampf, W.C. and Werrell, W.L. 2001. *Ground-Water Flow to Death Valley, as Inferred from the Chemistry and Geohydrology of Selected Springs in Death Valley National Park, California and Nevada.* Water-Resources Investigations Report 98-4114. Denver, Colorado: U.S. Geological Survey. TIC: 251734.

101159 Stuckless, J.S.; Whelan, J.F.; and Steinkampf, W.C. 1991. "Isotopic Discontinuities in Ground Water Beneath Yucca Mountain, Nevada." *High Level Radioactive Waste Management, Proceedings of the Second Annual International Conference, Las Vegas, Nevada, April 28-May 3, 1991. 2,* 1410-1415. La Grange Park, Illinois: American Nuclear Society. TIC: 204272.

101933 Thomas, J.M.; Welch, A.H.; and Dettinger, M.D. 1996. *Geochemistry and Isotope Hydrology of Representative Aquifers in the Great Basin Region of Nevada, Utah, and Adjacent States.* Professional Paper 1409-C. Denver, Colorado: U.S. Geological Survey. ACC: MOL.20010803.0369.

106585 Thordarson, W. 1965. *Perched Ground Water in Zeolitized-Bedded Tuff, Rainier Mesa and Vicinity, Nevada Test Site, Nevada.* TEI-862. Washington, D.C.: U.S. Geological Survey. ACC: NN1.19881021.0066.

126827 Thorstenson, D.C.; Weeks, E.P.; Haas, H.; Busenberg, E.; Plummer, L.N.; and Peters, C.A. 1998. "Chemistry of Unsaturated Zone Gases Sampled in Open Boreholes at the Crest of Yucca Mountain, Nevada: Data and Basic Concepts of Chemical and Physical Processes in the Mountain." *Water Resources Research, 34,* (6), 1507-1529. Washington, D.C.: American Geophysical Union. TIC: 246315.

101490 Tompson, A.F.B. and Gelhar, L.W. 1990. "Numerical Simulation of Solute Transport in Three-Dimensional, Randomly Heterogeneous Porous Media." *Water Resources Research, 26,* (10), 2541-2562. Washington, D.C.: American Geophysical Union. TIC: 224902.

178576 Tonkin, M.J. and Doherty, J. 2005. "A Hybrid Regularized Inversion Methodology for Highly Parameterized Environmental Models." *Water Resources Research, 41,* (W10412), 1-16. Washington, D.C.: American Geophysical Union. TIC: 258946.

179068 Tseng, P-H. and Zyvoloski, G.A. 2000. "A Reduced Degree of Freedom Method for Simulating Non-Isothermal Multi-Phase Flow in a Porous Medium." *Advances in Water Resources, 23,* 731-745. New York, New York: Elsevier. TIC: 254768.

101060 Tucci, P. and Burkhardt, D.J. 1995. *Potentiometric-Surface Map, 1993, Yucca Mountain and Vicinity, Nevada.* Water-Resources Investigations Report 95-4149. Denver, Colorado: U.S. Geological Survey. ACC: MOL.19960924.0517.

155410 Tucci, P. 2001. Segment of SN-USGS-SCI-126-V1: Revision of Water Level AMR (ANL-NBS-HS-000034, Rev 00/ICN 01). Scientific Notebook SN-USGS-SCI-126-V1. ACC: MOL.20010712.0271.

154625 USGS (U.S. Geological Survey) 2001. *Water-Level Data Analysis for the Saturated Zone Site-Scale Flow and Transport Model.* ANL-NBS-HS-000034 REV 00 ICN 01. Denver, Colorado: U.S. Geological Survey. ACC: MOL.20010405.0211.

168473 USGS 2004. *Water-Level Data Analysis for the Saturated Zone Site-Scale Flow and Transport Model.* ANL-NBS-HS-000034 REV 01 Errata 002. Denver, Colorado: U.S. Geological Survey. ACC: MOL.20020209.0058; MOL.20020917.0136; DOC.20040303.0006.

105946 Vaniman, D.T.; Bish, D.L.; Chipera, S.J.; Carlos, B.A.; and Guthrie, G.D., Jr. 1996. *Chemistry and Mineralogy of the Transport Environment at Yucca Mountain.* Volume I of *Summary and Synthesis Report on Mineralogy and Petrology Studies for the Yucca Mountain Site Characterization Project.* Milestone 3665. Los Alamos, New Mexico: Los Alamos National Laboratory. ACC: MOL.19961230.0037.

157427 Vaniman, D.T.; Chipera, S.J.; Bish, D.L.; Carey, J.W.; and Levy, S.S. 2001. "Quantification of Unsaturated-Zone Alteration and Cation Exchange in Zeolitized Tuffs at Yucca Mountain, Nevada, USA." *Geochimica et Cosmochimica Acta, 65,* (20), 3409-3433. New York, New York: Elsevier. TIC: 251574.

178577 Vecchia, A.V. and Cooley, R.L. 1987. "Simultaneous Confidence and Prediction Intervals for Nonlinear Regression Models with Application to a Groundwater Flow Model." *Water Resources Research, 23,* (7), 1237-1250. Washington, D.C.: American Geophysical Union. ACC: MOL.20070108.0002.

143606 Verma, S. and Aziz, K. 1997. "A Control Volume Scheme for Flexible Grids in Reservoir Simulation." *Proceedings, SPE Reservoir Simulation Symposium, 8-11, June 1997, Dallas, Texas.* SPE 37999. Pages 215-227. Richardson, Texas: Society of Petroleum Engineers. TIC: 247097.

154706 Vesselinov, V.V.; Illman, W.A.; Hyun, Y.; Neuman, S.P.; Di Federico, V.; and Tartakovsky, D.M. 2001. "Observation and Analysis of a Pronounced Permeability and Porosity Scale-Effect in Unsaturated Fractured Tuff." *Fractured Rock 2001, An International Conference Addressing Groundwater Flow, Solute Transport, Multiphase Flow, and Remediation in Fractured Rock, March 26-28, 2001, Toronto, Ontario, Canada.* Kueper, B.H.; Novakowski, K.S.; and Reynolds, D.A., eds. Smithville, Ontario, Canada: Smithville Phase IV. TIC: 249909.

101062 Waddell, R.K. 1982. *Two-Dimensional, Steady-State Model of Ground-Water Flow, Nevada Test Site and Vicinity, Nevada-California.* Water-Resources Investigations Report 82-4085. Denver, Colorado: U.S. Geological Survey. ACC: NNA.19870518.0055.

103022 Walker, G.E. and Eakin, T.E. 1963. *Geology and Ground Water of Amargosa Desert, Nevada-California.* Ground-Water Resources – Reconnaissance Series Report 14. Carson City, Nevada: State of Nevada, Department of Conservation and Natural Resources. TIC: 208665.

178643 Watermark Computing 2004. *Groundwater Data Utilities Part B: Program Descriptions*. Brisbane, Australia: Watermark Computing. ACC: MOL.20070115.0009.

178642 Watermark Numerical Computing 2003. *Groundwater Data Utilities Part A: Overview*. Brisbane, Australia: Watermark Numerical Computing. ACC: MOL.20070115.0008.

178612 Watermark Numerical Computing 2004. *PEST, Model-Independent Parameter Estimation User Manual.* 5th Edition. Brisbane, Australia: Watermark Numerical Computing. ACC: MOL.20070111.0002.

130510 Wen, X-H. and Gomez-Hernandez, J.J. 1996. "The Constant Displacement Scheme for Tracking Particles in Heterogeneous Aquifers." *Ground Water, 34,* (1), 135-142. Worthington, Ohio: Water Well Journal Publishing. TIC: 246656.

137305 Whelan, J.F.; Moscati, R.J.; Allerton, S.B.M.; and Marshall, B.D. 1998. *Applications of Isotope Geochemistry to the Reconstruction of Yucca Mountain, Nevada, Paleohydrology—Status of Investigations: June 1996.* Open-File Report 98-83. Denver, Colorado: U.S. Geological Survey. ACC: MOL.19981012.0740.

108865 Whelan, J.F.; Moscati, R.J.; Roedder, E.; and Marshall, B.D. 1998. "Secondary Mineral Evidence of Past Water Table Changes at Yucca Mountain, Nevada." *High-Level Radioactive Waste Management, Proceedings of the Eighth International Conference, Las Vegas, Nevada, May 11-14, 1998.* Pages 178-181. La Grange Park, Illinois: American Nuclear Society. TIC: 237082.

101165 White, A.F. 1979. *Geochemistry of Ground Water Associated with Tuffaceous Rocks, Oasis Valley, Nevada.* Professional Paper 712-E. Washington, D.C.: U.S. Geological Survey. TIC: 219633.

108871 White, A.F. and Chuma, N.J. 1987. "Carbon and Isotopic Mass Balance Models of Oasis Valley - Fortymile Canyon Groundwater Basin, Southern Nevada." *Water Resources Research, 23,* (4), 571-582. Washington, D.C.: American Geophysical Union. TIC: 237579.

101166 White, A.F.; Claassen, H.C.; and Benson, L.V. 1980. *The Effect of Dissolution of Volcanic Glass on the Water Chemistry in a Tuffaceous Aquifer, Rainier Mesa, Nevada.* Geochemistry of Water. Geological Survey Water-Supply Paper 1535-Q, Washington, D.C.: U.S. Government Printing Office. TIC: 221391.

155614 Wilson, C. 2001. *Data Qualification Report: Stratigraphic Data Supporting the Hydrogeologic Framework Model for Use on the Yucca Mountain Project.* TDR-NBS-HS-000013 REV 00. Las Vegas, Nevada: Bechtel SAIC Company. ACC: MOL.20010725.0225.

170977 Williams, N.H. 2003. "Contract No. DE-AC28-01RW12101 - Transmittal of Report Technical Basis Document No. 11: Saturated Zone Flow and Transport Revision 2 Addressing Twenty-Five Key Technical Issue (KTI) Agreements Related to Saturated Zone Flow and Transport." Letter from N.H. Williams (BSC) to C.M. Newbury (DOE/ORD), September 30, 2003, MP:cg - 0930038958, with enclosure. ACC: MOL.20040105.0270.

108882 Winograd, I.J. and Pearson, F.J., Jr. 1976. "Major Carbon 14 Anomaly in a Regional Carbonate Aquifer: Possible Evidence for Megascale Channeling, South Central Great Basin." *Water Resources Research, 12,* (6), 1125-1143. Washington, D.C.: American Geophysical Union. TIC: 217731.

101167 Winograd, I.J. and Thordarson, W. 1975. *Hydrogeologic and Hydrochemical Framework, South-Central Great Basin, Nevada-California, with Special Reference to the Nevada Test Site.* Geological Survey Professional Paper 712-C. Washington, D.C.: United States Government Printing Office. ACC: NNA.19870406.0201.

100094 Winograd, I.J.; Coplen, T.B.; Landwehr, J.M.; Riggs, A.C.; Ludwig, K.R.; Szabo, B.J.; Kolesar, P.T.; and Revesz, K.M. 1992. "Continuous 500,000-Year Climate Record from Vein Calcite in Devils Hole, Nevada." *Science, 258,* 255-260. Washington, D.C.: American Association for the Advancement of Science. TIC: 237563.

178405 Winterle, J. 2005. *Simulation of Spring Flows South of Yucca Mountain, Nevada, Following a Potential Future Water Table Rise.* San Antonio, Texas: Center for Nuclear Waste Regulatory Analyses. ACC: MOL.20061120.0234.

178404 Winterle, J.R. 2003. *Evaluation of Alternative Concepts for Saturated Zone Flow: Effects of Recharge and Water Table Rise on Flow Paths and Travel Times at Yucca Mountain.* San Antonio, Texas: Center for Nuclear Waste Regulatory Analyses. ACC: MOL.20061120.0233.

129796 Winterle, J.R. and La Femina, P.C. 1999. *Review and Analysis of Hydraulic and Tracer Testing at the C-Holes Complex Near Yucca Mountain, Nevada.* San Antonio, Texas: Center for Nuclear Waste Regulatory Analyses. TIC: 246623.

149596 Yang, I.C. and Peterman, Z.E. 1999. "Chemistry and Isotopic Content of Perched Water." In *Hydrogeology of the Unsaturated Zone, North Ramp Area of the Exploratory Studies Facility, Yucca Mountain, Nevada.* Rousseau, J.P.; Kwicklis, E.M.; and Gillies, D.C., eds. Water-Resources Investigations Report 98-4050. Denver, Colorado: U.S. Geological Survey. ACC: MOL.19990419.0335.

100194 Yang, I.C.; Rattray, G.W.; and Yu, P. 1996. *Interpretation of Chemical and Isotopic Data from Boreholes in the Unsaturated Zone at Yucca Mountain, Nevada.* Water-Resources Investigations Report 96-4058. Denver, Colorado: U.S. Geological Survey. ACC: MOL.19980528.0216.

101441 Yang, I.C.; Yu, P.; Rattray, G.W.; Ferarese, J.S.; and Ryan, J.N. 1998. *Hydrochemical Investigations in Characterizing the Unsaturated Zone at Yucca Mountain, Nevada.* Water-Resources Investigations Report 98-4132. Denver, Colorado: U.S. Geological Survey. ACC: MOL.19981012.0790.

179430 YMP (Yucca Mountain Site Characterization Project) 2001. Sample Collection Report, Characterization of the Yucca Mountain Unsaturated-Zone Percolation Surface-Based Studies, May 17, 1995 through May 18, 1995. Las Vegas, Nevada: Yucca Mountain Site Characterization Office. ACC: MOL.20011030.0681.

101171 Zyvoloski, G. 1983. "Finite Element Methods for Geothermal Reservoir Simulation." *International Journal for Numerical and Analytical Methods in Geomechanics, 7,* (1), 75-86. New York, New York: John Wiley & Sons. TIC: 224068.

163341 Zyvoloski, G.; Kwicklis, E.; Eddebbarh, A.A.; Arnold, B.; Faunt, C.; and Robinson, B.A. 2003. "The Site-Scale Saturated Zone Flow Model for Yucca Mountain: Calibration of Different Conceptual Models and their Impact on Flow Paths." *Journal of Contaminant Hydrology, 62-63,* 731-750. New York, New York: Elsevier. TIC: 254340.

9.2 CODES, STANDARDS, REGULATIONS, AND PROCEDURES

176567 10 CFR 50. 2006. Energy: Domestic Licensing of Production and Utilization Facilities. Internet Accessible.

176544 10 CFR 63. 2006. Energy: Disposal of High-Level Radioactive Wastes in a Geologic Repository at Yucca Mountain, Nevada. Internet Accessible.

AP-2.22Q, Rev. 1, ICN 1. *Classification Analyses and Maintenance of the Q-List.* Washington, D.C.: U.S. Department of Energy, Office of Civilian Radioactive Waste Management. ACC: DOC.20040714.0002.

AP-2.27Q, Rev. 1, ICN 5. *Planning for Science Activities.* Washington, D.C.: U.S. Department of Energy, Office of Civilian Radioactive Waste Management. ACC: DOC.20041014.0001.

AP-SI.1Q, Rev. 5, ICN 2. *Software Management.* Washington, D.C.: U.S. Department of Energy, Office of Civilian Radioactive Waste Management. ACC: DOC.20030902.0003.

AP-SIII.10Q, Rev. 2, ICN 7. *Models.* Washington, D.C.: U.S. Department of Energy, Office of Civilian Radioactive Waste Management. ACC: DOC.20040920.0002.

176399 ASME NQA-1-2004. 2004. Quality Assurance Requirements for Nuclear Facilities Applications. New York, New York: American Society of Mechanical Engineers. TIC: 256850.

177092 DOE (U.S. Department of Energy) 2006. *Quality Assurance Requirements and Description*. DOE/RW-0333P, Rev. 18. Washington, D.C.: U.S. Department of Energy, Office of Civilian Radioactive Waste Management. ACC: DOC.20060602.0001.

IT-PRO-0011, *Software Management*.

IT-PRO-0012, *Qualification of Software*.

IT-PRO-0013 *Software Independent Verification and Validation*.

LP-SI.11Q-BSC, Rev. 0, ICN 1. *Software Management.* Washington, D.C.: U.S. Department of Energy, Office of Civilian Radioactive Waste Management. ACC: DOC.20041005.0008.

LS-PRO-0203, *Q-List and Classification of Structures, Systems, and Components*.

SCI-PRO-001, *Qualification of Unqualified Data*.

SCI-PRO-003, Rev. 2, ICN 0. *Document Review.* Washington, D.C.: U.S. Department of Energy, Office of Civilian Radioactive Waste Management. ACC: DOC.20070418.0002.

SCI-PRO-006, *Models*.

9.3 SOURCE DATA, LISTED BY DATA TRACKING NUMBER

149155 GS000308312322.003. Preliminary Release of Field, Chemical, and Isotopic Data from the Nye County Early Warning Drilling Program (EWDP) Wells in Amargosa Valley, Nevada Collected Between 12/11/98 and 11/15/99. Submittal date: 03/16/2000.

149947 GS000508312332.001. Water-Level Data Analysis for the Saturated Zone Site-Scale Flow and Transport Model. Submittal date: 06/01/2000.

150842 GS000700012847.001. Chemical and Isotopic Data from Cind-R-Lite Well Samples Collected on 5/17/95 and 9/6/95. Submittal date: 07/10/2000.

171433 GS001208312312.009. Ground-Water Altitudes from Manual Depth-to-Water Measurements at Various Boreholes January through June 2000. Submittal date: 12/29/2000.

162908 GS010208312322.001. Uranium Concentrations and 234U/238U Activity Ratios Analyzed Between August, 1998 and April, 2000 for Saturated-Zone Well Water, Springs, and Runoff Collected between April, 1998 and November 1999. Submittal date: 03/30/2001.

162910 GS010308312322.002. Chemical and Isotopic Data from Wells in Yucca Mountain Area, Nye County, Nevada, Collected between 12/11/98 and 11/15/99. Submittal date: 03/29/2001.

154734 GS010308312322.003. Field, Chemical and Isotopic Data from Wells in Yucca Mountain Area, Nye County, Nevada, Collected Between 12/11/98 and 11/15/99. Submittal date: 03/29/2001.

155307 GS010608312332.001. Potentiometric-Surface Map, Assuming Perched Conditions North of Yucca Mountain, in the Saturated Site-Scale Model. Submittal date: 06/19/2001.

156187 GS010608315215.002. Uranium and Thorium Isotope Data for Waters Analyzed Between January 18, 1994 and September 14, 1996. Submittal date: 06/26/2001.

156007 GS010808312322.004. Uranium and Uranium Isotopic Data for Water Samples from Wells and Springs in the Yucca Mountain Vicinity Collected Between December 1996 and December 1997. Submittal date: 08/29/2001.

163555 GS010908312332.002. Borehole Data from Water-Level Data Analysis for the Saturated Zone Site-Scale Flow and Transport Model. Submittal date: 10/02/2001.

168699 GS010908312332.003. Vertical Head Differences from Water-Level Data Analysis for the Saturated Zone Site-Scale Flow and Transport Model. Submittal date: 10/20/2001.

162874 GS010908314221.001. Geologic Map of the Yucca Mountain Region, Nye County, Nevada. Submittal date: 01/23/2002.

158690 GS011008314211.001. Interpretation of the Lithostratigraphy in Deep Boreholes NC-EWDP-19D1 and NC-EWDP-2DB Nye County Early Warning Drilling Program. Submittal date: 01/16/2001.

162911 GS011108312322.006. Field and Chemical Data Collected between 1/20/00 and 4/24/01 and Isotopic Data Collected between 12/11/98 and 11/6/00 from Wells in the Yucca Mountain Area, Nye County, Nevada. Submittal date: 11/20/2001.

174112 GS020108314211.001. Interpretation of the Lithostratigraphy in Deep Boreholes, NC-EWDP-7SC and NC-EWDP-15P, Nye County Early Warning Drilling Program. Submittal date: 01/16/2001.

162913 GS021008312322.002. Stable Isotopic Data for Water Samples Collected between 02/20/98 and 08/20/98 in the Yucca Mountain Area, Nye County, Nevada. Submittal date: 11/12/2002.

163483 GS030108314211.001. Interpretation of the Lithostratigraphy in Deep Boreholes NC-EWDP-18P, NC-EWDP-22SA, NC-EWDP-10SA, NC-EWDP-23P, NC-EWDP-19IM1A, and NC-EWDP-19IM2A, Nye County Early Warning Drilling Program, Phase III. Submittal date: 02/11/2003.

166467 GS031108312322.003. Uranium Concentrations and $^{234}U/^{238}U$ Ratios for Ground-Water Samples from Boreholes ER-EC-7, ER-18-2, and UE-18R Collected between December 1999 and June 2000. Submittal date: 11/25/2003.

174113 GS031108314211.004. Interpretation of the Lithostratigraphy in Deep Boreholes NC-EWDP-16P, NC-EWDP-27P, and NC-EWDP-28P, Nye County Early Warning Drilling Program, Phase IV A. Submittal date: 11/26/2003.

179431 GS031208312322.004. Dissolved Organic Carbon-14 (DOC-14) Hydrochronology Data for Groundwater from Wells in the Yucca Mountain Area for Samples Analyzed through 1/30/2003. Submittal date: 01/26/2004.

179422 GS040108312322.001. Field and Chemical Data Collected Between 10/4/01 and 10/3/02 and Isotopic Data Collected Between 5/19/00 and 5/22/03 from Wells in the Yucca Mountain Area, Nye County, Nevada. Submittal date: 06/07/2004.

172396 GS040208312322.003. Uranium Concentrations and 234U/238U Ratios from Spring, Well, Runoff, and Rain Waters Collected from the Nevada Test Site and Death Valley Vicinities and Analyzed between 01/15/98 and 08/15/98. Submittal date: 04/01/2004.

179432 GS040708312322.004. Strontium Isotope Ratios and Strontium Concentrations on Groundwater Samples from Springs in the Area of Amargosa Valley and Desert. Submittal date: 09/08/2004.

179433 GS040808312322.005. Strontium Isotope Ratios and Strontium Concentrations on Groundwater Samples in Support of Nye Co. Early Warning Drilling Program (EWDP) and the Alluvial Tracer Complex (ATC). Submittal date: 09/20/2004.

179434 GS040808312322.006. Field, Chemical, and Isotope Data for Spring and Well Samples Collected Between 03/01/01 and 05/12/04 in the Yucca Mountain Area, Nye County, Nevada. Submittal date: 11/15/2004.

174114 GS040908314211.001. Interpretation of the Lithostratigraphy in Deep Boreholes NC-EWDP-24P and NC-EWDP-29P, Nye County Early Warning Drilling Program, Phase IV B. Submittal date: 10/26/2004.

179435 GS050708314211.001. Description and Interpretation of Core Samples from Alluvial Core Holes NC-EWDP-19PB and NC-EWDP-22PC, Nye County Early Warning Drilling Program. Submittal date: 07/27/2005.

105937 GS920408312321.003. Chemical Composition of Groundwater in the Yucca Mountain Area, Nevada 1971 - 1984. Submittal date: 04/24/1987.

148109 GS930108315213.002. Water Chemistry and Sample Documentation for Two Samples from Lathrop Wells Cone and USW VH-2. Submittal date: 01/15/1993.

145525 GS930108315213.004. Uranium Isotopic Analyses of Groundwaters from SW Nevada – SE California. Submittal date: 01/21/1993.

145530 GS930308312323.001. Chemical Composition of Groundwater and the Locations of Permeable Zones in the Yucca Mountain Area. Submittal date: 03/05/1993.

145404 GS930908312323.003. Hydrochemical Data from Field Test and Lab Analyses of Water Samples Collected at Field Stations: USW VH-1, JF3, UE-29 UZN#91, Virgin Spring, Nevares Spring, UE-25 J#12, UE-25 J#13, UE-22 ARMY#1, and USW UZ-14. Submittal date: 09/30/1993.

149611 GS931100121347.007. Selected Ground-Water Data for Yucca Mountain Region, Southern Nevada and Eastern California, Through December 1992. Submittal date: 11/30/1993.

164673 GS940908315213.005. U Concentrations and 234U/238U Ratios for Waters in Yucca Mountain Region. Submittal date: 09/22/1994.

106516 GS950708315131.003. Woodrat Midden Age Data in Radiocarbon Years Before Present. Submittal date: 07/21/1995.

148114 GS950808312322.001. Field, Chemical, and Isotopic Data Describing Water Samples Collected in Death Valley National Monument and at Various Boreholes in and Around Yucca Mountain, Nevada, Between 1992 and 1995. Submittal date: 08/16/1995.

151649 GS951208312272.002. Tritium Analyses of Porewater from USW UZ-14, USW NRG-6, USW NRG-7A and UE-25 UZ#16 and of Perched Water from USW SD-7, USW SD-9, USW UZ-14 and USW NRG-7A from 12/09/92 to 5/15/95. Submittal date: 12/15/1995.

106517 GS960308315131.001. Woodrat Midden Radiocarbon (C14). Submittal date: 03/07/1996.

162915 GS960408312323.002. Chemical and Isotopic Data Describing Water Samples Collected from 11 Springs and One Stream Within Death Valley National Park in 1993, 1994, and 1995. Submittal date: 04/02/1996.

114124 GS960908312232.012. Comparison of Air-Injection Permeability Values to Laboratory Permeability Values. Submittal date: 09/26/1996.

162916 GS960908312323.005. Hydrochemical Data Obtained from Water Samples Collected at Water Well ER-30-1 on 1/31/95 and 2/1/95. Submittal date: 09/10/1996.

145405 GS970708312323.001. Delta 18-O and Delta D Stable Isotope Analyses of a Bore-Hole Waters from GEXA Well 4 and VH-2. Submittal date: 07/22/1997.

164674 GS970708315215.008. Strontium Isotope Ratios and Isotope Dilution Data for Strontium for Two Samples Collected at UE-25 C#3, 12/4/96 and 2/19/97. Submittal date: 07/29/1997.

145921 GS970808315215.012. Uranium and Thorium Isotope Data from Secondary Minerals in the ESF Collected Between 02/15/97 and 09/15/97. Submittal date: 09/17/1997.

149617 GS980108312322.005. Water Chemistry Data from Samples Collected at Borehole USW WT-24, Between 10/06/97 and 12/10/97. Submittal date: 01/26/1998.

146065 GS980208312322.006. Uranium Isotopic Data for Saturated- and Unsaturated-Zone Waters Collected by Non-YMP Personnel Between May 1989 and August 1997. Submittal date: 02/03/1998.

145412 GS980908312322.008. Field, Chemical, and Isotopic Data from Precipitation Sample Collected Behind Service Station in Area 25 and Ground Water Samples Collected at Boreholes UE-25 C #2, UE-25 C #3, USW UZ-14, UE-25 WT #3, UE-25 WT #17, and USW WT-24, 10/06/97 to 07/01/98. Submittal date: 09/15/1998.

118977 GS980908312322.009. Uranium Concentrations and $^{234}U/^{238}U$ Ratios from Spring, Well, Runoff, and Rain Waters Collected from the Nevada Test Site and Death Valley Vicinities and Analyzed between 01/15/1998 and 08/15/1998. Submittal date: 09/23/1998.

145692 GS990308312272.002. Isotopic Composition of Pore Water from Boreholes USW UZ-14 and USW NRG-6. Submittal date: 03/02/1999.

149393 GS990808312322.001. Field and Isotopic Data From Ground Water Samples From Wells in the Amargosa Valley and NTS. Submittal date: 08/23/1999.

162917 GS990808312322.002. Chemical and Isotopic Data from Ground Water Samples Collected from Wells in the Amargosa. Submittal date: 08/23/1999.

145263 GS991208314221.001. Geologic Map of the Yucca Mountain Region. Submittal date: 12/01/1999.

147077 LA0002JF831222.001. Apparent Infiltration Rates in Alluvium from USW UZ-N37, USW UZ-N54, USW UZ-14 and UE-25 UZ#16, Calculated by Chloride Mass Balance Method. Submittal date: 02/25/2000.

147079 LA0002JF831222.002. Apparent Infiltration Rates in PTN Units from USW UZ-7A, USW UZ-N55, USW UZ-14, UE-25 UZ#16, USW NRG-6, USW NRG-7A, and USW SD-6, SD-7, SD-9 and SD-12 Calculated by the Chloride Mass Balance Method. Submittal date: 02/25/2000.

165507 LA0202EK831231.002. Calculation of Corrected and Uncorrected Groundwater Carbon-14 Ages. Submittal date: 02/25/2002.

180317 LA0202EK831231.004. Calculation of the Maximum Possible Percentage of 1000Year-Old Water Present in Selected Yucca Mountain Area Groundwater Samples. Submittal date: 02/25/2002.

163561 LA0303PR831231.002. Estimation of Groundwater Drift Velocity from Tracer Responses in Single-Well Tracer Tests at Alluvium Testing Complex. Submittal date: 03/18/2003.

163788 LA0304TM831231.002. SZ Site-Scale Flow Model, FEHM Files for Base Case. Submittal date: 04/14/2003.

171890 LA0308RR831233.001. Regional Groundwater Flow Pathways in the Yucca Mountain Area Inferred from Hydrochemical and Isotopic Data. Submittal date: 08/25/2003.

165471 LA0309EK831223.001. UTM Coordinates for Selected Amargosa Desert Wells. Submittal date: 09/05/2003.

171887 LA0309EK831231.001. SZ Flow and Transport Model, FEHM Files for Tracer Transport. Submittal date: 09/02/2003.

166546 LA0309RR831233.001. Regional Groundwater Hydrochemical Data in the Yucca Mountain Area Used as Direct Inputs for ANL-NBS-HS-000021, REV 01. Submittal date: 09/05/2003.

166548 LA0309RR831233.002. Regional Groundwater Hydrochemical Data in the Yucca Mountain Area Used as Corroborative Data for ANL-NBS-HS-000021, REV 01. Submittal date: 09/05/2003.

171889 LA0310EK831231.001. SZ Geochemical Calculations, Groundwater Travel Times for Selected Wells. Submittal date: 10/16/2003.

165995 LA0310EK831232.001. SZ Geochemical Models, PHREEQC Files for Selected Groundwater Parameters. Submittal date: 10/02/2003.

165985 LA0311EK831223.001. Well Completion Summary Information for the Nye County EWDP, Phases I and II. Submittal date: 11/04/2003.

166068 LA0311EK831232.001. Hydrochemical Data Obtained from GEOCHEM.02 Database. Submittal date: 11/06/2003.

166069 LA0311EK831232.002. Groundwater Hydrochemical Data from Nye County Early Warning Drilling Project Boreholes as Reported by Nye County. Submittal date: 11/04/2003.

122733 LA9909JF831222.010. Chloride, Bromide, Sulfate, and Chlorine-36 Analyses of ESF Porewaters. Submittal date: 09/29/1999.

122736 LA9909JF831222.012. Chloride, Bromide, and Sulfate Analyses of Porewater Extracted from ESF Niche 3566 (Niche #1) and ESF 3650 (Niche #2) Drillcore. Submittal date: 09/29/1999.

145401 LAJF831222AQ97.002. Chlorine-36 Analyses of Packrat Urine. Submittal date: 09/26/1997.

145402 LAJF831222AQ98.011. Chloride, Bromide, Sulfate and Chlorine-36 Analyses of Springs, Groundwater, Porewater, Perched Water and Surface Runoff. Submittal date: 09/10/1998.

163044 LB03023DSSCP9I.001. 3-D Site Scale UZ Flow Field Simulations for 9 Infiltration Scenarios. Submittal date: 02/28/2003.

148744 MO0003SZFWTEEP.000. Data Resulting from the Saturated Zone Flow and Transport Expert Elicitation Project. Submittal date: 03/06/2000.

151492 MO0007GNDWTRIS.002. Isotopic Content of Groundwater from Yucca Mountain Project Borehole, USW G-2, Extracted from ANL-NBS-HS-000021, Geochemical and Isotopic Constraints on Groundwater Flow Directions, Mixing and Recharge at Yucca Mountain, Nevada. Submittal date: 07/27/2000.

151493 MO0007GNDWTRIS.003. Isotopic Content of Groundwater from Yucca Mountain Project Boreholes UZ-14, WT-17, and WT #3, Extracted from ANL-NBS-HS-000021, Geochemical and Isotopic Constraints on Groundwater Flow Directions, Mixing and Recharge at Yucca Mountain, Nevada. Submittal date: 07/27/2000.

151494 MO0007GNDWTRIS.004. Isotopic Content of Groundwater from Borehole TW-5 Extracted from ANL-NBS-HS-000021, Geochemical and Isotopic Constraints on Groundwater Flow Directions, Mixing and Recharge at Yucca Mountain, Nevada. Submittal date: 07/27/2000.

151495 MO0007GNDWTRIS.005. Isotopic Content of Groundwater from Yucca Mountain Project Borehole JF #3, Extracted from ANL-NBS-HS-000021, Geochemical and Isotopic Constraints on Groundwater Flow Directions, Mixing and Recharge at Yucca Mountain, Nevada. Submittal date: 07/28/2000.

151496 MO0007GNDWTRIS.006. Isotopic Content of Groundwater from Selected Yucca Mountain Project WT Boreholes Extracted from ANL-NBS-HS-000021, Geochemical and Isotopic Constraints on Groundwater Flow Directions, Mixing and Recharge at Yucca Mountain, Nevada. Submittal date: 07/28/2000.

151497 MO0007GNDWTRIS.007. Isotopic Content of Groundwater from Yucca Mountain Project Boreholes WT #14, WT #15, and WT #12, Extracted from ANL-NBS-HS-000021, Geochemical and Isotopic Constraints on Groundwater Flow Directions, Mixing and Recharge at Yucca Mountain, Nevada. Submittal date: 07/28/2000.

151508 MO0007GNDWTRIS.008. Isotopic Content of Groundwater from Yucca Mountain Project Borehole UE-25 P #1 Extracted from ANL-NBS-HS-000021, Geochemical and Isotopic Constraints on Groundwater Flow Directions, Mixing and Recharge at Yucca Mountain, Nevada. Submittal date: 07/28/2000.

151509 MO0007GNDWTRIS.009. Isotopic Content of Groundwater from Selected Yucca Mountain Project Boreholes Extracted from ANL-NBS-HS-000021, Geochemical and Isotopic Constraints on Groundwater Flow Directions, Mixing and Recharge at Yucca Mountain, Nevada. Submittal date: 07/28/2000.

151500 MO0007GNDWTRIS.010. Isotopic Content of Groundwater from Selected Yucca Mountain Project Boreholes Extracted from ANL-NBS-HS-000021, Geochemical and Isotopic Constraints on Groundwater Flow Directions, Mixing and Recharge at Yucca Mountain, Nevada. Submittal date: 07/28/2000.

151501 MO0007GNDWTRIS.011. Isotopic Content of Groundwater from Selected Boreholes Not Drilled for the Yucca Mountain Project Extracted from ANL-NBS-HS-000021, Geochemical and Isotopic Constraints on Groundwater Flow Directions, Mixing and Recharge at Yucca Mountain, Nevada. Submittal date: 07/28/2000.

151504 MO0007GNDWTRIS.013. Isotopic Content of Perched Groundwater from Yucca Mountain Project Boreholes Extracted from ANL-NBS-HS-000021, Geochemical and Isotopic Constraints on Groundwater Flow Directions, Mixing and Recharge at Yucca Mountain, Nevada. Submittal date: 07/28/2000.

151507 MO0007MAJIONPH.002. Major Ion Content of Groundwater from Borehole TW-5 Extracted from ANL-NBS-HS-000021, Geochemical and Isotopic Constraints on Groundwater Flow Directions, Mixing and Recharge at Yucca Mountain, Nevada. Submittal date: 07/27/2000.

151513 MO0007MAJIONPH.003. Major Ion Content of Groundwater from Yucca Mountain Project Borehole USW G-2, Extracted from ANL-NBS-HS-000021, Geochemical and Isotopic Constraints on Groundwater Flow Directions, Mixing and Recharge at Yucca Mountain, Nevada. Submittal date: 07/27/2000.

151516 MO0007MAJIONPH.004. Major Ion Content of Groundwater from Borehole ONC #1, Extracted from ANL-NBS-HS-000021, Geochemical and Isotopic Constraints on Groundwater Flow Directions, Mixing and Recharge at Yucca Mountain, Nevada. Submittal date: 07/27/2000.

151517 MO0007MAJIONPH.005. Major Ion Content of Groundwater from Boreholes UZ-14, WT-17 and WT #3, Extracted from ANL-NBS-HS-000021, Geochemical and Isotopic Constraints on Groundwater Flow Directions, Mixing and Recharge at Yucca Mountain, Nevada. Submittal date: 07/27/2000.

151518 MO0007MAJIONPH.006. Major Ion Content of Groundwater from Selected Boreholes Not Drilled on the Yucca Mountain Project, Extracted from ANL-NBS-HS-000021, Geochemical and Isotopic Constraints on Groundwater Flow Directions, Mixing and Recharge at Yucca Mountain, Nevada. Submittal date: 07/25/2000.

151519 MO0007MAJIONPH.007. Major Ion Content of Groundwater from Yucca Mountain Project Borehole UE-25 UZ #16, Extracted from ANL-NBS-HS-000021, Geochemical and Isotopic Constraints on Groundwater Flow Directions, Mixing and Recharge at Yucca Mountain, Nevada. Submittal date: 07/27/2000.

151521 MO0007MAJIONPH.008. Major Ion Content of Groundwater from Selected YMP and Other Boreholes Extracted from ANL-NBS-HS-000021, Geochemical and Isotopic Constraints on Groundwater Flow Directions, Mixing and Recharge at Yucca Mountain, Nevada. Submittal date: 07/27/2000.

151522 MO0007MAJIONPH.009. Major Ion Content of Groundwater from Borehole NDOT Extracted from ANL-NBS-HS-000021, Geochemical and Isotopic Constraints on Groundwater Flow Directions, Mixing and Recharge at Yucca Mountain, Nevada. Submittal date: 07/27/2000.

151523 MO0007MAJIONPH.010. Major Ion Content of Groundwater from Borehole UE-25 P #1 Extracted from ANL-NBS-HS-000021, Geochemical and Isotopic Constraints on Groundwater Flow Directions, Mixing and Recharge at Yucca Mountain, Nevada. Submittal date: 07/27/2000.

151524 MO0007MAJIONPH.011. Major Ion Content of Groundwater from Selected Yucca Mountain Project Boreholes Extracted from ANL-NBS-HS-000021, Geochemical and Isotopic Constraints on Groundwater Flow Directions, Mixing and Recharge at Yucca Mountain, Nevada. Submittal date: 07/27/2000.

151529 MO0007MAJIONPH.012. Major Ion Content of Groundwater from Selected YMP and Other Boreholes Extracted from ANL-NBS-HS-000021, Geochemical and Isotopic Constraints on Groundwater Flow Directions, Mixing and Recharge at Yucca Mountain, Nevada. Submittal date: 07/27/2000.

151530 MO0007MAJIONPH.013. Major Ion Content of Groundwater from Selected YMP and Other Boreholes Extracted from ANL-NBS-HS-000021, Geochemical and Isotopic Constraints on Groundwater Flow Directions, Mixing and Recharge at Yucca Mountain, Nevada. Submittal date: 07/27/2000.

151531 MO0007MAJIONPH.014. Major Ion Content of Groundwater from Selected Boreholes Not Drilled on the Yucca Mountain Project Extracted from ANL-NBS-HS-000021, Geochemical and Isotopic Constraints on Groundwater Flow Directions, Mixing and Recharge at Yucca Mountain, Nevada. Submittal date: 07/27/2000.

151532 MO0007MAJIONPH.015. Major Ion Content of Groundwater from NC-EWDP Boreholes Extracted from ANL-NBS-HS-000021, Geochemical and Isotopic Constraints on Groundwater Flow Directions, Mixing and Recharge at Yucca Mountain, Nevada. Submittal date: 07/27/2000.

151533 MO0007MAJIONPH.016. Major Ion Content of Perched Groundwater from Selected YMP Boreholes with Perched Water Extracted from ANL-NBS-HS-000021, Geochemical and Isotopic Constraints on Groundwater Flow Directions, Mixing and Recharge at Yucca Mountain, Nevada. Submittal date: 07/28/2000.

151534 MO0008MAJIONPH.017. Major Ion Content of Groundwater from Selected WT Boreholes Drilled for the Yucca Mountain Project Extracted from ANL-NBS-HS-000021, Geochemical and Isotopic Constraints on Groundwater Flow Directions, Mixing and Recharge at Yucca Mountain, Nevada. Submittal date: 08/02/2000.

153777 MO0012MWDGFM02.002. Geologic Framework Model (GFM2000). Submittal date: 12/18/2000.

153384 MO0012URANISOT.000. Water - Selected Uranium Abundance and Isotope Ratios. Submittal date: 12/06/2000.

154733 MO0102DQRBTEMP.001. Temperature Data Collected from Boreholes Near Yucca Mountain in Early 1980's. Submittal date: 02/21/2001.

155523 MO0102DQRGWREC.001. Groundwater Recharge Rate Data for the Four Reaches of Fortymile Wash Near Yucca Mountain, Nevada. Submittal date: 02/26/2001

157187 MO0112DQRWLNYE.018. Well Completion Diagram for Borehole NC-EWDP-19D. Submittal date: 12/05/2001.

168375 MO0203GSC02034.000. As-Built Survey of Nye County Early Warning Drilling Program (EWDP) Phase III Boreholes NC-EWDP-10S, NC-EWDP-18P, and NC-EWDP-22S - Partial Phase III List. Submittal date: 03/21/2002.

168378 MO0206GSC02074.000. As-Built Survey of Nye County Early Warning Drilling Program (EWDP) Phase III Boreholes, Second Set. Submittal date: 06/03/2002.

179372 MO0206NYE04926.119. NC-EWDP-7SC Well Completion Diagram. Submittal date: 06/19/2002.

165876 MO0306NYE05259.165. Revised NC-EWDP-19IM1 Well Completion Diagram. Submittal date: 07/02/2003.

165877 MO0306NYE05260.166. Revised NC-EWDP-19IM2 Well Completion Diagram. Submittal date: 07/02/2003.

179373 MO0306NYE05261.167. Revised NC-EWDP-10S Well Completion Diagram. Submittal date: 07/03/2003.

179374 MO0306NYE05262.168. Revised NC-EWDP-10P Well Completion Diagram. Submittal date: 07/03/2003.

179375 MO0306NYE05263.169. Revised NC-EWDP-18P Well Completion Diagram. Submittal date: 07/03/2003.

170556 MO0307GSC03094.000. As-Built Survey of Nye County Early Warning Drilling Program Phase IV Boreholes EWDP-16P, EWDP-27P & EWDP-28P. Submittal date: 07/14/2003.

165529 MO0309THDPHRQC.000. Input Data File (PHREEQC.DAT) for Thermodynamic Data Software Code PHREEQC, Version 2.3. Submittal date: 09/22/2003.

174103 MO0312GSC03180.000. As-Built Survey of Nye County Early Warning Drilling Program, Phase IV Boreholes: NC-EWPD-24P & NC-EWDP-29P. Submittal date: 12/03/2003.

174102 MO0408GSC04123.000. Nye County Early Warning Drilling Program, Phase IV, As-Built Location of NC-EWDP-19PB Borehole. Submittal date: 08/12/2004.

179336 MO0409SEPPSMPC.000. Potentiometric-Surface Map Showing Possible Changes After Including EWDP Phases III and IV Wells. Submittal date: 09/23/2004.

179599 MO0505NYE06464.314. NC-EWDP-22PC Well Completion Diagram. Submittal date: 05/16/2005

177372 MO0507NYE06631.323. EWDP Manual Water Level Measurements through February 2005. Submittal date: 07/21/2005.

174523 MO0507SPAINHFM.000. Input Data for HFM - USGS-Supplied Data to Supplement Regional Hydrogeologic Framework Model. Submittal date: 02/22/2005.

177371 MO0602SPAMODAR.000. Model Archives from USGS Special Investigations Report 2004-5205, Death Valley Regional Ground-Water Flow System, Nevada and California-Hydrogeologic Framework and Transient Ground-Water Flow Model. Submittal date: 02/10/2006.

179352 MO0610MWDHFM06.002. Hydrogeologic Framework Model (HFM2006) Stratigraphic Horizon Grids. Submittal date: 11/01/2006.

179486 MO0612NYE07008.366. NC-EWDP-32P WELL COMPLETION DIAGRAM. Submittal date: 12/04/2006.

179487 MO0612NYE07011.368. NC-EWDP-33P WELL COMPLETION DIAGRAM. Submittal date: 12/04/2006.

179337 MO0612NYE07122.370. EWDP Manual Water Level Measurements through November 2006. Submittal date: 12/15/2006.

129714 SNT05082597001.003. TSPA-VA (Total System Performance Assessment-Viability Assessment) Saturated Zone (SZ) Base Case Modeling Analysis Results. Submittal date: 02/03/1998.

9.4 OUTPUT DATA, LISTED BY DATA TRACKING NUMBER

LA0612RR150304.001. UTM Coordinates for Selected Nye County Early Warning Drilling Program Boreholes: NC-EWDP-7SC and Phases III and IV. Submittal date: 12/18/2006.

LA0612RR150304.002. Hydrochemical Data Obtained from the Underground Test Area (UGTA) Program's Geochem05 Database. Submittal date: 12/18/2006.

LA0612RR150304.003. Geochemical and Isotopic Data for Selected NC-EWDP Wells, Phases II, III, and IV. Submittal date: 01/02/2007.

LA0612RR150304.004. Regional Groundwater Flow Pathways In The Yucca Mountain Area Inferred From Hydrochemical And Isotopic Data. Submittal date: 01/02/2007.

LA0612RR150304.005. Uranium Activity Ratios Calculated from Isotopic Ratios Reported for Nye County EWDP Boreholes and McCracken Well by Geochron Laboratories, for Samples Collected between November 1999 and June 2000. Submittal date: 12/21/2006.

LA0612TM831231.001. SZ Site-Scale Flow Model, LaGriT Files for Base-Case FEHM Grid. Submittal date: 12/21/2006.

MO0611SCALEFLW.000. Water Table for the Saturated Zone Site Scale Flow Model. Submittal date: 11/15/2006.

SN0610T0510106.001. Water Level Data, Well Location Data, and Open Well Interval Data. Submittal date: 10/02/2006.

SN0612T0510106.003. Recharge and Lateral Groundwater Flow Boundary Conditions for the Saturated Zone (SZ) Site-Scale Flow Model. Submittal date: 12/04/2006.

SN0612T0510106.004. Saturated Zone (SZ) Site-Scale Flow Model PEST and FEHM Files Using HFM2006. Submittal date: 01/17/2007.

SN0702T0510106.006. Saturated Zone (SZ) Site-Scale Flow Model with "Water Table Rise" Alternate Conceptual Model - FEHM Files Using HFM2006. Submittal date: 02/19/2007.

SN0702T0510106.007. Nye County Early Warning Drilling Program (EWDP) Well Data for Period 2/2001 through 11/2006 Used for Saturated Zone (SZ) Flow Model Potentiometric Surface, Calibration and Validation. Submittal date: 02/22/2007

SN0704T0510106.008. Flux, head and particle track output from the qualified, calibrated saturated zone (SZ) site-scale flow model. Submittal date: 05/01/2007.

SN0705T0510106.009. PEST V11.1 Predictive Uncertainty Analysis Including The Prediction Maximizer. Submittal date: 05/24/2007.

9.5 SOFTWARE CODES

155082 Software Code: CORPSCON V. 5.11.08. 2001. WINDOWS NT 4.0. STN: 10547-5.11.08-00.

167994 Software Code: EARTHVISION V. 5.1. 2000. IRIX 6.5. STN: 10174-5.1-00.

163072 Software Code: EXT_RECH V. 1.0. 2002. Sun O.S. 5.7. STN: 10958-1.0-00.

179539 Software Code: FEHM V. 2.24. 2006. SUN 9.S. 5.7 & 5.8, Windows XP, RedHat Linux 7.1. STN: 10086-2.24-02.

173140 Software Code: LaGriT V. 1.1. 2004. Sun OS 5.7, 5.8, 5.9, IRIX64 OS 6.5. STN: 10212-1.1-00.

164654 Software Code: fehm2tec VV 1.0. 2003. Sun, Solaris 2.7 and 2.8. 11092-1.0-00.

164653 Software Code: maketrac VV 1.1. 2003. Sun, SunOS 5.7 and 5.8. 11078-1.1-00.

157837 Software Code: PHREEQC VV2.3. 2002. PC. 10068-2.3-01.

164652 Software Code: reformat_sz VV 1.0. 2003. Sun, Solaris 2.7 and 2.8. 11079-1.0-00.

161564 PEST V. 5.5. 2002. SUN O.S. 5.7 & 5.8, WINDOWS 2000, RedHat 7.3. STN: 10289-5.5-00.

179480 PEST V11.1. 2007. Windows. 611582-11.1-00.

155323 PHREEQC V. 2.3. 2001. WINDOWS 95/98/NT, Redhat 6.2. STN: 10068-2.3-00.

163070 Software Code: Extract VV 1.0. 2002. Sun UltraSPARC - SunOS 5.7. 10955-1.0-00.

163071 Software Code: Extract VV 1.1. 2002. Sun UltraSPARC - SunOS 5.7. 10955-1.1-00.

163073 Software Code: Mult_Rech VV 1.0. 2002. Sun UltraSPARC - SunOS 5.7. 10959-1.0-00.

180546 Software Code: SPDIS.EXE VV0.0, Windows XP. 611598-00-00.

163074 Software Code: Xread_Distr_Rech VV 1.0. 2002. Sun UltraSPARC - SunOS 5.7. 10960-1.0-00.

163075 Software Code: Xread_Distr_Rech_-UZ VV 1.0. 2002. Sun UltraSPARC - SunOS 5.7. 10961-1.0-00.

163076 Software Code: Xread_Reaches VV 1.0. 2002. Sun UltraSPARC - SunOS 5.7. 10962-1.0-00.

163077 Software Code: Xwrite_Flow_New VV 1.0-125. 2002. Sun UltraSPARC - SunOS 5.7. 10963-1.0-125-00.

163078 Software Code: Zone VV 1.0. 2002. Sun UltraSPARC - SunOS 5.7. 10957-1.0-00.

INTENTIONALLY LEFT BLANK